Thermal Resistance of U-tube Borehole Heat Exchanger System: Numerical Study

A thesis submitted to The University of Manchester for the degree of

Master of Philosophy

in the Faculty of Engineering and Physical Sciences

2013

Raghdah Al-Chalabi

School of Mechanical, Aerospace and Civil Engineering

List of Contents

List of Figures

List of Tables

The University of Manchester
Raghdah Al-Chalabi
Master of Philosophy
Thermal Resistance of U-tube Borehole Heat Exchanger System: Numerical Study
June 12, 2013

Abstract

This research aims to enhance the efficiency of Ground Source Heat Pump (GSHP)system, specifically the U-tube Borehole Heat Exchanger (BHE)system, through reducing the required loop depth to decrease the installation cost. This will assess in promoting the use of BHE system in commercial and small industrial facilities in the UK. Ground source heat pump (GSHP) systems, due to their high coefficient of performance (COP) and low CO_2 emissions are great substitute for fossil fuel to provide more comfortable coexistence of humans and the environment

The design optimisation of the BHE is attempted in this research through the reduction of the total thermal resistance value (R_t). This reduction will lead to lower the required loop depth, and therefore enhance the thermal efficiency of the system and decrease the installation cost. The total thermal resistance is a sum of borehole thermal resistance (R_b) and ground thermal resistance (R_g) values. The ground thermal resistance is influenced by soil thermal properties around the borehole, while borehole resistance is influenced by borehole thermal materials and geometric configurations. Measuring the components of the total resistance accurately and finding technique to reduce R_t is highly required in BHE design field.

Several equations are available to calculate the value of borehole thermal resistance, however, there is no definite decision about their validity. Furthermore, although there are methods suggested in the literature to reduce R_b, none of them were able to reduce it to satisfactory level. Extensive numerical experimental program was conducted in this study to provide better understanding in the field of the thermal resistance of BHE. The originally of this work rests on the following pillars:

I. Conducting a thorough numerical assessment for the available equations in the literature that predict the value of borehole thermal resistance.

II. Conducting an intensive numerical characterization for borehole thermal resistance.

III. Exploring several methods to reduce the R_b, and R_t and assessing their efficiency numerically.

Declaration

No portion of the work referred to in this thesis has been submitted in support of an application for another degree or qualification to this or any other university or institute of learning.

Copyright Statement

Acknowledgements

I would like to express my deepest gratitude to my supervisor, Dr. Hossam Abul Naga, for his inspiring guidance and encouragement through my work and for the invaluable influence he has made in my academic life.

I am hugely grateful to my husband, Samer, for always being there to help and support me, to care and encourage me, and for always being patient with me. Without his support , this work and thesis would never have been realised. My loving thanks for my son Zain for being always patient with me throughout the year.

Also huge thanks to my parents and my parents in law , for their endless love, and consistent support and complete understanding all the way through.

Glossary

ASHP... Air Source Heat Pump.

BHE… Borehole Heat Exchanger.

COP… Coefficient of Performance .

GSHP… Ground Source Heat Pump.

GWHP... Ground Water Heat Pump.

HDPE... High Density Polyethylene.

VGHE... Vertical Ground Heat Exchanger.

Notation

COPc... cooling coefficient of performance [W].

COP_h... heating coefficient of performance [W].

C_p ... heat capacity [J/Kg K].

Cρ… specific heat capacity [J/kg.K].

d_b ... diameter of the borehole [m].

d_{eq} ... equivalent diameter he borehole [W/m].

F_c ... cooling run factor dimensionless.

F_h ... heating run factor dimensionless.

h ... convective coefficient of the fluid [W/m^2k].

k_g ... grout thermal conductivity[W/K.m].

k_p ... pipe thermal conductivity[W/K.m].

k_s ... thermal conductivity of the ground [W/mK].

L … total borehole length [m].

q... heat flux per unit length of the borehole [W/m].

q'… thermal power per unit length [W/m].

q"… thermal power per unit area [W/m^2].

q_h ... peak hourly ground load [W].

q_m ... highest monthly ground load [W].

q_y... yearly average ground heat load [W].

r... radial distance from the line source [m].

r_1 ... inside radius of the pipe [m].

R_{10y}... effective thermal resistance corresponding to 10 years load [m.K/W].

R_{1m}... ground resistance corresponding of one month's load [m.K./W].

r_2 ... outer pipe radius [m].

R_{6h}... ground thermal resistance corresponding to six hours' load [m.K/W].

r_b... borehole radius [m].

R_b ... unit length borehole resistance excluding pipe resistance [K.m/W].

Re… Reynolds number [dimensionless].

r_p ... U-pipe radius [m].

R_p ... U-pipe thermal resistance [K m/W].

r_{rock} … rock radius at a given distance from the borehole centre [m].

R_s... soil thermal resistance [K m/W].

T... temperature of the ground at radius r [°C].

t… time [sec].

T_{bhw}… borehole wall temperature [°C].

T_f … fluid mean temperature of the inlet and outlet pipes [°C].

T_g... undisturbed ground temperature [°C].

T_h ... high soil temperature at peak day of the year [°C].

T_L... low soil temperature at low point day of the year [°C].

T_{max}... maximum entering water temperature to unit in cooling mode [°C].

T_{min}.. minimum entering water temperature to unit in heating mode [°C].

$T_{o....}$ initial temperature of the ground [°C].

T_p... temperature correction to undisturbed ground temperature [°C].

UC... unit capacity-cooling [J/Kg K].

UH... unit capacity-heating [J/Kg K].

x_c ... half the centre-to-centre distance between the two legs of the U-tube [m].

z… borehole depth [m].

α... thermal diffusivity of the ground [m^2/s].

γ... Euler's constant [dimensionless].

λ ... thermal conductivity [W/K.m].

ρ ... soil density [Kg/m^3].

Chapter 1: Introduction to The Research

1.0. Research Background

It was common to believe that most people could afford energy supply with reasonable prices. However, this has been questioned lately due to the limitations of fossil fuels. Furthermore, the energy supplied by fossil fuels generates harmful emissions on the environment, such as carbon dioxide. Reducing carbon dioxide and other greenhouse gases by at least 80% by 2050, relative to the 1990 baseline, is required for the UK by Climate Change Act (2008).

The good news is that some sustainable technologies and methods have been developed and they would save the situation if the researches have reached feasible solutions for practical use. The fact that around 30% of the total final energy consumed, and a total of 25% of carbon dioxide emissions is used in the UK for residential heating and cooling purposes, makes renewable energy a great alternative in UK to provide more comfortable coexistence of humans and the environment (Kannan and Strachan, 2009).

Extracting renewable energy is achieved through the use of sustainable technologies such as solar panels and heat pumps. Heat pumps classified according to the energy source into two types ,Air Source Heat Pump (ASHP) in case of using air or Ground Source Heat pump (GSHP) in case of using the ground. However, some renewable source, for example, ground source energy at great depth, is uncertain, therefore large investment on the field measurements is required to gather the required data (Mori,2010). Therefore, the evaluation of the system performance has to be based on reliable database to minimise the negative effects of the selective and fluctuating BHE characteristic.

Unlike fossil fuels, renewable energy's density is low; therefore, the needed energy will requires more space and time to be collected (Mori,2010). Therefore, facilities with high energy demands are generally built in highly dense regions, where large

space for the energy collection is difficult to expect, such as in the city centre. For this reason, high efficiency of renewable energy source is crucial to defeat this dilemma (Mori,2010).Benefit of the heat pump mechanisms from a practical viewpoint is the use of low grade energy, which does not have attractive energy density and temperature level.

This chapter will highlight the problems facing the feasible design in sustainable technology with appropriate solutions. Finally, aims and objective will be presented followed by a structure of this research.

1.1. Problem Definition

Geothermal energy has the potential to become a flexible heat source for heat pump systems because of the low grade energy that is required to operate. Therefore, the ground source heat pump system could contribute to solving the global energy shortage. In fact, enhancing the benefits of heat pumps can be carried out by finding the most feasible and economical designs to extract the geothermal energy. In general geothermal energy for heat pump could be obtained by system of heat exchangers that need to be buried for a long distance, either horizontally or vertically.

In fact, the installation cost of the ground heat exchanger system is the main obstacle facing the Ground Source Heat Pump (GSHP) technology as it is generally higher than the alternative conventional systems such as Air Source Heat Pump (ASHP). For example, in case that long vertical heat exchangers are selected, the initial costs for the practical depth, 50 to 100 m, generally discourage potential users (Mori,2010).

The ground loop must be sized to meet the required heating demand. Over sized ground loops will significantly increase the installation costs, whereas under sizing the system may result in ground temperatures not being able to recover and heat extraction from the ground being unsustainable. The recovery of the ground temperatures begins After shut-down of heat extraction. During the production

period of a BHE, the drawdown of the temperature around the BHE is strong during the first few years of operation. Later, the yearly deficit decreases to zero.

During the recovery period after a virtual stop-of-operation, the ground temperature shows a similar behaviour: during the first years, the temperature increase is strong and tends with increasing recovery time asymptotically to zero. These effects are shown in Figure1.1. The time to reach a complete recovery depends on how long the BHE has been operational. Principally, the recovery period equals nearly the operation period. This is shown in Figure 7 for different distances from the BHE and for different final temperature deficits (Walter,2000).

Therefore, precise sizing/designing of the ground heat exchanger system is crucial to optimise the performance and to minimise the cost of a GSHP system as much as possible (Mori,2010).

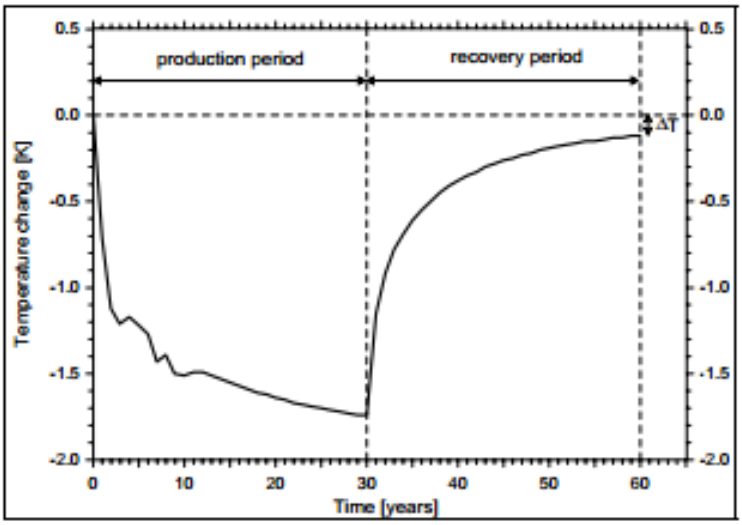

Figure1.1: Calculated temperature change in a depth of 50 m and in a distance of 1m from the BHE over a production and a recovery period of 30 years each (Walter,2000).

The amount of heat extracted from the soil per linear meter of Borehole Heat Exchanger(BHE) is mainly controlled by the total thermal resistance of BHE. This resistance is the sum of the ground thermal resistance and the borehole thermal resistance. In fact, 15 to 25 % of the total thermal resistance is attributed to the borehole thermal resistance, whereas the rest is attributed to the ground thermal resistance (Kavanaugh, 2010). Therefore, the size/length of BHEs, L, is mainly controlled by the total thermal resistance and can be expressed as follows (Mikael Philippe,2010):

$$L = \frac{q_h R_b + q_y R_{10y} + q_m R_{1m} + q_h R_{6h}}{T_f - (T_g + T_p)} \quad (1.1)$$

where L is the total borehole length, T_f is the mean fluid temperature in the borehole, T_g is the undisturbed ground temperature, T_p is the temperature, representing a correction to the undisturbed ground temperature due to thermal interference between the borehole (in the case of a single borehole T_p=0), q_y, q_m and q_h represent, respectively, the yearly average ground heat load, the highest monthly ground load, and the peak hourly ground load, R_{10y}, R_1m and R_{6h} are the effective ground thermal resistance corresponding to 10 years, one month, and six hours ground load and R_b is borehole thermal resistance.

Based on the above discussion it is cleared that the precise determination of the borehole length depends mainly on the confidence in the approach used to calculate the thermal resistance components of the Borehole Heat Exchanger system. Therefore, there is a great need to have accurate methods to determine the total thermal resistance. Furthermore, methods to decrease the total thermal resistance should be explored to decrease the loop length and the overall cost of the system.

1.2. Aims and Objectives of The Study

This study aims to enhance the knowledge in the field of BHE by reducing the design uncertainties in calculating BHE resistance and propose some methods to

decrease the total borehole thermal resistance. For this purpose, a 2D numerical study of BHEs was conducted.

The primary tasks to this study:

a) Discuss the factors influencing ground thermal resistance and borehole thermal resistance of BHE systems.
b) Assess numerically the validity of borehole thermal resistance values using wide range of equations available in the literature.
c) Produce new simple charts to obtain the exact values of borehole thermal resistance for any borehole thermal materials and geometry conditions.
d) Optimize the design of the BHE system by reducing the value of thermal resistance using 2D steady state simulations.

1.3. Thesis Structure

This thesis is structured according to the aims of the study and is presented in eight chapters. The first chapter introduces a geothermal energy definition and the possible savings achieved through improving thermal performance. It also highlights the history of geothermal energy, as well as the aims and objectives of the study.

Chapter two provides a review of the details of GSHP and ASHP types and fundamentals. It also presents an extensive review to the design models of the ground source heat pump system.

Chapter three presents a comprehensive review and discussion of ground geology and hydrology effects on BHE systems. It also defines soil thermal properties and highlights their effect on ground thermal resistance. A review to the factors influencing the value of borehole thermal resistance is also presented.

Chapter four deals with research methodology in this thesis, where numerical solutions using Flex PDE program is discussed. This followed by validation case to estimated numerical borehole thermal resistance using some well known analytical equation.

Chapter five discusses the analytical and semi-analytical equations used to determine the value of BHE resistance. Numerical assessment was conducted by comparing the results to numerical borehole resistance obtained from the Flex PDE program.

Chapter six investigates the most influential factors on BHE thermal resistance. In addition, this chapter introduces, for the first time, contour charts to obtain the exact value borehole resistance for any borehole geometry without the need for complex equations or setting numerical simulations.

Chapter seven introduces several solutions that led to total elimination of borehole thermal resistance. It also discusses the affects that the deep mixing technique on the total thermal resistance of the BHE system, and evaluates the effective deep mixing radius.

Chapter eight presents a summary of the key findings from this work and a discussion of the contribution to knowledge. The achievement of the aims and objectives are highlighted, and potential areas for future research are suggested.

Chapter 2: Literature Review of The Ground Source Heat Pump System

2.0 Introduction

The physical law tells us that heat normally flows from a warmer medium to a colder one, but how do we move heat from our cooler house and dump it to a higher outside environment in the summer? And how can we extract heat from a lower temperature outside to warm rooms in the winter? The answer is by using a heat pump. The heat pump does this by "pumping" heat up the temperature scale and transferring it from a cold material to a warmer one by adding energy, usually in the form of electricity (Ruqun Wu, 2009).

Hence, this chapter will address the component, and the common types of the heat pump. In particular, the GSHP is going to be introduced in details. Moreover, some GSHP design models are described in order to assess their feasibilities.

2.1. Heat Pumps

a heat pump is defined as a device or machine that extracts heat from a low temperature source and supplies it to a heat sink at a higher temperature. Thus, such a device can be used for heating in the winter or for cooling in the summer. Even though heat pumps have some impact on the environment, as they require electricity to run, the heat they extract from the ground or air is constantly being renewed naturally. These machineries are more efficient than electric heating in mild and moderate climates. Unlike gas or oil boilers, heat pumps deliver heat at lower temperatures over much longer periods. This means that during the winter they may be required to be left on 24/7 to heat buildings efficiently. It also means that radiators should never feel as hot to the touch as they would do when using a gas or oil boiler (Jenkins et. al., 2009).

Heat Pump has number of components namely are: Evaporator, compressor, condenser, expansion valves, and reversing valves. Both the heating and cooling cycles' working concepts and heat pump components are presented in Figure 2.1 (Cengel and Boles, 1994).

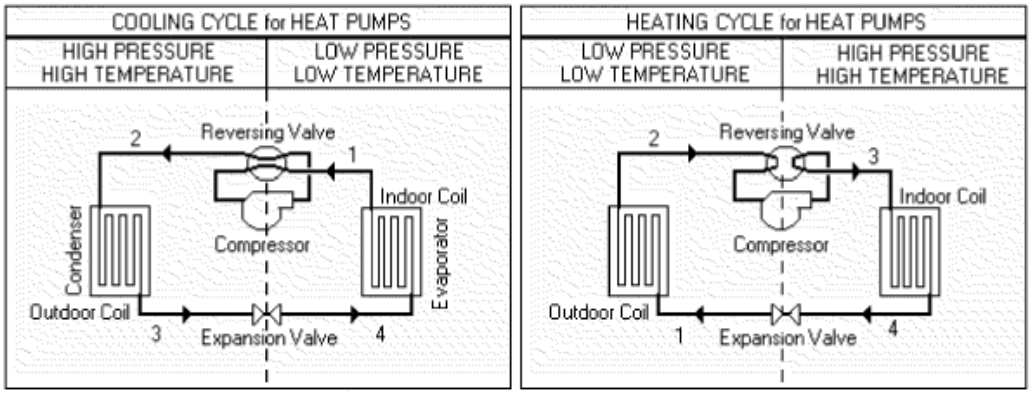

Figure 2.1: Heat pump cooling and heating cycles (Vanderburg, 2002).

- **Cooling cycle**

1. Cool, low-pressure refrigerant vapour enters the compressor after absorbing heat from the air in the building (heat source) through the evaporator/cooling coil. The compressor then compresses the cool vapour.

2. The refrigerant exits the compressor as a hot vapour under high-pressure, which then enters the condenser (heat sink). The loop condenses the vapour until it is mostly liquid.

3. The refrigerant then leaves the condenser (heat sink) as a warm liquid. The expansion valve regulates the flow from the condenser so that only liquid refrigerant passes through.

4. The refrigerant expands as it exits the expansion valve and becomes a cold liquid. The liquid evaporates as it passes through the cooling coil (located in the indoor air unit). The refrigerant then absorbs indoor heat from the air blowing over the coil surface, and thus cools the building. The refrigerant is now a cool vapour and the cycle continues.

- **Heating Cycle**

1. The refrigerant enters the outdoor coil as a cool liquid.

2. The cold liquid absorbs heat from its surroundings (air or a geothermal earth source) and exits as a cool vapour. The cool vapour then enters the compressor.

3. The refrigerant exits the compressor as an extremely hot vapour, which is much hotter than the inside air. A fan blows over the hot coils to transfer the heat into the building.

4. The refrigerant leaves the indoor coil as a warm liquid and then enters the expansion valve to cool the liquid.

There are two types of heat pumps. The most common type of heat pump is the air source heat pump (ASHP), which transfers heat between indoor and outside air. Ground source heat pumps (GSHPs) have been used since the late 1940s, which use the constant temperature of the ground as the heat exchange medium instead of outside air temperature (Ruqun Wu, 2009).In the next sections the detail of the working principles for both the ASHP and GSHP will be discussed.

2.2. Types of Heat Pumps

2.2.1. Air Source Heat Pump (ASHP)

In the case of ASHPs, the heat is removed from the indoor air and rejected to the outdoor air in the cooling cycle, while the reverse happens during the heating cycle. ASHPs are classified as either air-to-air or air-to-water depending on whether the heat distribution system in the building uses air or water (Ruqun Wu, 2009).Types of air source heat pump components are presented in Figure 2.2.

For application, an ASHP will typically be a roof top unit, which is either completely packaged or a split package system. Split package heat pumps are designed with an air handling unit located inside the conditioned spaced, while the condenser and compressor are packaged for outdoor installation on the roof.

Packaged systems usually have both coils and the fan outdoors. Heated or cooled air is then delivered to the interior from ductwork that protrudes through a wall or roof (Aye, 2003).

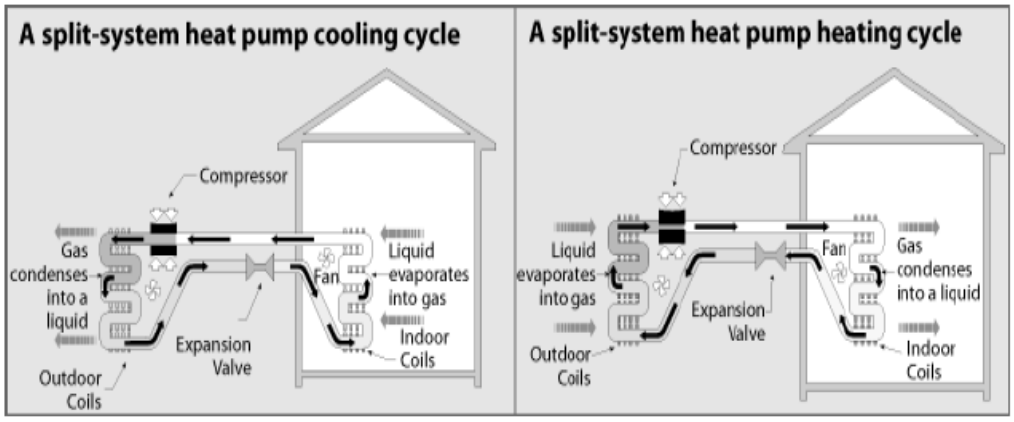

Figure 2.2: ASHP split system (Source: U.S. Department of Energy, 2008).

2.2.2. Ground Source Heat Pump

Ground source heat pumps (also called earth-coupled heat pumps or geothermal heat pumps) are able to provide heating or cooling for buildings using ground thermal energy. The Earth preserves a lot of thermal energy, partly from its formation (30-50%) and partly from the radioactive decay inside the earth (50-70%). There are temperatures of around 4,800-7,700°C inside the inner core of the Earth. All in all 99 % of the Earth is hotter than 1,000°C and the rest is still hotter than 100°C, which advises the use of this energy (Robin, 1999).

Although public awareness of this beneficial technology is limited, GSHP have been in commercial use for over 50 years. Archaeological evidence discloses that the first human use of geothermal recourses was in North America over 10,000 years ago, by a settlement of Paleo-Indians in Hot Springs. The spring worked as a source of warmth and cleansing, and its minerals were used as a source of healing by people soaking in heated pools that were heated by the Earth. However, the first successful GSHP application occurred back in 1946 at the Commonwealth Building in Portland, Oregon (Stuebi, 2000).

GSHPs have gained more popularity and have experienced an annual increase of 10 % in about 33 countries, including the UK, over the last ten years. There is not complete data, but it is estimated that the number of installed plants recently reached 1,700,000 throughout the world (Lund, 2007).

Generally, geothermal energy can be classified in one of the three following categories (as defined by ASHRAE, 2003):

(1) High-temperature (>150^{o}C) electric power production.

(2) Intermediate- and low-temperature (<150^{o}C) direct-use applications.

(3) GSHP general applications (<32 ^{o}C).

All types of GSHP consist of the following (starting from the inside to the outside) components:

- The interior heating and cooling distribution system.
- A heat pump.
- The earth connection (coils).

In GSHP, the outdoor coil is placed within the earth at specific depths depending on the type of system. This will be where ground level temperatures remain relatively constant regardless of outside ambient air temperature (Brandl et al., 2006).

Sizing the depth of the BHE varies between local meteorological properties, soil type and technical properties of designing the heat pump. The required length of GHEs for heating and cooling are given below (Mils et al., 1994).

Total heating pipe length:

$$L_H = \frac{UH\frac{COP_h - 1}{COP_h}(R_F + R_S.F_b)}{T_L - T_{min}} \quad (2.1)$$

Total cooling pipe length:

$$L_c = \frac{UC\frac{COP_C+1}{COP_c}(R_p+R_s.F_c)}{T_{max}-T_h} \quad (2.2)$$

where UH: unit capacity-heating, UC: unit capacity-cooling, COP_h: heating coefficient of performance, COPc: cooling coefficient of performance, R_p: pipe thermal resistance, R_s: soil thermal resistance, T_L: low soil temperature at low point day of the year, T_h: high soil temperature at peak day of the year, T_{min}: design minimum entering water temperature to unit in heating mode, T_{max}: design maximum entering water temperature to unit in cooling mode, F_h: heating run factor, F_c: cooling run factor,

The pipe length for both operating modes is calculated and then the longer length used for the application. The evaluation of the total length of the BHE is crucial since it is an important part of the initial costs of the system.

2.3. Types of Ground Source Heat Pump

The first step in producing a feasible design of the ground source heat pump is achieved by choosing a suitable type of heat pump. Ground Heat Pump systems (GHPs) are divided into two categories depending on the source/sink utilized. If the Ground Heat pump (GHP) utilizes a water body to extract or reject heat then it is called a ground water heat pump (GWHP), whereas in cases of the pump using the earth it is called a Ground Source Heat Pump (GSHP).

When underground water is available and used as a heat carrier, it is brought directly to the heat pump where there is no barrier between the soil, ground water, and the heat pump evaporator – this type is called an “open-loop” ,as shown in Figure 2.3. There is always a risk of ground water contamination due to direct contact between the loops and groundwater (Omer, 2006).

However , underground water is not available everywhere, on the other side, the GSHPs can be installed anywhere (Brandl, 2006).GSHPs are divided into two types open loops and closed loops.

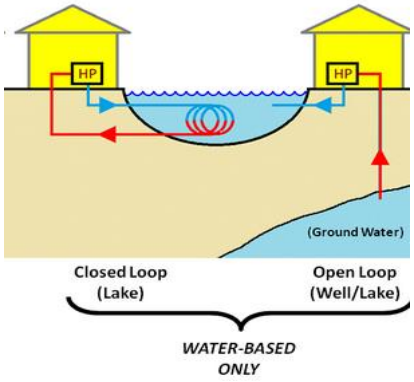

Figure 2.3: Ground water heat pump system(Omer, 2006).

2.3.1.Types of Closed Loop System

A closed loop network of tubing is buried in the ground where there is no direct contact between the circulating fluid and ground water, and this can be either horizontal or vertical. The most common method of ground-coupling is to bury thermally fused plastic piping either vertically or horizontally. These plastic pipes are typically made from a pair of straight pipes, which are then attached to the bottom by U-shape joints and typically made of high density polyethylene pipes (HDPE) with a diameter ranging from 19mm to 38mm. In the USA and in Central Europe it is common practice, and sometimes required, to backfill the boreholes with some material such as bentonite, concrete or quartz sand. Special mixtures, called thermally enhanced grouts, have been developed to provide for better heat transfer than pure bentonite (Remund and Lund, 1993). The grout has the following roles:

1. Connects the U-pipe to the surrounding soil.
2. Protects from ground water contamination, as it isolates the pipe from the surrounding ground water.
3. Guarantees the stability of the formation.

These U-pipes are then filled with solution (water or antifreeze) that circulates in closed loops, where heat is released to, or absorbed from, the ground (see Figure

2.4). Therefore, closed loops represent the connection between the GSHP and the ground. There are two types of closed loops, vertical closed loops and horizontal closed loops. These loops will be discussed in the following sections.

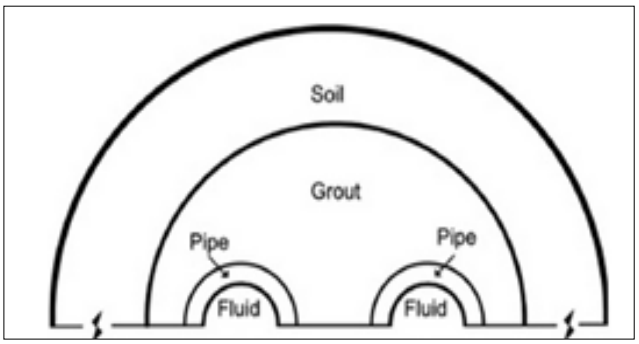

Figure 2.4: A half cross section to the closed loop system (Austin, 1995).

2.3.1.1. Horizontal Ground Closed Loops

This type is the most cost effective as they are easy to dig, however, the size of the installing location has to be sufficient. In general, trenchers are utilized to dig the trenches one to three metres below the ground in which a series of parallel plastic pipes are laid ,as illustrated in Figure 2.5.

The fact that these trenches are installed at shallow depths means they are more exposed to seasonal temperature variance, as thermal properties of the soil will fluctuate with season and rainfall. Trenching costs are typically lower than well-drilling costs. A typical horizontal loop will be 100 to 200 metres long for each ton of heating and cooling (Omer, 2006).

Since the main thermal recharge for all horizontal systems is supplied mainly by solar radiation to the Earth's surface, it is vital that the surface above the ground heat collector is not covered. The horizontal loop system can be buried beneath lawns, landscaping, and parking areas.

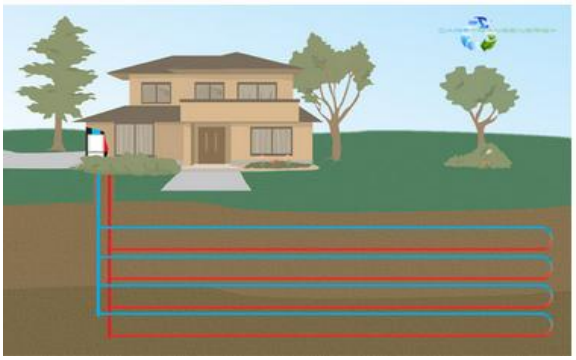

Figure 2.5: Horizontal closed loop system.

(Source: British Eco Renewable Energy Solutions, 2013)

2.3.1.2. Vertical Ground Closed Loops

Vertical heat exchangers, commonly called borehole heat exchangers (BHEs), are generally employed when land surface is limited, surface rocks make trench digging impractical. Several bores are typically used with spacing not less than 5-6m in order to achieve total heat-transfer requirements as shown in Figure 2.6.

Vertical loops are generally more expensive to install, but these require less piping than horizontal loops because the earth's temperature is more stable below the surface. Typically, the BHE is 0.1-0.2 m in diameter and 15-20m in depth (Brandl, 2006).

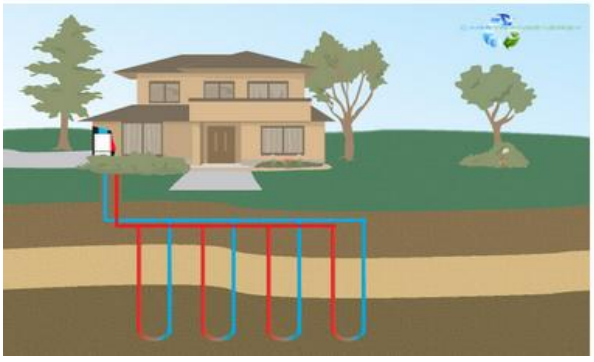

Figure 2.6: Vertical closed loop system.

(Source: British Eco Renewable Energy Solutions, 2013)

2.4. Vertical Loops Versus Horizontal Loops

- **Cost**

Horizontal loops are more cost effective than vertical loops due to their drilling depths being quite a lot less. However, the piping used in vertical loops is much less due to the stable temperatures where it is installed.

- **Area**

Horizontal loops, unlike vertical loops, require sufficient area for installation and it is important not to cover the surface above the ground heat collector. Hence, vertical loops are a better choice when little land disturbance is required.

- **Efficiency**

Horizontal trenches are installed at a shallow depth unlike the vertical loops, so it is more exposed to seasonal temperature variances. Therefore, vertical loops are more efficient than horizontal ones. The next section will discuss developments in vertical heat exchanger models.

2.5. Existing Design Models For Borehole Heat Exchanger

Over the years, different analytical and numerical models have been refined and employed to evaluate heat exchanged within the borehole and the bedrock to:

1. Estimate the required BHE depth.
2. Predict BHE thermal performance.

A number of models have been created to predict the heat transfer rate and thermal resistance of the ground and BHE (Bose et al., 1985; Eskilson and Classon, 1988; Deerman and Kavanaugh, 1991; Bi et al., 2002; Zeng et al., 2003; Li et al., 2006). These models are analytical models, and numerical models.

Analytical models use line or cylinder heat source theory to solve the heat transfer rate from the borehole wall to the surrounding soil. In these analytical models the

internal region of the borehole has been neglected. However, the numerical models finite differences are used to solve temperature distribution in the whole domain, including the surrounding and the inertial of the borehole region (Sharqawy et. al., 2009).

The next section will review the Analytical models according to the two categories above. Each model is explained starting with its conceptual modelling and followed by the mathematical formulation. The advantages and limitations of the models are highlighted to clear some of the present flaws in modelling BHEs.

2.5.1. The Line Source Model

The main assumption in the line source model is made by considering the whole borehole as an infinitely long line source and neglecting of the thermal properties of the borehole, such as the thermal mass of the fluid, pipes, and backfilling materials. The earliest application of this approach was introduced by Lord Kelvin (1882)to determine thermal performance through ground heat exchanger pipes. Therefore, this model is also called "Kelvin's line source theory".

Ingersoll and Plass (1948) employed this model in ground loop heat exchangers. However, the method neglects the heat transfer in the direction of the borehole axis. Thus, the heat conduction process in the ground is simplified as one dimensional.

A number of improvements for this approach have been proposed to account for some complicated factors and enhance the accuracy in estimation of the BHE, as listed in Table 2.1(Yang et al., 2010). For example, one major improvement to this method by Hart and Couvillion (1986) utilized the line source model to estimate continuous time-dependent heat transfer between a line source and the ground.

Despite the fact that Kelvin's line source theory neglects the axial heat flow, the theory can be regarded as a simple, suitable starting point for analysis of BHE and the most practical model. However, it is not suitable for a long-term response.

Assuming an initial uniform temperature and a constant heat flux per unit depth at the borehole centre, the expression given by Ingersoll (1954) for the temperature at any time and at any radius is expressed as:

$$T - T_o = \frac{q}{2\,\pi\,k}\int_x^{\infty}\frac{e^{-B^2}}{\beta}d\beta = \frac{Q}{2\pi\,k}\,I(x) \tag{2.3}$$

and

$$\beta = \frac{r}{2\sqrt{\alpha(t-t')}} \tag{2.4}$$

$$x = \frac{r}{2\sqrt{\alpha t}} \tag{2.5}$$

where T is the temperature of the ground at radius r (°C), T_o is the initial temperature of the ground (°C), q is the heat flux per unit length of the borehole (W/m), r is the radial distance from the line source (m), k is the thermal conductivity of the ground (W/mK), α is the thermal diffusivity of the ground (m^2/s), and t is the time since the start of the operation (s).

For X < 0.2, the values of the integral term can be evaluated using the following approximation:

$$I(x) = 2.303\ \log_{10}\frac{1}{x} + \frac{x^2}{2} - \frac{x^4}{8} - 0.2886 \tag{2.6}$$

Carslaw and Jaeger (1947) utilized the exponential integral E_1 to approximate the solution of the line source model and derive the most commonly used equation to estimate the thermal conductivity of the ground during in situ thermal response tests. This line source equation is given as:

$$T - T_0 = \frac{Q}{4\,\pi\,k}\int_{r^2/4\alpha t}^{\infty}\frac{e^{-u}}{\beta}du = \frac{Q}{4\pi\,k}\,E_1\left(\frac{r^2}{4\alpha t}\right) \tag{2.7}$$

The exponential integral E_1 can be estimated by:

$$E_1\left(\frac{r^2}{4\,\alpha\,t}\right) = -\gamma - \ln\left(\frac{r^2}{4\,\alpha\,t}\right) - \sum_{n=1}^{\infty}(-1)^n \frac{\left(\frac{r^2}{4\,\alpha\,t}\right)^n}{nn!} \cong \ln\left(\frac{r^2}{4\,\alpha\,t}\right) - \gamma \qquad (2.8)$$

where γ is Euler's constant, which is equal to (0.577). The natural logarithm approximation of the exponential integral E_1 in the equation (2.7) provides errors less than 10%for the time criterion $t_c \geq 5r^2/\alpha$. The temperature at the borehole wall (r_b) at time *t* can then be expressed as:

$$T_b = \frac{Q}{4\pi k}\left[\ln\left(\frac{4\alpha\,t}{r_b^2}\right) - \gamma\right] + T_0 \qquad (2.9)$$

with $t_c \geq {5r_b^2}/{\alpha}$, which ranges from 3-10 hours in practice.

Assuming the heat transfer within the borehole is in a steady-state, at any time, the relationship between the mean fluid temperature and the borehole temperature can be defined using a thermal borehole resistance, so that:

$$T_f = T_{bhw} + Q.R_b$$

$$= \frac{Q}{4\pi K}\ln(t) + Q\left[R_b + \frac{1}{4\pi k}\left(\ln\left\{\frac{4\alpha}{r_b^2}\right\} - \gamma\right)\right] + T_0 \qquad (2.10)$$

where T_f is the mean fluid temperature, T_{bhw} is the borehole temperature, and R_b is the borehole thermal resistance. There are other solutions developed from Kelvin's line source theory, such as Hart and Couvillion's approach (1986) and the IGSHPA approach (Bose, 1991).

Steady-state borehole models are mainly developed to estimate borehole thermal resistance using analytical models. The primary assumption made in steady-state borehole models is that the heat transfer in the borehole is in a steady state. The ratio between the heat flux of the borehole and the temperature difference between the fluid and the borehole wall is a constant value. Thus, thermal resistance can be employed to define the relationship between the heat flux, the temperature difference of the fluid, and the borehole wall as follows (He, 2012):

$$R_b = \frac{T_f - T_b}{Q} \quad (2.11)$$

where R_b is the borehole thermal resistance (Km/W), Q is the heat flux per unit length of the borehole (W/m), T_f is the average temperature of the fluid (°C), and T_b is the average temperature of the borehole wall (°C).

The borehole thermal resistance consists of the convective resistance of the fluid, the conductive resistance of the pipes, and the conductive resistance of the grout. The relationship of the borehole's thermal resistance and the thermal resistance of the fluid, pipe and grout can be presented as:

$$R_b = \frac{R_f + R_p}{2} + R_g \quad (2.12)$$

where R_f is the convective resistance of the fluid within one pipe, R_p is the conductive resistance of one pipe, and R_g is the conductive resistance of the grout. The conductive resistance of the fluid within one pipe can be estimated by (Incorpera et al., 2007):

$$R_f = \frac{1}{2\pi\, h\, r_1} \quad (2.13)$$

where r_1 is the inside radius of the pipe (m) and h is the convective coefficient of the fluid (W/m^2k). If the fluid flow is kept under turbulent conditions then fluid resistance is typically less than 1%, and can therefore be neglected. The conductive resistance of the one pipe can be determined by (Incorpera et al., 2007):

$$R_p = \frac{\ln(\frac{r_2}{r_1})}{2\pi k_p} \quad (2.14)$$

where r_1 is the inside radius of the pipe (m) k_p is the pipe thermal conductivity, r_2 is the outer pipe radius, and r_1 is the inner radius of the pipe. A number of steady state borehole models have been developed. These models are the equivalent diameter

model by Gu and O'Neal's (1998), multipole model by Bennet et al., (1987) models and numerical models. These models will be discussed below.

Table 2.1: Brief development history for the line source approach (Yang et. al., 2010).

Year	Line Source Approach
1882	Lord Kelvin Kelvin's line source model
1948	Ingersoll and Plass Modified line source model
1986	Hart and Couvillion Enhanced line source model

2.5.1.2. Equivalent Diameter Model

Gu and O'Neal's (1998) equivalent diameter method is a simple method of calculating steady state borehole thermal resistance and is based on the assumption of concentricity of one pipe within the borehole as shown in Figure 2.7. It determines a steady state borehole resistance value that is satisfactory for most simple calculations. This method is presented by an algebraic equation to combine the U-tube fluid into one circular region inside the centre of the borehole, such that the resistance between the equivalent diameter and the borehole wall is equal to the steady-state borehole resistance of the grout.

$$R_b = \frac{\ln\left(\frac{d_b}{d_{eq}}\right)}{2\pi k_g} \tag{2.15}$$

$$D_{eq} = \sqrt{2d_P . s} \qquad d_p \leq s \leq r_b \qquad (2.16)$$

where R_b is borehole thermal resistance(K.m/W), k_g is conductivity of the grout (W/K.m), d_b is the diameter of the borehole (m), d_{eq} is the equivalent diameter using Gu-O'Neal's method (m), d_p is the diameter of the U-shaped pipe (m), and s is the centre-to-centre distance between the two legs (m).

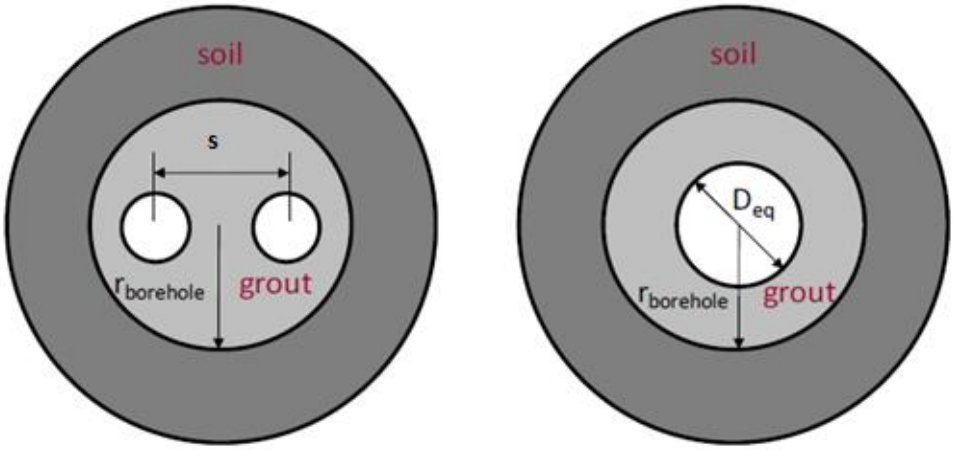

Figure 2.7: Diagram of equivalent diameter of a BHE with a single U-tube (He, 2012).

It over simplifies the 2D heat transfer occurring inside the borehole into a 1D heat flow process and neglects temperature variations over the borehole's cross-section. Since they might lead to overestimating the value of borehole thermal resistance, this model may be used to provide rough estimates for design considerations, consequently, this may lead to over-sizing the ground heat exchanger.

2.5.1.3. Multipole Method

The multipole method, developed by Bennet et al. (1987) ,introduces an analytical solution for R_b based on line source theory. It assumes a constant heat flux from each pipe source and that heat transfer is through conduction. Multipole resistance

was found using a modified version of the Fortran 77 source code given in Bennet et al. (1987).

Within the multipole method, borehole resistance is obtained by establishing a temperature at the U-tube wall and then determining a heat flux and a temperature profile around the circumference of the borehole wall (T_{bhw}), as shown in Figure 2.8. The temperature at the borehole was calculated by taking an average of 180 points along the circumference of the borehole wall. Averaging 180 points, versus an average of 360 points, produced a temperature difference of less than 0.00001°C (Bennet and Claesson, 1987; He, 2012).

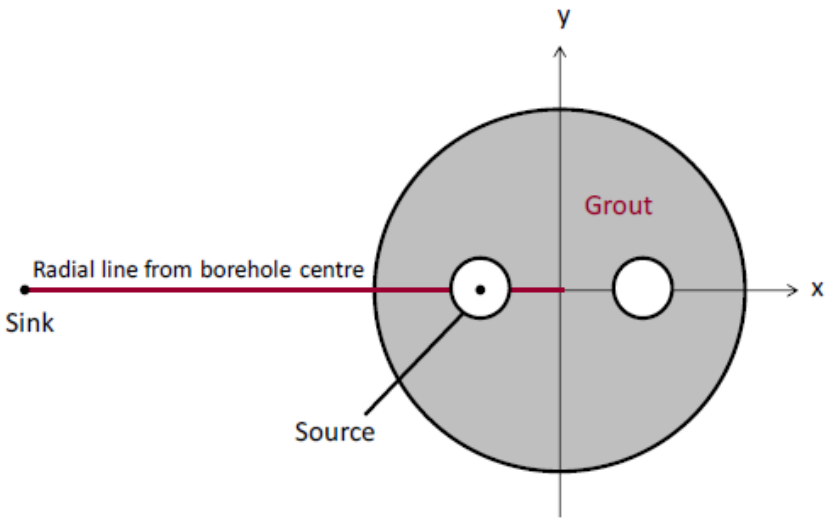

Figure 2.8: Single line source with a single line sink (He, 2012).

By setting a specific temperature for each pipe, the multipole method is used to estimate the heat flux of each pipe and the average temperature of the borehole wall so that the borehole resistance can be derived as follows:

$$R_b = \frac{1}{4\pi k_g}\left[\ln\left(\frac{\lambda_1\,\lambda_2^{1+4\sigma}}{2(\lambda_2^4)^{\sigma}}\right) - \frac{\lambda_3^2(1-(4\sigma/(\lambda_2^4-1)))^2}{1+\lambda_3^2(1+(16\sigma/(\lambda_2^2-\frac{1}{\lambda_2^2})^2))}\right] \tag{2.17}$$

where $\lambda_1 = \frac{r_b}{r_p}$,$\lambda_2 = \frac{r_b}{0.5\ s}$, $\lambda_3 = \frac{r_b}{s} = \frac{\lambda_2}{2\lambda_1}$, $\sigma = \frac{k_g - k_s}{k_g + ks}$,$R_b$ is the borehole resistance (K.m/W),s is the shank spacing, which defines the centre-to centre distance between the two legs of the U-tube , r_b is the borehole radius (m), r_p is the pipe radius (m), k_g is the grout thermal conductivity (W/K.m).

2.5.2.4. Numerical Models

A number of numerical models have been developed to calculate the temperature distribution around U-tube boreholes, as well as borehole thermal resistance. These numerical models have been developed to examine the nature of heat transfer around borehole heat exchangers for research purposes.

In addition, the models have been used in system simulations to field data. Whereas both line source models and cylindrical models using analytical solutions ignored the axial heat transfer in the direction of the borehole axis, numerical solutions can account for the axial heat transfer by considering a borehole with finite length. In a number of the numerical BHE models that have been developed, as shown in Table 2.2, two numerical approaches are the most common:

- The g-function model developed by Eskilson in 1988.
- The duct storage (DST) model developed by Hellström in 1991.

In Eskilson's model a two-dimensional numerical calculation was utilized for a single borehole in homogeneous ground, with constant initial and boundary temperature. The thermal capacitance of the borehole elements, such as the pipe wall and the grout, are ignored. Eskilson's g-function calculates the temperature change at the borehole wall in response to a stepped heat input for a unit time. This model aimed to provide the response for the ground to heat rejection/extraction over long periods of time (up to 25 years). However, as the numerical model that provides the g-functions does not account for the local borehole geometry, it cannot accurately provide the shorter term response.

However, this calculation is time-consuming and it can hardly be incorporated directly into an hourly, building design and energy analysis programme for practical applications. This is because the g-functions of BHEs with different configurations have to be pre-computed and stored in a massive database (Yang et al., 2010). In addition, the g-function model developed by Eskilson does not explain the thermal resistance effects of the borehole elements, such as the pipe wall, the grout, and the fluid flow.

Yavuzturk and Spitler (1999) enhanced Eskilson's g-function algorithm to account for the influences of the thermal properties of the grouting material and the thermal properties of the anti-freeze on BHEs heat transfer performance. The enhanced g-function model by Yavuzturk and Spitler is named the short time-step model.

Hellstrom (1991) developed a numerical model for vertical ground heat stores, which are densely packed ground loop heat exchangers used for seasonal thermal energy storage, where the borehole thermal resistance is calculated as follows:

$$R_b = \frac{1}{4\pi k_g}\left[\ln\left(\frac{r_b}{r_p}\right) + \ln\left(\frac{r_b}{2x_c}\right) + \sigma \ln\left(\frac{(r_{b/x_c})^4}{(r_b/x_c)^4 - 1}\right)\right] \quad (2.18)$$

where R_b is the unit length borehole resistance excluding pipe resistance (Km/W), x_c is the shank spacing – defined here as half the centre-to-centre distance between the two legs of the U-tube – r_b is the borehole radius (m), r_p is the pipe radius (m), and k_g is grout thermal conductivity.

Zeng et al. (2003) have developed a quasi-three dimensional model to determine R_b inside single and double U-tubes. The borehole thermal resistance

$$R_b = \frac{1}{2\pi k_g}\left[\ln\left(\frac{r_b}{s}\right) - \frac{k_g - k_s}{k_g + k_s}\ln\left(\frac{r_b^2 + (0.5\,s)^2}{r_b^2}\right)\right] \quad (2.19)$$

where k_g is the grout thermal conductivity(W/K.m), k_s is the soil thermal conductivity(W/K.m), r_b is the borehole radius(m),s is the shank spacing between the U-tube legs (m).

Thornton et al. (1997) used Hellstrom's approach as part of a detailed component based simulation model of a ground source heat pump system. It was calibrated to monitored data from a family housing unit by adjusting input parameters such as the far-field temperature and the ground formation thermal properties. When calibrated, the model was able to accurately match measured entering water temperatures.(Yavuzturk et al., 1999)

Table 2.2: Brief history of the numerical solution (Yang et al., 2010).

Year	**Numerical Approach**
1985	Mei and Emerson
1987	Eskilson
1991	Hellstrom
1996	Berger et al. Murya et al.
1997	Rottmayer et al. Thornton et al.
1999	Yavuzturk and Spliter
2003	Zeng et al.

2.5.2. Cylinder Source Model

In another development, Carslaw and Jaeger (1947) developed the cylindrical source model, which considers the two legs of the U-tube as a single pipe that is co-axial with the borehole. However, the thermal mass of the fluid, pipes and grout are neglected in this approach (Carslaw and Jaeger, 1947).

Ingersoll et al. (1954) modified this model to size buried heat exchangers. Then, Kavanaugh (1985) refined the model to determine the temperature distribution or the heat transfer rate around a buried pipe ,as shown in Table 2.3. ASHRAE's (2007) procedure uses the cylinder source model developed by Kavanaugh, and Table 2.2 illustrates the history development of the cylindrical source approach.

Considering the two pipes as one infinitely long pipe, and coaxial with the borehole with infinite length, the cylinder source solution (Carslaw and Jaeger, 1947) can be utilized to evaluate the temperature distribution of the infinite ground with the initial temperature around the borehole, at any time.

Assuming a constant heat flux along the borehole, the governing equation for the one-dimensional heat transfer problem is presented as:

$$\frac{\partial^2\theta}{\partial r^2}+\frac{1\partial\theta}{r\partial r}-\frac{1}{\alpha}\frac{\partial\theta}{\partial t}=0 \qquad r_0<r<\infty \tag{2.20}$$

while the boundary conditions and initial condition can be expressed as:

$$-2\pi.r_0.k\frac{\partial\theta}{\partial r}=Q \qquad r=r_0.t>0 \tag{2.21}$$

$$\frac{\partial\theta}{\partial r}=0 \quad r_0=0 \tag{2.22}$$

$$\theta=0 \qquad t=0, r>r_0 \tag{2.23}$$

where $\theta=T-T_0$ is the temperature difference between the ground temperature at radial distance r from the cylinder source, at time t and the initial temperature (°C).

Taking the Laplace transform and inverse Laplace transform, the solution can be expressed as:

$$\theta(r,t) = \frac{2Q}{\pi k}\int (1 - e^{-\alpha t u^2}) \frac{J_0(u,r)Y_1(u\alpha) - Y_0(ur)J_1(u\alpha)}{u^2\left[J_1^2(u\alpha) + Y_1^2(u\alpha)\right]} du \quad (2.24)$$

where J_0, J_1, Y_0, and Y_1 are the zero and first order functions.

Kavanaugh (1985) tested this model using experimental data from two test sites. Due to the fact that the cylinder source solution considers the two pipes as one, the short circuit heat transfer within the borehole, presented by the temperature difference between these two pipes, is, therefore, neglected (Young, 2004).

Since both ASHP and GSHP use renewable energy, the question is which type of heat pump has higher thermal efficiency and lower installation costs. The next section, therefore, will present a comparison between these types of heat pumps.

Table2.3: Brief development history for the cylindrical source approach (Yang et. al., 2010).

Year	**Line Source Approach**
1947	Carslaw and Jaeger Cylinder source model
1954	Ingersoll et al. Modified cylinder source model
1985	Kavanaugh Modified cylinder source model

2.6. GSHP versus ASHP

- **Operating efficiency**

The classical parameter used to describe heat pump performance efficiency is Coefficient of Performance (COP). The COP of a heat pump is the ratio of the heating or cooling provided over the electrical energy consumed, which provides a metric of performance for heat pumps that is analogous to thermal efficiency for power cycles (Lu Aye, 2003; ASHRAE, 2003). It is defined by:

$$COP = \frac{\text{Cooling or heating energy obtained from heat pump(kW)}}{\text{Energy input for operation(kW)}} \qquad (2.24)$$

For example, a value of 4 COP means that from one portion of electrical energy, three portions of environmental energy (from the air or ground), and four portions of usable energy are derived. A good performing system should give a COP of at least 3 (Reynolds, 1977). This coefficient is inversely proportional to the temperature difference between sink and source; thus, heat pumps operating over a small temperature difference are more efficient than those attempting to supply a sink at a much higher temperature than the source. In other words, heat pump efficiency is primarily dependent upon the temperature difference between the building interior and the outdoor environment. If this difference can be minimized then heat pump efficiency will improve.

In fact, the ASHP system suffers from the disadvantage that the greatest requirement for building heating or cooling necessarily coincides with the times when the external air temperature, which is generally colder in winter and warmer in summer, is less effective as a heat source or sink, respectively. However, GSHPs avoid this problem by extracting/rejecting heat from liquid-filled buried coils, which are not subject to large annual swings in temperatures as they are buried in the earth that has moderate temperatures all year round (Mils et. al., 1994).

The temperature within the zone of five metres depth is a dampened version of the air temperature at the surface. The temperature in intervals of 5m, and up to 50m in depth, is constant throughout the year as a result of a complex interaction of heat fluxes from above (the sun and the atmosphere) and below (the Earth's interior) the ground (Hart and Couvillion, 1986). Below this zone (greater than about 50 metres) the temperature begins to rise according to the natural geothermal gradient (30°C/km), as shown in Figure 2.9 (Chiasson, 1992). Furthermore, ground temperatures are almost always closer to the required room temperature than outdoor air temperatures (Grant et. al., 1982).

Figure 2.10, shows the performance curves of GSHP and ASHP for cooling operations in the Japanese environment, where the temperature of the ground and outdoor air during the summer are 15°C and 35°C, respectively. The results show that the primary benefit of ground-source heat pumps is the increased operating efficiency (COP) that arises from the reduced and more steady temperature difference they are required to work over.

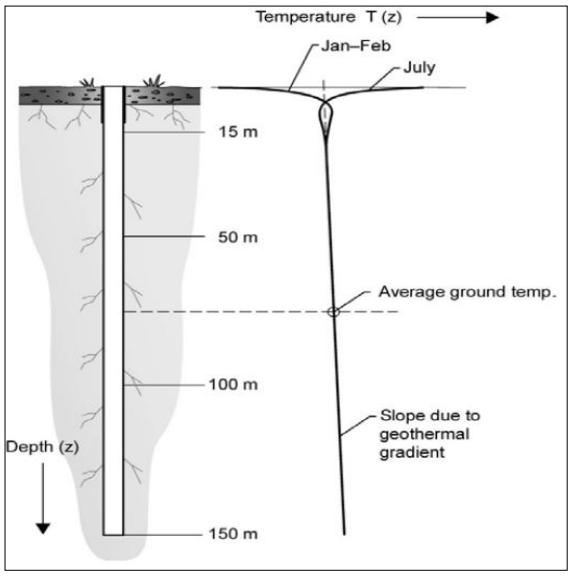

Figure 2.9: Temperature variation in the ground. Seasonal variations do not reach 15 metres from the ground surface (Gehlin, 2002).

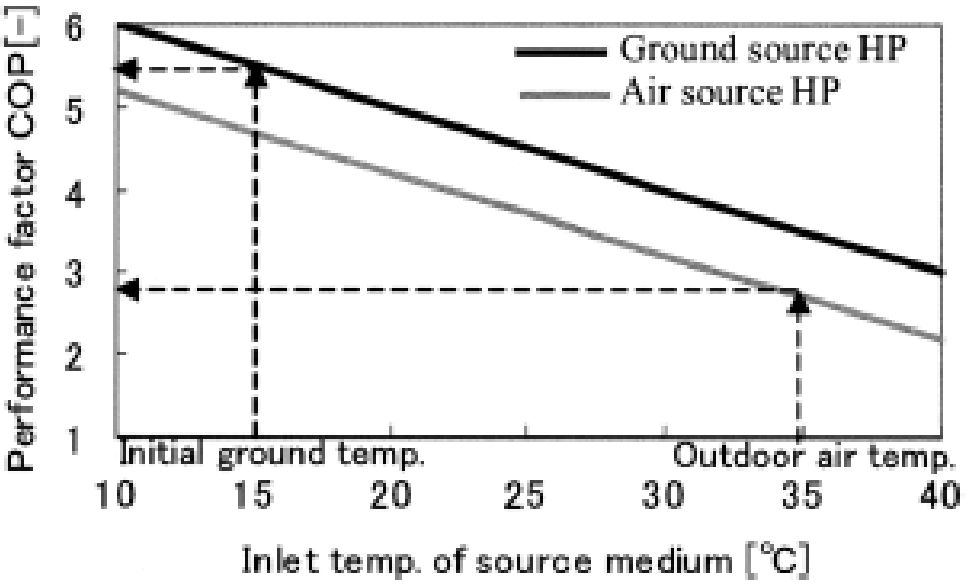

Figure 2.10: Performance curves for cooling operations (Nippon Steel Corporation, 2005).

- **Environmental aspects**

Environmentally, GSHP represents a superior alternative in many aspects when compared to ASHP. These are as follows:

- As GSHP consumes less primary energy than ASHP, it is an important technology to help reduce the emissions of gases that harm the environment, such as carbon dioxide (CO_2). Genchi et al. (2002) estimate that replacing ASHP with GSHP in Japan would result in a reduction of 54 % of the total CO_2 emissions per year. Genchi et al. (2002) calculated the CO_2 payback time (CPT) from the point when the conventional ASHP regional heating and cooling system is disposed of and replaced by a GSHP system. The CPT is calculated by the equation below:

$$\text{CPT} = \frac{\text{CO}_2 \text{ emisions during the intial construction phase}}{\text{annual CO}_2 \text{ emission reduction by the introduction of new systems}} \tag{2.25}$$

- Unlike ASHP, the GSHP system does not emit waste heat into the air. Instead, GSHP sequesters the heat underground that would have been released into the ambient air of the city by ASHP. Therefore, it does not propagate the Urban heat Island (UHI) phenomenon. UHI is a metropolitan area which is significantly warmer than its surrounding rural areas. Genchi (2002) estimated that full installation of GSHP in the central part of Tokyo may reduce the daily maximum atmospheric temperature in the summer by 1.2^{o}C.
- The heat released underground by GSHP in the summer could be retrieved for winter heat demand. Thus, it is expected that year-round energy consumption for climate control in the city would be reduced by the GSHP system.
- GSHP typically uses less refrigerant than ASHP. Also, GSHP are generally sealed when manufactured, therefore GSHP have reduced potential of contamination, when compared to ASHP, when refrigerant leaks on site (Phetteplace, 2007).

- **Durability**

GSHPs, unlike ASHPs, have few mechanical components and most of those components are underground, being isolated from the weather. Hence, they are considered more durable, are quieter to operate, and little maintenance is required (Kasuda and Archenbach, 1965).

- **Heat transfer through outdoor coil**

As water is far superior to air with regards to convecting heat through coil surfaces, the water coils in GSHP are smaller and much more efficient in transferring heat than in ASHP. Furthermore, although water is heavier than air, a given volume of water contains 3,500 times the thermal capacity of atmospheric air. Therefore, the pump motors circulating water through a GSHP system are much smaller than outdoor air fan motors of conventional ASHP systems. Therefore, the GSHP

system is more efficient than the ASHP system because its auxiliary power requirements are less compared to a conventional ASHP system.

Through the comparison between GSHP and ASHP, it can be seen that GSHP has several advantages over ASHP through the following aspects: higher efficiency, lower impact on environment, and hence better reliability.

Since GSHP systems are more efficient than ASHPs, they are chosen to be optimised in this study. However, problems in the design of GSHP systems will be highlighted in the following section.

2.7. Summary and Conclusion

The GSHP system has high thermal performance and is thus recommended as a priority choice, especially for large buildings where the upfront cost is not a pressure for the owners. It is also recommended for local climate with large seasonal variations in temperature and with feasible soil or water conditions.

BHE models were surveyed in this chapter in order to understand the factors influencing efficiency. These models have been reviewed according to three categories: (1) analytical models, and (2) numerical models. All of the above models studied the heat transfer rate from the BHE to the surrounding soil (or vice versa).

The analytical models were developed by making a number of simplifying assumptions which were then applied to both the design of the BHEs and an analysis of in situ test data. One of the most common assumptions is ignoring the geometry and thermal capacity of the components in the borehole.

For example, the line source method is based on classical theory, and the ground heat exchanger can be modelled as a line heat source in an infinite medium (Carslaw and Jaeger, 1947; Ingersoll, 1954). In addition, this method assumes that

the rate of heat input to the water loop is constant. However, this is rarely the case since in the field the heater is usually powered by a portable generator.
In the cylinder source method, ground heat exchangers are modelled as a cylindrical, constant heat source in an infinite medium (Ingersoll et al., 1954).

Both Kelvin's theory and the cylindrical source model neglected the axial heat flow along the borehole depth, and thus are incompetent for analyzing the long-term operation of BHE systems (Yang et.al., 2010). The other common assumption is to consider the borehole to be infinitely long. The heat transfer below the BHEs, as a result, is considered. However, this assumption makes analytical models unsuitable for multi-annual simulations (Cenk Yavuztruk et. al., 1999).

Although analytical solutions require less computing effort, they are less suited to design and simulation tasks where one would like to take account of time varying heat transfer rates and the influence of surrounding boreholes on long timescales.

The main purpose of all of the analytical and numerical models is to calculate the heat flux and borehole thermal resistance value, i.e. the rate of heat transferred from the borehole to the surrounding soil (or vice versa). The resistance to this transfer is crucial when estimating GSHP efficiency.

In addition, sensible sizing to ground loop length is important, since the efficiency of vertical loops – defined by loop length and the amount of heat extracted from the soil – varies significantly depending on the rate at which the heat transfers through the soil to the loops. This rate is mainly controlled by total thermal resistance of the borehole wall and the ground. Therefore, the next chapter will thoroughly discuss the most influential factors on total thermal resistance faced by the borehole heat exchanger system.

Chapter 3: Factors Influencing The Total Thermal Resistance of GSHP Systems

3.0 Introduction

It is clear that thermal resistance has significant influence in sizing of the borehole heat exchanger system, and hence the installation cost. Adding both borehole and ground thermal resistances together will estimate the values of total thermal resistance affecting the BHE systems, as shown in the equation below (Incorpera and Dewitt, 2002; Sagia et. al., 2012).

$$R_{total} = R_b + R_g \quad (3.1)$$

where R_{total} is the total thermal resistance (K.m/W), R_b is the borehole thermal resistance (K.m/W), and R_g is the ground thermal resistance (K.m/W).

According to Kavanaugh (2010), typical completed borehole heat exchanger system of 20 to 25 mm in diameter, the borehole thermal resistance ranges from 15% to 25% of the total resistance at design conditions. The remainder of the resistance is attributed to the ground.

Both borehole and ground thermal resistances affect the thermal efficiency of the heat pump system. Therefore, this chapter will discuss the factors affecting both ground and borehole thermal resistance values.

3.1. Ground Thermal Resistance

In order to calculate the total ground thermal resistance value, investigations of the geological and hydrological conditions of soils' subsurface layers are crucial. Soil geological conditions include properties such as soil thermal conductivity, soil diffusivity, and soil volumetric heat capacity. The higher the ground thermal conductivity the higher heat transferred per unit of piping. In turn, this will reduce the installation costs due to shorter U-tubes being required. Intemann et. al., 1982

Heat transfer by conduction is the flow of thermal energy within solids and non-flowing fluids, which are driven by thermal non-equilibrium (i.e. the effect of a non-uniform temperature field), as illustrated in Figure 3.1, commonly measured as a heat flux (vector), i.e. the heat flow per unit time (and usually a unit's normal area) at the control surface (Intemann et. al., 1982).

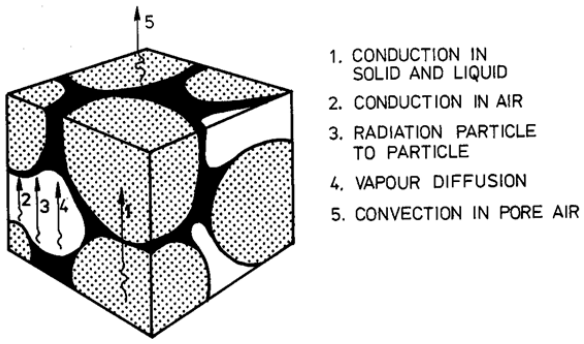

Figure 3.1 Different mechanisms that can contribute to heat transport in moist soil material (Johansen, 1975).

The lack of heat conductivity in soils may require, according to Intemann et al. (1982), an increase in the collector loops of up to 50% when compared to highly conductive soil. This is because the fluid in the pipes needs to be in contact with the ground for longer periods. Therefore, the soil thermal impacts the proposed sizing of the total system. Table 3.1 shows some examples of thermal conductivity and the required borehole depth for a vertical closed loop system for typical houses.

Table 3.1: Soil conductivity and the corresponding amount of piping required (Intemann et. al., 1982).

Soil Thermal Conductivity (W/k.m)	**Depth of the U-tube (m)**
0.952	60.55
1.212	57.3
1.471	56.9
2.336	54.86

3.1.1. Soil Thermal Properties

The thermal properties of the soil including soil thermal conductivity and heat capacity, are the primary parameters to affect the transfer of heat energy through soil layers. In the case of a borehole heat exchanger, these properties will vary according to the depth; therefore, in the design effective or average thermal properties over the length of the borehole are generally obtained.

The value of heat capacity (C_p) (J/Kg K), thermal conductivity (λ) (W/K.m), and soil density (ρ) (Kg/m^3) determine the soil's thermal diffusivity (α) (the rate at which the heat is conductive thorough a medium) (m^2/s) as follows:

$$\alpha = \frac{\lambda}{C_p . \rho} \tag{3.2}$$

Values of thermal diffusivity commonly range between 0.005×10^{-4} and 0.02×10^{-4} m^2/s. Experiments carried out on porous materials by Johansen (1975) show that the diffusion rates are strongly reduced as porosity decreases in dry materials.

Soil consists of three phases: air phase, water phase, and solid phase. Soil thermal conductivity is largely dependent on the volume fraction and the thermal conductivity of each phase. Hence, the proportion of each phase is an important factor in determining the thermal conductivity of the overall system. The thermal conductivity of different soil classes are presented in Table 3.2 (Johansen, 1975; Intemann et al., 1982).

Below the water table's ground layers is a two-phase system of water and solid. Above the water table, in the unsaturated zone, the subsurface consists of a three-phase system of air, water, and solid materials with large temperature variations of relative proportions of air and water. The relative proportions of air and water above the water table vary continuously due to the process of rain infiltration, evaporation, and transport by the planet. As a result, the thermal properties of each phase above the water table vary continuously(Intemann et al., 1982).

Table 3.2: Thermal properties for common types of soils have been well documented and here are some examples (British Geological Survey, 2011).

Class	Thermal Conductivity W m^{-1} K^{-1}
Sand (gravel)	0.77
Silt	1.67
Clay	1.11
Loam	0.91
Saturated sand	2.50
Saturated silt or clay	1.67

Since thermal conductivity λ (W/m K) is defined as the capacity of the material to conduct or transmit heat, it is significantly influenced by moisture content and dry density. Moisture content describes the amount of water contained in a soil, while dry density refers to the mass of soil particles per unit volume. An increase in either the moisture or dry density of a soil will result in an increase in its thermal conductivity. Other factors that have a secondary effect on soil thermal conductivity include soil temperature, texture, and air volume (Kersten, 1949; Salomone et al., 1984; Brandon and Mitchell, 1989; Mitchell, 1991; Becker et al., 1992; Ochsner, et.al., 2001).

It is also crucial to evaluate soil heat capacity c (J/kg K), as this demonstrates the amount of energy stored in the material per unit mass and per unit change in temperature; the greater its heat capacity, the more heat can be obtained (or lost) per unit rise (or fall) in temperature (Rees et al., 2000). The heat capacity of soil is the sum of the heat capacities of the soil components. This measurement is very important for GSHP system feasibility because the more heat that can be stored, the more heat can be released.

The primary focus of the next few sections is to clarify the impact of different influential variables mainly on soil thermal conductivity; these variables are: dry density, moisture content soil texture, air volume, and soil temperature.

3.1.1.1 Moisture Content

One important factor to be considered is the extent to which the voids (or pore spaces) are filled with water. Moisture content is defined as the weight of water expressed as a percentage of the dry weight of a given soil volume, while the degree of saturation is defined as the volume of water expressed as a percentage of the volume of voids. The moisture content changes depending on both climate and type of subsurface materials at a particular location (Lawrence, 1979).

Heat transfer in moist soils occurs as a result of vapour diffusion. Water vapour molecules diffuse from warm regions, where evaporation occurs to cold regions and where condensation occurs as a result of a vapour pressure gradient caused by temperature differences. For partially saturated soils, the effect of water vapour diffusion at a higher temperature contributes to increasing the thermal conductivity of air (Sepaskhah et. al., 1979).

There are three stages at which thermal conductivity of a soil increases depending upon the moisture content. These stages are (Smith, 1939; Nakshabandi et. al., 1965):

- At low moisture content water will first coat the soil particles. The amount of water required to create the coating depends on the specific surface area of the particles, which is a function of particle size and shape. The clay particles, for example, have a much larger specific surface than the sand particles, and therefore require more water to produce a film of given thickness. At this stage the gaps between the soil particles are not filled rapidly, and thus there is a slow increase in thermal conductivity.

- When the particles are fully coated with moisture, any further increase in the moisture content fills the voids between particles and leads to an increase in the contact areas between particles (as shown in Figure 3.5). Thus, heat flow between particles will increase and result in a rapid increase in thermal conductivity. At this stage, any further increase of the moisture content will no longer increase the heat flow; therefore, thermal

conductivity does not significantly increase. At this point, the moisture content is called optimum moisture content (OMC) (Salomone et al., 1984).

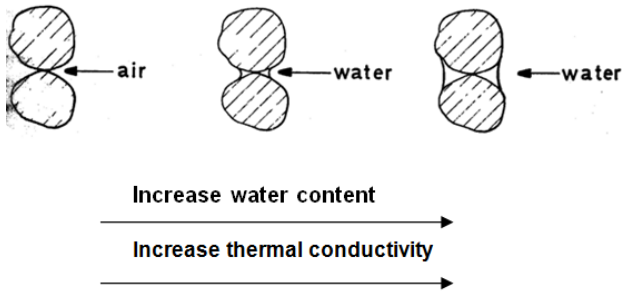

Figure 3.2: Formation of water at particles contact.

Therefore, the greatest increase in thermal resistivity (the inverse of thermal conductivity) is found from dryness to about 10 per cent of the volume of voids saturated, and there is very little change above 30 % (as can see in Figure 3.3; Lawrence, 1979).

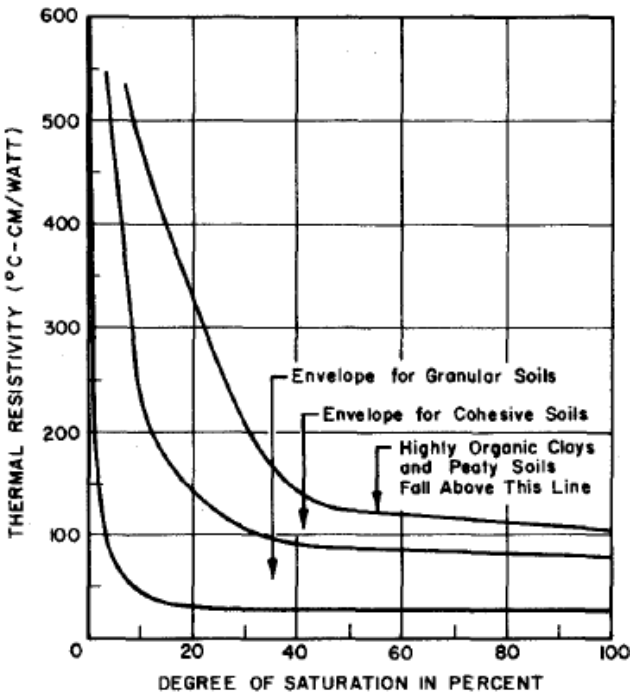

Figure 3.3: Thermal resistivity test data showing the effect of degree of saturation (Johansen, 1975).

As can be seen from Figure 3.4, water content in the sandy soil has the highest thermal conductivity among other moisture contented soils (such as clay, litter loam, and salty sand). Sandy soils are less porous than clay soils, which means they tend to have higher thermal conductivity; and organic soils are often extremely porous. Since the thermal conductivity of water is more than twenty times that of air, thermal conductivity of the soil increases greatly with an increase in the soil's water content. Similarly, the heat capacity of water is 3,500 times that of air and the heat capacity of soil increases with water content.

Therefore, the existence of moisture may impact the design process and lead to artificially increasing the soil thermal conductivities from in situ. This may lead for the borehole depth to be over- or under-sized, and conductivity values may be over- or under-designed too.

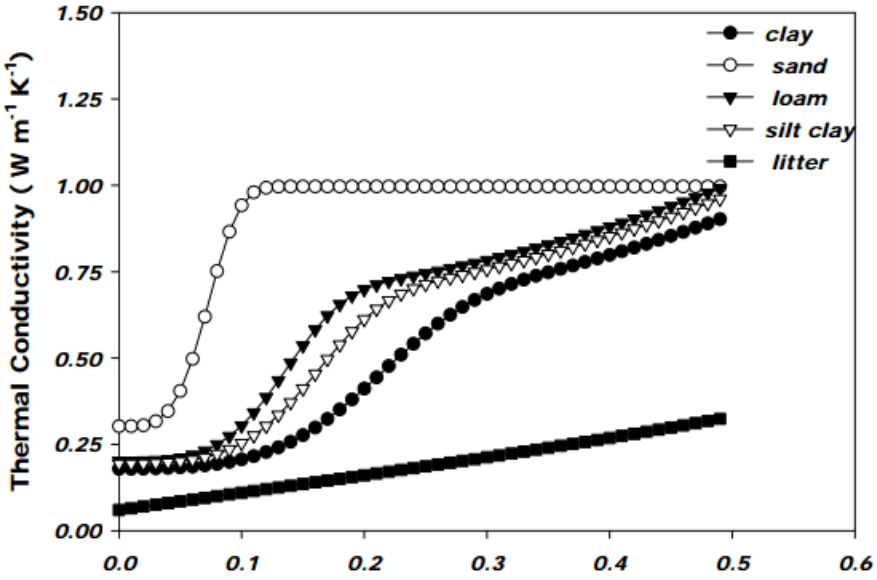

Figure 3.4: Thermal conductivity as a function of soil texture and moisture.

(Source: Lecture of Nature Resources of California University, Berkeley, 2013)

3.1.1.2. Dry Density

Dry density refers to a mass of soil particles per unit volume and an increase in dry density will result in an increase in thermal conductivity. Morinl and Silva (1984) concluded that the thermal conductivity of soil increases as soil porosity decreases (dry density increases).

The experimental results conducted on saturated Illite specimens, as shown in Figure 3.5, indicate that the thermal conductivity of soil tends to increase with a decrease in porosity. They attributed this behaviour to the thermal evolution of thermal conductivity of the air being much less than soil particles.

The density of a soil exerts one of the most important influences on the thermal resistivity of soil. Not only may the density of soils be changed by artificial means, such as compaction or disturbance of in situ soils, but also through natural factors such as consolidation, shrinkage or swelling. In the case of the greatest amount of soil material per unit volume, the least resistivity is achieved ,as demonstrated in Figure 3.6. Lawrence, 1979

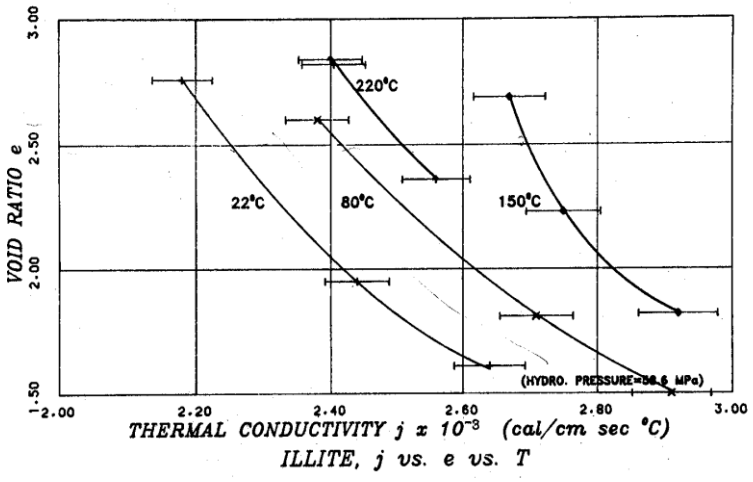

Figure 3.5: Thermal conductivity versus void ratio at four temperature intervals for undisturbed illitic clay (Morinl and Silva, 1984).

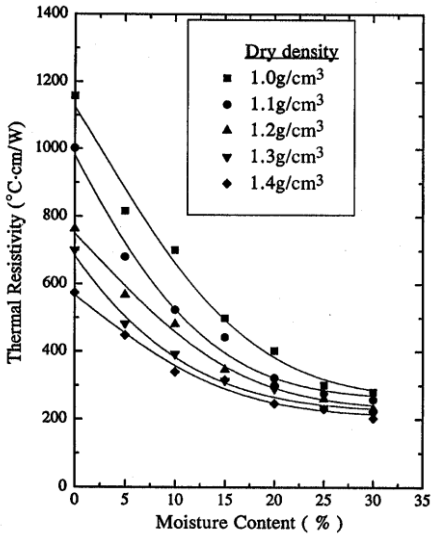

Figure 3.6: Thermal resistivity vs. moisture content for black cotton soil at different dry densities (Rao and Singh, 1999).

3.1.1.3. Temperature Level

The soil temperature level during the operating of BHE is an important consideration because it establishes the thermal gradient with adjacent soil once the moisture content has fallen below the field capacity. In addition, moisture migration is controlled by magnitude of temperature gradient. Also, the thermal conductivity of each individual soil constituent may depend on temperature (Sepaskhah et al., 1979).

Sepaskhah and Boersma (1979) studied the thermal conductivity of soils as a function of temperature and water content. They concluded that, at low saturation levels as soil temperature increases, thermal conductivity increased due to the more contribution of vapour diffusion to thermal conductivity of air at high temperatures. However, as the degree of saturation increased, the effect of temperature decreased (Johansen, 1975).

Also, measurement of thermal conductivity was carried out by Birch and Clarkes (1940), who, for a number of rock materials over the temperature range 0 to 400^{o}C, showed that the conductivity in most materials decreases

with an increase in temperature (as demonstrated in Table 3.3). Sepaskhah et al., 1979; Johansen,1975.

In Table (3.3), it is clear that the thermal conductivity of air increases with an increase in temperature, unlike granite soil where the conductivity decreases with an increase in temperature.

Similarly, Kersten (1949) concluded a 4% decrease in resistivity for a 17°C increase in temperature and about a 10 % decrease in resistivity for an increase in temperature ranging 20°C to 60°C. This change is a function of the moisture content and temperature (Johansen, 1975).

Table 3.3: Conductivity for air and granite at different temperatures W/m k. (Johansen, 1975).

Temperature °C	-30	0	30	100	150	200
Air	0.004	0.0241	0.0277	0.0310	0.0339	0.0367
Granite	3.91	3.65	3.37	3.11	2.94	2.79

The temperature of the soil near the surface is influenced more by changes in the air temperature than the ground temperature below ten metres. Therefore, soil deeper than ten metres will store more useful thermal energy for the GSHP. This means that the soil temperature should be defined by the mean annual ground temperature and is dependent on its geographic location. For this reason, installing deep boreholes will help to reduce the required exchange length by 30 to 50 % over burying shallow heat exchangers. Nevertheless, the dilemma with the intensive initial cost should be overcome (Mori, 2010).

3.1.1.4. Air Volume

Ochsner et al. (2001) reveal the dominant influence of air volume on the thermal conductivity of soil. Based on the test results of 59 soil specimens of four different soils at different ranges of porosities, volume fractions of water, and volume fractions of air, they found that thermal conductivity is more strongly correlated

with the volume fraction of air. They attributed to the fact of the thermal conductivity of air is one order of magnitude less than the thermal conductivity of water and two orders of magnitude less than the thermal conductivity of soil.

3.1.2 Hydrological Conditions

Some theoretical studies have been published to evaluate the effect of underground water flow (Eskilson, 1987; Claesson & Hellstom, 2000; Chiasson et al., 2000). These studies introduce models for the impact of regional ground water flow based on the assumption that natural groundwater movement is reasonably homogeneously spread over ground volume. This applies well on homogeneously and porous ground material. Eskilson, Claesson and Hellstrom used line source theory to model the influence of groundwater on a single vertical borehole. They concluded that under normal conditions the impact of regional groundwater flow is negligible. Chiasson et al. (2000) used a 2D finite element groundwater flow and mass/heat transport model. It was concluded that geologic materials with high hydraulic conductivity (e.g. sand and gravel) and rocks with secondary porosities, could have a significant impact on borehole performance (Signhild Gehlin, 2002).

For sandy materials the effect of ground water flow is slight, except in the case of very coarse sands where the dispersion effects may increase conductivity by up to 20 % (Johansen, 1975).

3.2. Predicting Ground Thermal Conductivity

Heat flow in saturated soil varies with thermal conductivities, volumetric proportions of constituents, shape, size, and structural arrangement of the soil particles. Many researches have been directed to predict the thermal conductivity of soils (e.g. Kersten, 1949; De Vries, 1963; McGaw, 1969; Morinl and Silva, 1984; Gemant, 1950; Webb, 1956; Woodside, 1958; Jackson and Kiham, 1958; Moench and Evens, 1970; Rao and Singh, 1999; Tarnawski et al., 2002). The basic equation for prediction of the thermal conductivity of saturated soils, λ_T, was formulated based on the geometric mean approach, as follows:

$$\lambda_T = \lambda_s^{(1-n)} \lambda_w^{n} \quad (3.3)$$

where λ_T, λ_s, and λ_w are the thermal conductivity of the soil, solid soil particles and water, respectively, and n is the soil porosity. Sass et al. (1971) show that when the thermal conductivities of the soil constituents do not contrast by more than one order of the magnitude, the geometric mean method provides satisfactory results. In fact, the solutions for the soil's thermal conductivity prediction have tended to fall into two main categories: empirical equation and theoretical equation, depending on Ohm's Law. However, it should be mentioned that the validity of the empirical predicting equations is always limited to certain conditions.

3.2.1 Empirical Equation

Morinl and Silva (1984), based on a laboratory test programme on four different saturated clay types, developed the following logarithmic relationship between the thermal conductivity of soil (λ_T) and the void ratio (e), taking into consideration the effect of soil temperature (T):

$$\text{Log } \lambda_T = \text{m (e) +b} \quad (3.4)$$

$$\text{m = a T +c} \quad (3.5)$$

where a, b, and c are constants and depend on soil mineralogy composition. Van Rooyen and Winterkorn's (1957) correlation, based upon data collected from sands and gravels, is given as follows:

$$\frac{1}{k} = A10^{-BS_r} + S \quad (3.7)$$

where k is the soil thermal conductivity, S_r is the degree of saturation, and A, B, and s_r are the functions of dry density, mineral type and granulometry, respectively.

The Van Rooyen-Winterkorn method is limited to sands and gravels with saturation levels between 1.5 and 10%. Johansen's (1975) correlation, which is based on thermal conductivity data for dry and saturated states at the same dry density, has the following form:

$$k = (K_{SAT} - K_D).K_e + K_D \quad (3.8)$$

where k is the soil thermal conductivity(W/K.m), k_{SAT} and k_D are soil thermal conductivity in the saturated and dry states, respectively, and k_e is the dimensionless function of soil saturation.

Johansen's method is suitable for calculating soil thermal conductivity of both coarse- and fine-grained soils in frozen and unfrozen states. However, it is limited to saturations greater than 20%.

The correlation given by De Vries (1952) assumes that soil is a two-phase material composed of uniform ellipsoidal particles dispersed in a fluid phase. The De Vries equation is given as:

$$K = \frac{x_f k_f + F x_s k_s}{x_f + F\, x_s} \tag{3.9}$$

where f and s are the fluid and solid phases, respectively, x is volume fraction, and k is the soil thermal conductivity.

The expression of thermal conductivity as a function of dry density can be expressed by the equation below (Misra et al., 1992):

$$k = k_a \left(10.68\, \frac{\rho_d}{\rho_s} - 4\right) (\ln \alpha^2 + b + wc - 3.9) \tag{3.10}$$

where K is the soil thermal conductivity (W/K.m), ρ_d is the soil dry density, ρ_s is the solid density, α is the soil diffusivity rate, wc is the water content, and b is the coefficient upon soils type.

3.2.2. Analytical Equations

3.2.2.1 Parallel Flow Equation

An equation derived originally by Maxwell and Lord Rayliegh for the calculation of the electrical conductivity (Ohm's Law) of porous materials. The procedure was then used by Cochran et al. (1967) (Sepaskhah and Boersma, 1979).

It is based on the parallel heat flow concept for each soil component and is weighted with the volumetric ratio of the soil components and the factor k, which expresses the ratio of the average temperature gradient in the particular soil component to the average temperature gradient in the continuous medium (soil water). The saturated soil thermal conductivity, λ_T, is estimated according to the following form:

$$\lambda_T = \frac{\theta_w \lambda_w + \sum_{i=1}^{n} k_i \, \theta_i \lambda_i}{\theta_w + \sum_{i=1}^{n} k_i \, \theta_i} \tag{3.11}$$

where θ is the volumetric fraction of the soil component, w is water, and n is number of individual types of soil solid components. Factor k is estimated in terms of the soil particles shape and the thermal conductivity of water and soil mineral constituents as follows:

$$k = \frac{1}{3} \sum_{x=1}^{3} [1 + g_x \, (\frac{\lambda_s}{\lambda_w} - 1)]^{-1} \tag{3.12}$$

$$\sum_{x=1}^{3} g_x = 1 \tag{3.13}$$

where g_x expresses the axial length of the ellipsoidal particles for spherical particles g_x=1/3, 1/3, 1/3. However, it should be mentioned that the empirical nature of factor k becomes clear when the prediction of the De Vries (1963) equation for saturated granular soils provides good agreement with the measured values for g_x= 1/8, 1/8, 6/8 (McGaw, 1969). In fact, the presumed particle, with a major axis six times the length of each minor axis, does not describe the actual soil particle shape of the tested soil. Therefore, the estimation of factor k, which has no physical meaning, considers the most limitation of this equation.

3.2.2.2. Series/Parallel Flow Equation

Tarnawski et al. (2000) introduced a model equation to predict the thermal conductivity of saturated soils in the framework of Gori's (1983) model. The model assumes a single cubic soil grain surrounded by water (as shown in Figure 3.7). The thermal conductivity of the soil has been estimated using the hypothesis of

parallel isothermal lines. Therefore, the thermal conductivity of the saturated soil was determined as follows (Tarnawski et al., 2000):

$$\frac{1}{\lambda_T} = \frac{\beta-1}{\lambda_w \beta} + \frac{\beta}{\lambda_w[\beta^2-1]+\lambda_2} \tag{3.14}$$

$$\beta = \frac{L_t}{L_s} = \sqrt[3]{\frac{1}{1-n}} = \sqrt[3]{\frac{G_s}{\gamma_d}} \tag{3.15}$$

where β is a geometric factor, G_s and γ_d are porosity, specific gravity and dry unit weight of the tested soil, respectively. However, the proposed model does not include the effect of the soil fabric.

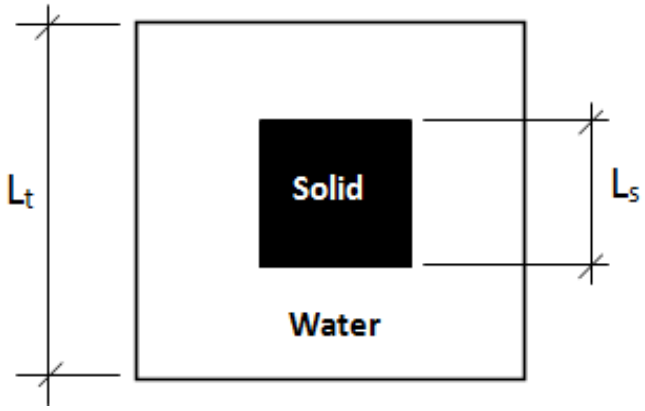

Figure 3.7: Conceptual thermal conductivity model of saturated soil (Tarnawski et al., 2002).

3.3. Borehole Thermal resistance

Many factors affect the borehole thermal resistance in the borehole heat exchanger. These include the pipe and borehole geometric properties, heat flow rate, backfill and grout properties, and soil properties.

3.3.1. Thermal Conductivity of the Back Filling Materials

Backfill materials play a significant part in the performance of the borehole loop heat exchanger system. This backfilling material is crucial for conducting heat when fluid goes down along the inlet pipe, and it resists heat when the fluid goes up along the outlet pipe. Therefore, when designing the borehole heat exchanger,

careful optimization of thermal resistivity for the grout is required to obtain an efficient geothermal system (Al-Khoury, 2012).

The grout material should be pumped and positioned between the U-loop and the ground material. Air gaps or separation between the ground and filling materials should be avoided as air is a natural insulator. If the grout does not efficiently conduct heat then it will be considered an insulator and will hence it will reduce the efficiency of the GHP system(Allan et al., 1998).

Grout material must contain readily available, environmentally safe, cost effective components, and it has to be easy to mixed and pumped with conventional geotechnical grouting equipment. In addition, the grout should have low shrinkage and good bonding characteristics to the U-loop and surrounding ground, as well as long-term durability (Allan et al., 1998).

In the past, Bentonite grouts were employed for GHP systems. Although Bentonite has good sealant properties, it has a relatively low thermal conductivity range between 0.65-0.90 W/m.K (Eckhart, 1991). Neat cement grout has also been used with some degree of success, but a high water to cementation materials (w/c) ratio often evolves pores in the grout, which may cause a significant decrease in thermal conductivity. Furthermore, neat cement grouts with high w/c ratios are prone to shrinkage and do not form a satisfactory bond with the U-loop (Allan et al., 1998).

However, it is possible to improve the thermal conductivity of Bentonite grouts by adding filler material, such as quartzite sand (Remund and Lund, 1993). Table 3.4 shows thermal conductivities for enhanced grouts, which can significantly amend the borehole thermal performance and lead to shallower boreholes (Allan et al., 1998).

3.3.2. Number of U-Tube Pipes In The Borehole

The borehole thermal resistance is quite large for single U-pipes, but usually decreases with a number pipes in the borehole. This is mainly due to the reduction in the grout resistance, and its being substituted by pipe and fluid resistance.

According to the study by Heya et al. (2003) on double and single U-pipe systems, the double U-tube boreholes are superior to those of the single U-tube with reduction in borehole resistance of 30 to 90 %.

Table 3.4: Typical thermal conductivity of backfill and grout materials(Allan et al. 1998).

Grout and Additives	**k_g (W/K.m)**	**Thermal Enhanced Grouts**	**k_g(W/K.m)**
20% Bentonite	0.726	**20% Bentonite-40% Quartzite**	1.47
30% Bentonite	0.744	**20% Bentonite-30% Quartzite**	1.211-1.29
Cement Mortar	0.69-0.78	**30% Bentonite-30% Iron Ore**	0.78

3.3.3.Borehole Geometric and Boundary Conditions

Based on all the equations discussed in the previous chapter, the borehole thermal resistance is actually a function of borehole diameter, U-tube pipe diameter, and shank spacing between the U-tube pipes.

In fact according to Lee et al. (2010), the value of borehole thermal resistance increase with increase of borehole diameter, and decease with increase of U-tube diameter. This is because increasing the borehole diameter leads to increase in the grout thermal resistance, which in turn leads to higher difference between the temperatures on borehole wall and the U-tube pipes, resulting in higher borehole thermal resistance.

According to Acuna (2010), the best U-pipe BHE configuration corresponds to when the pipes are completely apart from each other, where the borehole thermal resistance value will be at its lowest value. These factors will be discussed more in depth in the upcoming chapters.

3.4. Summary and Conclusion

The efficiency of the borehole heat pumps are greatly influenced by total thermal resistance of the system. The total thermal resistance of the GSHP system is the sum of both ground thermal resistance and borehole thermal resistance.

The thermal properties of the soil around the borehole closed loop system play a significant part in determining the value of the ground resistance and ground thermal resistance. The soil thermal properties are thermal conductivity, heat capacity, and thermal diffusivity.

Soil thermal conductivity is significantly influenced by saturation and dry density. An increase in either the saturation or dry density of soil will result in an increase in its thermal conductivity. The higher the thermal conductivity of the soil, the less ground resistance and more heat is transferred per unit of piping. This would reduce installation costs due to shorter U-tubes being required. Therefore, soil thermal properties influences the sizing of the total system.

In addition to geological conditions, hydrological conditions should also be considered for their influence on soil thermal conductivity. Underground water movement can have a significant impact on the heat transfer mechanism in soil, which can greatly influence the design and performance of the GSHP system. It may impact the design process, where thermal conductivities derived from in situ tests may appear artificially high. Therefore, GSHPs may be over- or under-designed .

Over sizing the heat pump system is not only influenced by the ground thermal resistance, but also by borehole thermal resistance. BHE resistance is affected many factors including the pipe and borehole geometric properties, heat flow rate, backfill and grout properties, and soil properties. The borehole thermal resistance is targeted in this thesis to optimise the system through the use of numerical analysis. Therefore, research methodology will be discussed in the following chapter.

Chapter 4: Research Methodology

4.0. Introduction

The main aim of this research is to evaluate the value of borehole thermal resistance for U-tube borehole model and propos different methods to decrease it, numerical approach will be used for this purpose.

In order to simulate the borehole heat exchanger and the surrounding ground, identification of the boundary and geometry conditions is required as a first step in the determination of the borehole resistance value. This will be followed by selection of the suitable software program to conduct the numerical simulations. Finally validation case to the numerical borehole thermal resistance values will to be conducted.

4.1. Heat Flow Theory

Heat flow by conduction is governed by Fourier's Law. Fourier's Law in differential form is as follows

$$q = -\lambda \nabla T \tag{4.1}$$

Fourier's Law states that the heat flux density(q) is proportional to the thermal conductivity (λ), and is the temperature gradient ∇T. The general partial differential equation for the for unsteady state energy balance to the differential equation is:

$$\frac{\partial}{\partial_x}\left(\lambda_x \frac{\partial T}{\partial x}\right) + \frac{\partial}{\partial_y}\left(\lambda_y \frac{\partial T}{\partial y}\right) + \left(\lambda_z \frac{\partial T}{\partial z}\right) = C\rho \frac{\partial T}{\partial t} \tag{4.2}$$

where λ_x ,λ_y ,and λ_z are the thermal conductivities of the soil in x , y, and z direction. Considering Cartesian's x-y coordinate system, the governing energy for steady state can be written as:

$$\frac{\partial^2 T}{\partial x^2} + \frac{\partial^2 T}{\partial y^2} = 0 \tag{4.3}$$

Therefore, equation (4.3) will be utilized to calculate the heat flux in the geothermal heat exchanger system. However, in order to conduct the simulation to the heat exchanger system, boundary and geometrical conditions are required. These conditions will be clarified in the following section.

4.2. Boundary and Geometry Conditions

The system being modelled consists of a borehole that has a diameter of (d_b) which is roughly between the common range of the borehole diameters 0.1-0.2 m (reported by Banks ,2008; and Sagia et al., 2012).

The borehole has two eccentric pipes each with an outside diameter (d_p) ranging between 0.03-0.07mm, separated by distance called shank spacing(s). Shank spacing refers to the centre to centre U-pipe distance.

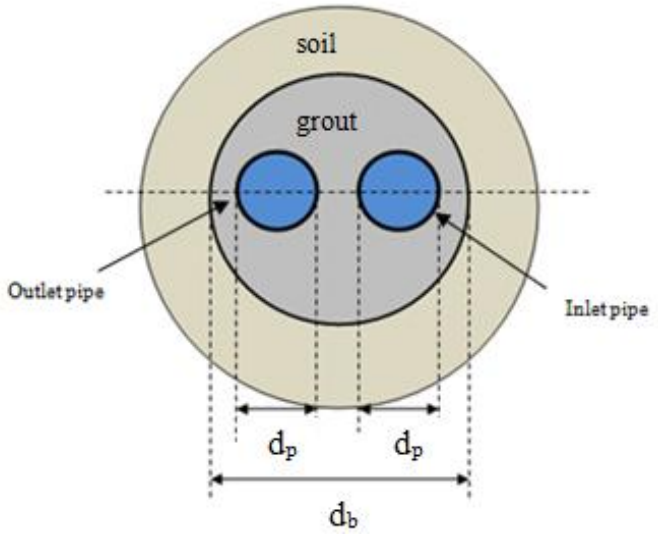

Figure 4.1: Cross section of the borehole heat exchanger system.

In order to carry out a numerical simulation to the borehole geometry, the following assumptions are made(Sagia et al., 2012):

1. The temperature of the ground is assumed to be constant (i.e. undisturbed ground temperature).
2. The material inside the borehole is treated as being homogeneous and all the thermal properties are independent of the temperature.
3. Steady state simulation is assumed to simulate the borehole with a single U-tube legs, for the following reasons(Sagia et al., 2012):
    a) The ability to store heat in the borehole is relatively small compared to the surrounding ground.
    b) The temperature variations within the borehole are usually minor and slow.
    c) The capacitance of the borehole is relatively small compared to the surrounding ground.
4. As the steady-state heat flow was assumed within homogeneous geologic material, it was only necessary to use a two-dimensional model.

The temperatures of upward and downward flow are in the heating mode, and have been chosen according to Kavanaugh and Raftty (1997). They implied that if the heat carrier fluid is streaming in heating mode through BHE, the temperature should typically be between 5˚C and 11˚C. Therefore, the temperatures of the inlet and outlet pipes was chosen to be 7 ºC and 9ºC respectively. All the parameters used in the 2D model simulations are presented in Table 4.1.

In order to simulate the ground surrounding the borehole heat exchanger, far field radius value is required. However, the question is whether the assumed far field radius of the soil in the numerical simulation will influence the numerically determined borehole resistance value? Finite element methods will be utilized to assess the influence of the far filed radius.

Table 4.1: Details of the sectional and thermal properties for the borehole system.

Parameter and Symbol	Value
Infinite ground	
Thermal conductivity Ks	1W/K..m
Grout	
Thermal conductivity K_g	1-4 W/K.m
Grout radius	0.05-0.1 m
U-tube pipe	
Thermal conductivity K_p	0.5W/K.m
Thickness of the pipe	0.0026-0.003m
Outlet pipe radius	0.015 m
Distance between two centre points of the pipes	0.0675-0.03 m
Operational conditions	
Undisturbed ground temperature T_o	12 ˚C
Temperature of upward flow in heating mode	9 ˚C
Temperature of downward flow in heating mode	7˚C

Note: some of the boundary conditions given in the above table might be changed in order to fit with investigation purposes.

4.3.Finite Element Analysis(FEA)

The development of the finite element method, has enabled engineers to solve extremely complex physical phenomena for a variety of boundary conditions and material properties.

Finite Element Analysis (FEA) is a numerical approach in which the domain under study is divided into a multitude of regions, each giving rise to one or more equations. (Mori, 2010).

It would be impossible to describe what is concretely involved in FEA calculations without referring to an existing software package. These programs could range from discipline specific products, such as the Geo-Slope software, to general partial differential equation solvers such as Flex PDE programs. The advantage of the latter is in their flexibility offered to researchers, allowing the modelling of a wide range of problems. Therefore ,Flex PDE software package will be utilised to simulate BHE models in this research.

4.3.1. Flex PDE Software Program

Flex PDE (PDE Solutions Inc., 1999) is one of many attractive applications of the Finite Element Methods for providing a framework for treating partial differential equation in general. In addition, Flex PDE provide a straight forward method in defining the domains and boundary conditions appropriate for wide range of application.

Major features of Flex PDE include(PDE Solutions Inc., 1999):

1. Capability to solve linear and non-linear partial differential equations of second order or less.
2. Represents static boundary values and time dependent initial/boundary value.
3. Adaptive grid refinement, eliminating the need for manually determining an appropriate mesh.
4. Can solve steady-state or time-dependent problems.
5. Any number of regions of different material properties may be defined.

In the case of borehole heat exchanger simulation, this program permits to change the following inputs: flow rate, properties of the ground, grout, and temperatures of the ground inlet and outlet fluid. From this description the program will create a finite element solution process tailored to the problem within quite broad limits(PDE Solutions Inc., 1999).

The problem description scrip in Flex PDE is presented in a readable text file. The contents of the file consist of a number of sections with each identified by a unique header. The most frequently used sections are as follows (PDE Solutions Inc., 1999):

TITLE – a descriptive label for the output.
SELECT – user controls over the default behaviour of Flex PDE.
VARIABLES – here the dependent variables are named.
DEFINITIONS – useful parameters, relationships or functions are defined.
EQUATIONS – each variable is associated with a partial differential equation.
INITIALVALUES – starting values for nonlinear or time-dependent problems.
BOUNDARIES – the geometry is described by walking the perimeter of the domain, stringing together line or arc segments to bound the figure.
PLOTS – the desired graphical output is listed. Plots may be any combination of CONTOUR, SURFACE, ELEVATION or VECTOR plots.

A sample of the numerical simulation, can be seen in Appendix B, created for this study to simulate a borehole with a single U-shape pipe. The borehole and U-tube diameters are assumed to be 0.1m and 0.03m, respectively. The borehole is assumed to be filled with grout that has 2 W/K.m thermal conductivity and surrounded by soil that has 1 W/K.m thermal conductivity.

Finite element meshes for a single borehole geometry and for a complete borehole field geometry in the sample case, have been constructed using triangular elements as shown in Figure 4.2. Nodal spacing was kept relatively fine around the borehole walls where the steepest temperature gradients were expected.

Borehole thermal resistance will be identified after calculating the rate at which heat transfer occurs inside the borehole, using numerical integration. Then the

borehole thermal resistance can be estimated using the equations given by Eskilson et al. (1988) and Sharaqawy et al. (2009):

$$R_b = \frac{T_{P1} - T_B}{q_{P1,B}} = R_b = \frac{T_{P2} - T_B}{q_{P2,B}} \quad (4.4)$$

where R_b is the borehole thermal resistance,$T_{p1,p2}$ is the inlet and outlet pipe temperature , T_b is the temperature on the borehole wall, q_B is determined using Fourier's Law of conduction. q_B as stated by Sharaqawy et al., (2009), is determined by:

$$q_B = q_{p1} + q_{p2} \quad (4.5)$$

where q_{p1} is the heat flow from the inlet pipe, q_{p2} is the heat flow from the put let pipe. It should be noted that the heat fluxes from the inlet and outlet pipes are calculated numerically by integrating the area of the two pipes as in Eqs. (4.6a, 4.6b). Hence, equation 4.5 can be used to check the accuracy of the numerical solutions. The variation between the two computed values of q_B should not exceed 10^{-8} W/m to assure grid independency and numerical solution convergence.

q_{inlet}= line_INTEGRAL(normal(-grad(temp)*k), 'inlet') (4.6a)

q_{outlet}= line_INTEGRAL(normal(-grad(temp)*k), 'outlet') (4.6b)

where q_{inlet} is the inlet heat flux, q_{outlet}, Temp is the initial value of undisturbed temperature, and k is the soil thermal conductivity.

Next section will utilise the Flex PDE program to assess the influence of the far filed radius on the value of borehole thermal resistance.

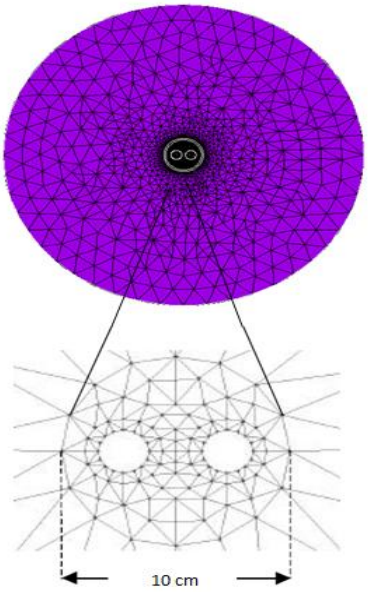

Figure 4.2: Finite element mesh representing a single borehole.

4.4. The Effect of The Far Field Radius on Borehole Resistance Value

This section is dedicated to investigate whether the assumed soil diameter(far field diameter) around the borehole could influence the calculated borehole thermal resistance, when the grout to soil thermal conductivity (k_g/k_s) ranged from 1 to 3. The case is constructed to simulate a borehole with a single U-shape pipe. The borehole and U-tube diameters are assumed to be 0.1m and 0.03m, respectively

The following Tables 4.2,4.3,an 4.4, present the values of the borehole resistance when 50mm shank separated the U-tube legs , and the far field radius ranging between 1m and 4m.

As it can be seen from Tables 4.2,4.3, and 4.4, that the percentage of errors in the values of the borehole resistance are very small for all ratios of k_g/k_s and far field radiuses employed. Therefore, the far field radius does not greatly influence the borehole resistance value. Hence, all the analyses in the upcoming investigations the soil diameter will be taken to be 1.0 m. Validation to the calculation of BHE

resistance using 2D model numerical model is going to be presented in the next section by reference to analytical models.

Table 4.2: Borehole thermal resistance values as a function of far field radius when $k_g/k_s = 1$.

Percentage of Difference		
Far Field Radius	Borehole Thermal(K.m./W)	Error%
1	0.0896	-
2	0.0897	0.115
3	0.0898	0.22
4	0.0898	0.22

Table 4.3: Borehole thermal resistance values as a function of far field radius when $k_g/k_s = 2$.

Percentage of Difference		
Far Field Radius	Borehole Thermal(K.m./W)	Error%
1	0.0464	-
2	0.0465	0.21
3	0.0466	0.43
4	0.0467	0.64

Table 4.4: Borehole thermal resistance values as a function of far field radius when $k_g/k_s = 3$.

Percentage of Difference		
Far Field Radius	Borehole Thermal(K.m./W)	Error%
1	0.0316	-
2	0.0317	0.32
3	0.0317	0.32
4	0.0318	0.63

4.5. Validation to The Numerical Values of Borehole Thermal Resistance

In order to validate the numerical BHE thermal resistance, two cases were solved and compared against known analytical solutions. In both cases, the thermal resistances were calculated by dividing the temperature difference between the pipe and the borehole wall by the rate of heat transfer, obtained by numerically integrating Fourier's Law over the pipe and borehole surfaces.

The first case is a single pipe concentric with the borehole, where the thermal resistance between the pipe and borehole, given by Incropera and Dewitt (2002), is:

$$R_b = \frac{ln\left(d_b/d_p\right)}{2\,\pi k_g} \tag{4.7}$$

where d_b is the borehole diameter (m), d_p is the pipe diameter (m), and k_g is the thermal conductivity of the grout material (W/K.m).

While the second case is a single pipe offset from the axis of the borehole, where the analytical solution for the thermal resistance between the pipe and borehole is given in Kerith (1980) as:

$$R_b = \frac{1}{2\pi k_g} cosh^{-1}\left(\frac{d_b^2+d_p^2-s^2}{2d_b d_p}\right) \tag{4.8}$$

Where d_b is the borehole diameter (m), d_p is the pipe diameter (m), k_g is the thermal conductivity of the grout material (W/K.m), and s is shank spacing (m).

The Flex PDE program is used to simulate the two cases above in order to find the numerical BHE resistance values. Figure 4.3 shows the isotherms corresponding to the concentric and eccentric cases.

The PDE solver Flex PDE has been verified against well-established analytical solutions for problems of conductive heat transfer. Comparisons between analytical expressions (Eqs. (4.7) and (4.8)), and numerical resistance, show close

agreement. These results in Table 4.5 not only show that Flex PDE behaves functionally the same as an analytical equation, but that the two-dimensional models run in Flex PDE appear to provide correct results in determining the borehole resistance.

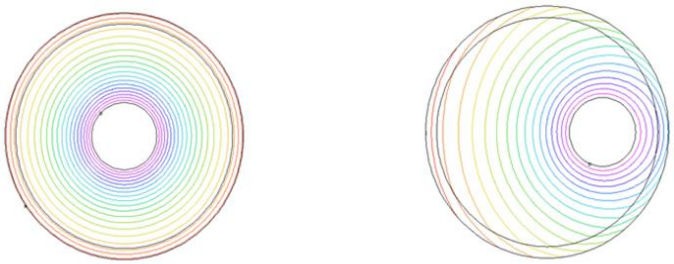

(a) (b)

Figure 4.3: Distribution of temperatures (in ◦C) within a borehole having a concentric pipe (a) and an eccentric pipe (b).

Table 4.5: Comparison of numerical and analytical results for the limiting cases studied.

	Concentric Pipe	Eccentric Pipe
Borehole diameter (d_b)(m)	0.1	0.1
Pipe diameter (d_p) (m)	0.03	0.03
Shank spacing (s) (m)	0	0.025
Thermal conductivity of the grout (k_g) (W/m.k.)	2	2
Heat transfer rate per unit length, q (W/m)	8.6	10.8
$2\pi\ k_g\ R_b$: numerical solutions	1.209	1.14
$2\pi\ k_g\ R_b$: analytical (Eq. 4.7 and 4.8).	1.204	1.132

4.5. Summary and Conclusion

It is clear from this chapter that Flex PDE software program provide sufficient result when calculating the values of borehole thermal resistance using 2D steady state simulations.

However, it is long process and time consuming to simulate each application in real life to calculate the borehole resistance. For this reason, there are few analytical equation presented by researchers to find the values of borehole resistance some of which are based on numerical analysis and others based on analytical theories.

Therefore , in order to investigate the accuracy of these equation , next chapter will provide extensive review to the analytical and semi analytical equation by comparing them to numerical BHE resistance.

Chapter 5: Numerical Assessment For Borehole Thermal Resistance.

5.0 Introduction

The accurate evaluation of the borehole thermal resistance is of a great importance for the design of the U-shaped BHE system. High resistance will result in a larger temperature difference between the borehole wall and the circulating fluid. This decreases the efficiency of the pump compared to lower resistance (Gustafsson et al., 2010). Although There are different methods to evaluate BHE resistance, there is no definite recommendation regarding their validity.

Therefore, in order to assess the validity these equations, 2D steady state numerical simulation using Flex PDE will be conducted. In another word, the assessment will be based on comparing numerical values of BHE resistance to resistance of methods in the literature.

5.1.Problem Configuration

The system being modelled consists of a borehole that has a diameter of 100mm. The borehole has two eccentric pipes each with an outside diameter (d_p) of 30 mm, separated by distance called shank spacing(s). Shank spacing refers to the centre to centre U-pipe distance.

The investigation will be conducted mainly on three geometric configurations: close together, average pipe, and along the outer wall, with shank spacing of 30mm,50mm,67.5mm shank spacings, respectively as shown in Figure 5.1. In addition, all the numerical simulation are function of the ratio of k_g/k_s that ranges between 1 to 4, where k_s is 1 W/K.m.

The difference between the borehole resistance calculated numerically,R_b^N, and those based on the available equations discussed in the literature, R_b^a, will be explained as ΔR^b, as follows

$$\Delta R^b = \frac{R_b^N - R_b^a}{R_b^N} \times 100 \quad (5.1)$$

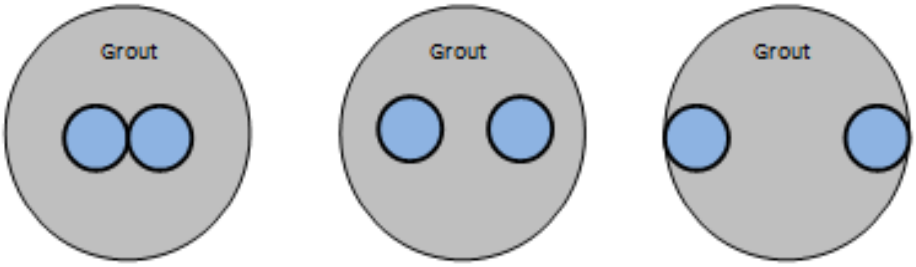

Figure 5.1: Pipe configurations. The inner circle corresponds to the two legs of the U-tube installed in the borehole (from left to right: close together configuration, average configuration, and along the outer wall configuration).

Number of equations will be assessed in this chapter numerically, including: Paul (1996) ,(Bennet et al., (1987); Hellstrom ,(1991); Gu and O' Neal, (1998); Shonder and beck ,(1999); and Sharqawy et al., (2009).

5.2.Paul (1996)

It is expensive to run in situ experiments on every borehole heat exchanger application to determine R_b, as they require a lots of equipment and software program for parameter identification. Therefore, laboratory experiments are sometimes considered as an alternative to calculate the value of borehole thermal resistance. A known equation based on laboratory experiment data was introduced by Paul (1996).

The test apparatus employed a single thick layer coil of wire wrapped around each side of the U-tube to form an electrical resistance heater. This provided a uniform, constant flux heat input for the system; however, a real borehole will not have uniform flux at the pipe wall. Heat was input until steady-state temperature conditions were reached at the borehole wall radius and along the circumference of the U-tube. The borehole resistance was then calculated from the temperatures and the flux (Thomas, 2001).

Paul(1996) equation measured the BHE thermal resistance of a single U-tube borehole for the three main configurations illustrated in Figure 5.1.The result of the best fit power correlation of the experimental data for the three configurations is as follow:

$$R_b = \frac{1}{\beta_o \left[\frac{d_b}{d_p}\right]^{\beta_i} k_g} \quad (5.2)$$

where d_b is borehole diameter (m), d_p is pipe diameter (m), and k_g is grout thermal conductivity (W/K.m). The coefficients β_o and β_i have been derived on the basis of the experimental data, as shown in Table 5.1.

Therefore Paul(1996) equation to determine R_b, depends on the modelling of several borehole parameters, including shank spacing, borehole diameter, U-tube diameter, and grout conductivity. (Paul, 1996; Thomas, 2001).

Table 5.1: Coefficients of eq. (5.2).

Configuration	**β_o**	**β_i**
Close Together	20.10	-0.9447
Average	17.44	-0.6052
Along Outer Wall	21.91	-0.3796

Paul's (1996) model suffers from the following downfalls:

a) The calculated parameters are typically fit to the tested samples.
b) The assumption of uniform temperature assumed around the borehole wall, as the value of soil thermal conductivity was neglected.

Therefore, different samples of the same materials and different borehole geometry might produce different results. In order to assess Paul's equation, numerical analysis has been established and a percentage of differences between Paul's

method and the numerical method have been determined ,as can be seen in Table 5.2.

Since the borehole diameter, U-pipe diameter and grout thermal conductivity are existed variable parameters in both the numerical and Paul's models, they may not be the main cause of the difference. In order to see the impact of the missing parameter in Paul (1996) expression (soil thermal conductivity) on the percentage of difference soil thermal conductivity will have the values of 1W/K.m, while grout thermal conductivity will be ranged from 1.0 to 4.0 W/K.m.

Figure 5.2 shows that Paul's method overestimated the value of BHE resistance by a maximum of 31.8 %, when average U-pipe configuration applied and the grout was equal to soil thermal conductivity.

Table 5.2: Borehole thermal resistance values resulting from using Flex PDE and Paul's equation, as a function of (k_g/k_s).

Borehole Thermal Resistance (K.m/W)				
Configuration	k_g/k_s	Flex PDE	Paul(1996)	ΔR_b(%)
Close Together	1	0.120	0.155	+29.1
	2	0.0606	0.0775	+27.8
	3	0.0406	0.0517	+27.3
	4	0.0306	0.0387	+26.4
Average	1	0.0895	0.118	+31.8
	2	0.0463	0.0594	+28.3
	3	0.0314	0.0396	+26.11
	4	0.0239	0.0297	+24.27
Along Outer Wall	1	0.0686	0.0720	+4.95
	2	0.0385	0.0360	-6.49
	3	0.0270	0.0240	-11.11
	4	0.0208	0.0180	-13.46

The difference between the numerical borehole resistance was quiet close to those resulted from close together configuration, where the values of BHE resistance were overestimated by a maximum of 29%, when the value of k_g was equal to the value of k_s. However, when the value of the grout thermal conductivity exceeded the value of soil thermal conductivity, the percentage of difference within the same configuration started to decreased.

Nevertheless, the best results were recorded when the maximum shank spacing applied with ratio of k_g/k_s ranged between 1and 2, where Paul' equation (1996) overestimated the numerical values of borehole resistance by only 4.95%.

To summarise, Paul's(1996) equation to calculate borehole resistance overestimated the borehole thermal resistance values in most cases. Overestimating the borehole

resistance will lead to overestimate the required depth for the borehole and hence substantially increase the installation cost.

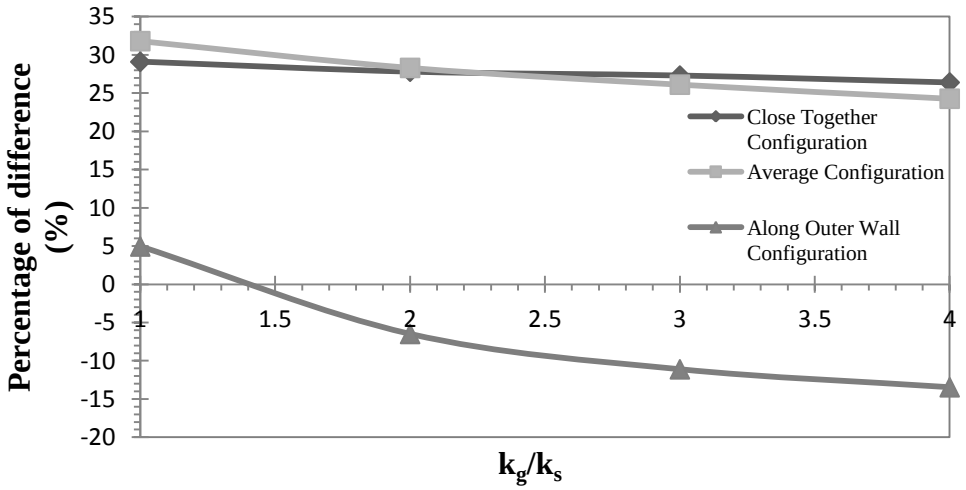

Figure 5.2: Percentage of difference between numerical and Paul's method as a function of the ratio of k_g/k

5.3. Bennet et al. (1987)

Bennet et al. (1987) proposed an equation based on multipole method that solve steady state problems in order to estimate the values of borehole thermal resistance. In the multipole method, borehole resistance is obtained by establishing a temperature at the U-tube wall and then determining a heat flux and a temperature

profile around the circumference of the borehole wall (T_{bhw}). The temperature at the borehole was calculated by taking an average of 180 points along the circumference of the borehole wall. Averaging 180 points, versus an average of 360 points, produced a temperature difference of less than 0.00001°C . (Bennet and Claesson, 1987; He, 2012).The equation is in the form of an infinite series (multipole expansion), presented is as follows :

$$R_b = \frac{1}{4\pi k_g}\left[\ln\left(\frac{\lambda_1\,\lambda_2^{1+4\sigma}}{2(\lambda_2^4-1)^{\sigma}}\right) - \frac{\lambda_3^2(1-(4\sigma/(\lambda_2^4-1)))^2}{1+\lambda_3^2(1+(16\sigma/(\lambda_2^2-\frac{1}{\lambda_2^2})^2))}\right] \quad (5.3)$$

where $\lambda_1 = \frac{d_b}{d_p}$, $\lambda_2 = \frac{d_b}{s}$, $\lambda_3 = \frac{d_p}{2s} = \frac{\lambda_2}{2\lambda_1}$, $\sigma = \frac{k_g - k_s}{k_g + ks}$, s is the shank spacing, d_b is the borehole radius (m), d_p is the pipe radius, k_g is grout thermal conductivity(W/K.m), and k_s is soil thermal conductivity (W/K.m).

Bennet et al.'s equation includes the influence of several parameters such as: borehole diameter, pipe diameter, shank spacing, and both grout and soil thermal conductivity. Therefore, this equation has the potential to produce an accurate estimation for borehole thermal resistance values. In Table 5.3, the borehole thermal resistance values are estimated as a function of U-pipe configuration and the ratio of k_g/k_s.

Figure 5.3, shows that despite the fact that Bennet's formula underestimated the values of borehole thermal resistances, by a maximum of 1.255 %, when Average pipe configuration applied. This proved that equations based on multipole theory can give accurate results of the BHE thermal resistance in any U-tube configurations used.

Table 5.3: Borehole thermal resistance values (K.m/W)using Flex PDE and Bennet et al. (1987) as a function of k_g/k_s .

Borehole Thermal Resistance (K.m/W)				
Configuration	k_g/k_s	Flex PDE	Bennet et al.(1987)	ΔR_b
Close Together	1	0.120	0.120	0.0
	2	0.0606	0.0606	0.0
	3	0.0406	0.0405	-0.24
	4	0.0306	0.0304	-0.65
Average	1	0.0895	0.0892	-0.335
	2	0.0463	0.0461	-0.431
	3	0.0314	0.0312	-0.636
	4	0.0239	0.0236	-1.255
Along Outer Wall	1	0.0686	0.0682	-0.583
	2	0.0385	0.0383	-0.519
	3	0.0270	0.0268	-0.740
	4	0.0208	0.0206	-0.961

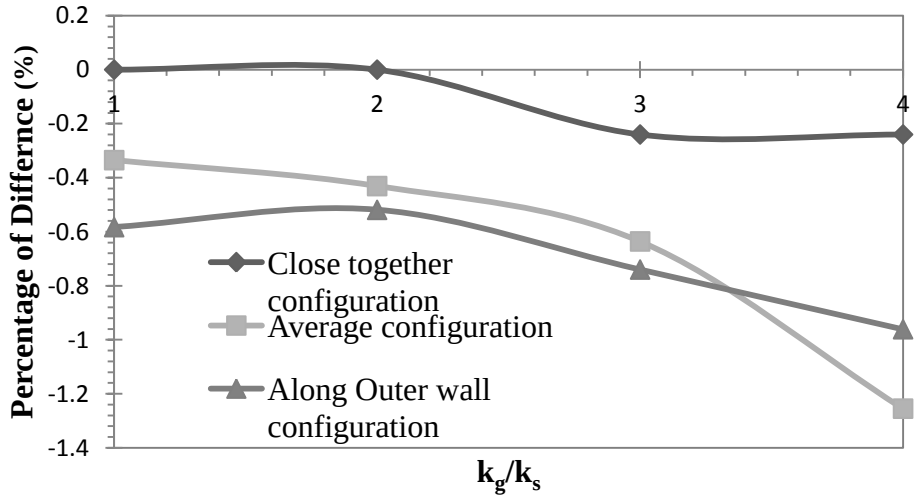

Figure 5.3: Borehole thermal resistance value as a function of k_g/k_s, using Flex PDE and Bennet et al. (1987), and using close, average and along the outer wall configurations, respectively.

5.4. Gu and O'Neal (1998)

Gu and O'Neal (1998) developed an expression based on the equivalent diameter theory for heat transfer in a vertical U-shaped BHE. It was derived assuming steady-state heat transfer and concentricity of one pipe with the borehole. Their expression reported by Sagia et al. (2012), is as follows:

$$R_b = \frac{\ln\left(\frac{d_b}{d_{eq}}\right)}{2\pi k_g} \tag{5.4}$$

where R_b is borehole thermal resistance(K.m/W), k_g is thermal conductivity of the grout(W/K.m), d_b is diameter of the borehole (m), r_b is radius of the borehole (m), d_{eq} is equivalent diameter which expressed as follows:

$$d_{eq} = \sqrt{2\ s\ d_p} \tag{5.4a}$$

where d_p is diameter of the U-shaped pipe (m), and s is the shank spacing between the centres of the U-tube legs.

Therefore, Gu and O'Neal(1998) equation shows that the borehole thermal resistance value depends on the pipe diameter, the shank spacing, and the grout thermal conductivity. Since the shank spacing was included in Gu and O'Neal (1998) equation, it is more flexible solution in calculating BHE resistance when changing the shank spacing.

Figure 5.4 shows that using Gu and O'Neal's equation, as the shank spacing increases, the difference between the obtained BHE resistance to the numerical solution decrease. However, when Average pipe configuration applied and the ratio of k_g/k_s equals 4, the borehole thermal resistance estimated by Gu and O'Neal equalised the value resulted from Flex PDE solution.

Figure 5.4 also illustrate that the equivalent diameter calculation is less accurate for small shank spacing's versus large shank spacing's. Unfortunately, the lower the value of shank spacing between the U-tube legs the closes the case to real life application.

Table 5.4: Borehole thermal resistance values(K.m/W) using Flex PDE and Gu and O'Neal (1998) as a function of k_g/k_s .

Borehole Thermal Resistance (K.m/W)				
Configuration	k_g/k_s	Flex PDE	Gu and O'Neal(1998)	ΔR_b(%)
Close Together	1	0.120	0.136	+13.33
	2	0.0606	0.0682	+12.54
	3	0.0406	0.0455	+12.06
	4	0.0306	0.0341	+11.43
Average	1	0.0895	0.0958	+7.03
	2	0.0463	0.0479	+3.45
	3	0.0314	0.0319	+1.59
	4	0.0239	0.0239	0.0
Along Outer Wall	1	0.0686	0.0719	+4.81
	2	0.0385	0.0359	-6.75
	3	0.0270	0.0239	-11.4
	4	0.0208	0.0179	-13.94

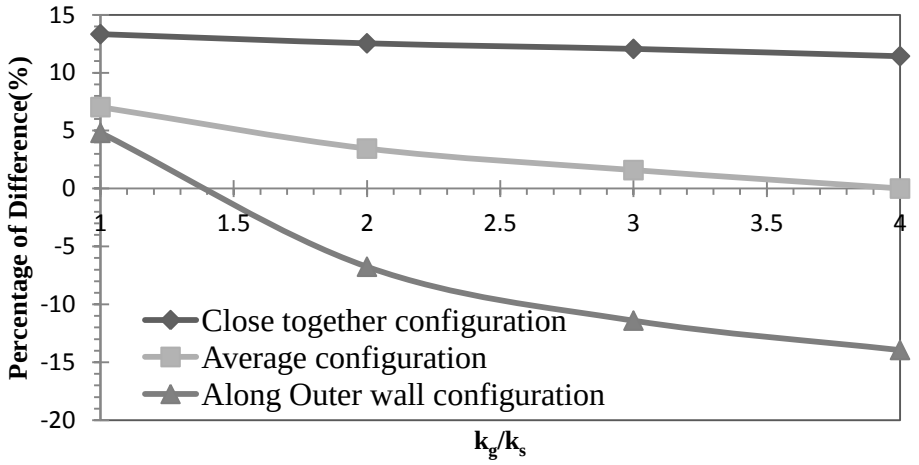

Figure 5.4:Borehole thermal resistance value as a function of k_g/k_s, using Flex PDE and Gu and O'Neal, and using close, average and along the outer wall configurations, respectively.

5.5. Hellstrom (1991)

Hellstrom (1991) used numerical program to simulate a vertical borehole field. The simulation resulted in creating an equation to determine the value of borehole thermal resistance. This equation reported by Lamarche et al.(2010), is as follows:

$$R_b = \frac{1}{4\pi k_g}\left[\ln\left(\frac{d_b}{d_p}\right) + \ln\left(\frac{d_b}{s}\right) + \sigma \ln\left(\frac{\left(d_b/0.5\,s\right)^4}{\left(d_b/0.5\,s\right)^4 - 1}\right)\right] \quad (5.5)$$

where d_b is the diameter of the borehole, d_p is the diameter of the pipe, s is the distance of the centre-to-centre pipe space, $\sigma = \frac{k_g - k_s}{k_g + k_s}$, k_g is the grout thermal conductivity (W/K.m), and k_s is soil thermal conductivity (W/K.m).

Obviously Hellstrom'(1991) equation has the same parameters as Bennet et al.'s equation(1987), however, the parameters were arranged differently in the equation. The question is, could this equation provide an accurate estimation to the borehole resistance as in Bennet et al.(1987) equation?

In order to assess Hellstom's equation, Table 5.5, will present the values of borehole thermal resistance as a function of σ, and the shank spacing between the U-tube pipes.

Figure 5.5 shows that Close Together pipe configuration with a ratio of k_g/k_s equals 1, the values of BHE thermal resistance were overestimated by a maximum of 13.13% as compare to the numerical U-tube borehole resistance.

However, when Average pipe configuration applied, the difference between numerical borehole resistance to those BHE resistance determinate using Hellstrom (1991) equation decreased to 7%.Furthermore, the difference equals zero as Along Outer wall configuration applied with k_g/k_s=3.

Table 5.5: Borehole thermal resistance values (K.m/W)using Flex PDE and Hellstrom,1991,as a function of k_g/k_s.

Borehole Thermal Resistance (K.m/W)				
Configuration	k_g/k_s	Flex PDE	Hellstrom(1991)	ΔR_b(%)
Close Together	1	0.120	0.136	+13.33
	2	0.0606	0.0683	+12.70
	3	0.0406	0.0456	+12.31
	4	0.0306	0.0342	+11.76
Average	1	0.0895	0.0958	+7.039
	2	0.0463	0.0487	+5.183
	3	0.0314	0.0328	+4.458
	4	0.0239	0.0247	+3.34
Along Outer Wall	1	0.0686	0.0719	+4.81
	2	0.0385	0.0390	+1.29
	3	0.0270	0.0270	0
	4	0.0208	0.0207	-0.48

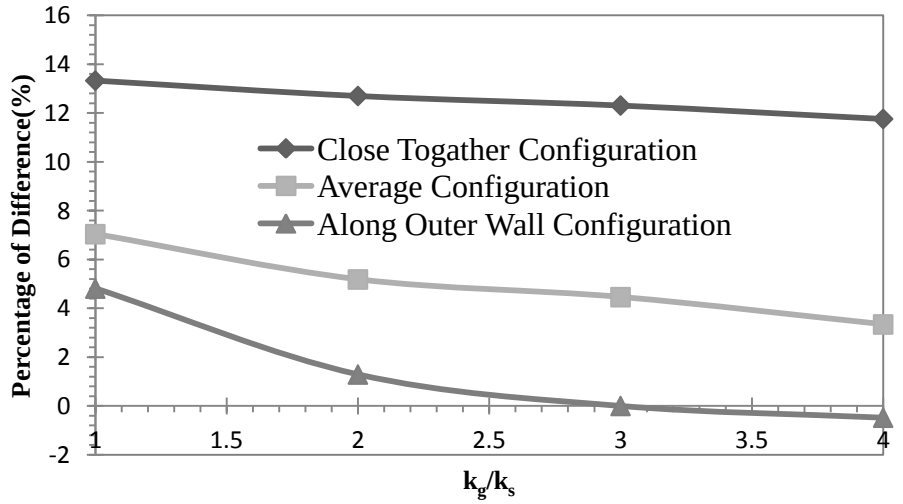

Figure 5.5: Borehole thermal resistance value as a function of k_g/k_s, using Flex PDE and Hellstrom (1991), and using close, average and along the outer wall configurations, respectively.

5.6. Shonder and Beck (1999)

Shonder and Beck (1999) purposed a 1D numerical model to obtain the value of borehole thermal resistance for BHE using a finite element model. In an attempt to simplify the complex geometry of the borehole, U-shaped pipes were modelled as a single pipe in the centre of the borehole, where the radius of the effective pipe matches to the area of U-tube pipes ,as shown in Figure 5.6 (Chiasson, 2007).The borehole thermal resistance equation proposed in this model, is as follows:

$$R_b = \frac{1}{2\pi K_g} \ln\left[\frac{d_b}{d_p\sqrt{n}}\right] \quad (5.6)$$

Where n is the number of pipes in the borehole (2 pipes in this study), k_g is the thermal conductivity of the grout, d_p is the U-pipe diameter ($dp\times\sqrt{2}$)(m), and d_b is outer diameter of the grout (m). Table 5.6 below will clarify the influence of using the U-pipe equivalent diameter as a function of k_g/k_s .

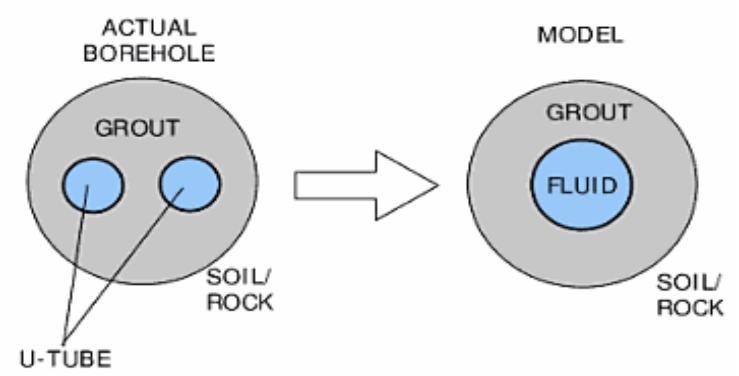

Figure 5.6:Schematic of the equivalent diameter approach used in Shonder and Beck's (1999) model (Chiasson, 2007).

Using Shonder and Beck's method, the borehole resistance values were overestimated by a maximum 98%, when Along Outer Wall configuration applied. Hence, this is considered the worse equation to determine BHE resistance in comparison to the previous tests. This may be because of the following:

1. It considers the two pipes as one, The short circuit heat transfer within the borehole presented by the temperature difference between these two pipes is, therefore, it is no considered.
2. It does not include soil thermal conductivity.
3. A constant undisturbed ground temperature was assumed at the outer boundary of the borehole.

Table 5.6: Borehole thermal resistance values using Flex PDE and Shonder and Beck (1999) (K.m/W) as a function of the ratio of k_g/k_s.

Borehole Thermal Resistance (K.m/W)				
Configuration	k_g/k_s	Flex PDE	Shonder and Beck(1999)	ΔR_b
Close Together	1	0.120	0.136	+13.33
	2	0.0606	0.0682	+12.54
	3	0.0406	0.0455	+12.06
	4	0.0306	0.0341	+11.43
Average	1	0.0895	0.136	+51.95
	2	0.0463	0.0682	+47.30
	3	0.0314	0.0455	+44.90
	4	0.0239	0.0341	+42.67
Along Outer Wall	1	0.0686	0.136	+98.25
	2	0.0385	0.0682	+77.14
	3	0.0270	0.0455	+68.51
	4	0.0208	0.0341	+63.91

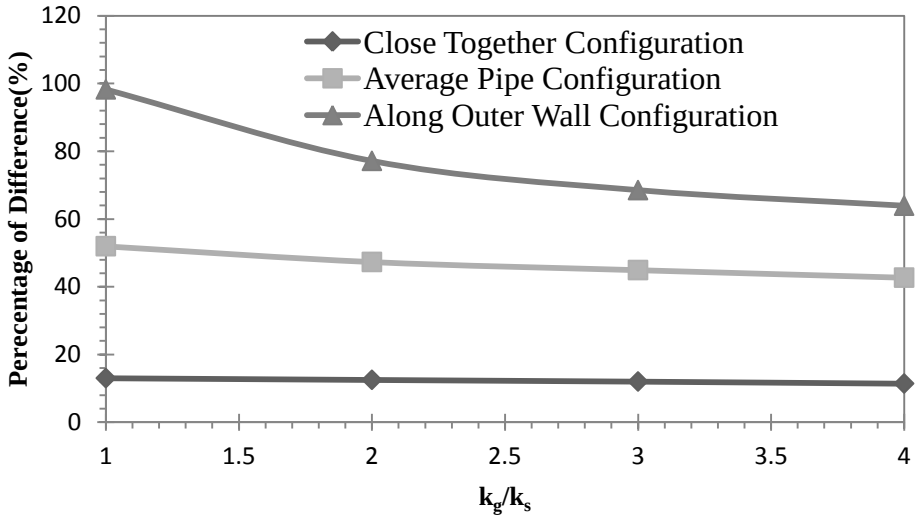

Figure 5.7: Borehole thermal resistance value as a function of k_g/k_s, using Flex PDE and Shonder and Beck, and using close, average and along the outer wall configurations, respectively.

5.7. Sharaqawy et al. (2009)

Sharaqawy et al. (2009) using finite element simulations produced an expression to calculate the value of borehole resistance within specific range of dimensionless geometrical parameters $2.5 \leq \frac{d_b}{d_p} \leq 7$ and $0.2 \leq \frac{s}{d_b} \leq 0.8$. The expression is as follows;

$$R_b = \frac{1}{2\pi k_g}\left[-1.49\left(\frac{s}{d_b}\right) + 0.656 \ln\left(\frac{d_b}{d_p}\right) + 0.436\right] \quad (5.8)$$

where d_b is the borehole diameter(m), d_p is the pipe diameter(m), k_g is the thermal conductivity of the grout material(W/K.m), and s is shank spacing(m).

Therefore, they based their equation on two dimensionless geometrical parameters to produce the values of the borehole thermal resistance. These dimensionless parameters are as follows:

$$R_b = \frac{1}{2\pi k_g} f\left\{\frac{d_b}{d_p}, \frac{s}{d_b}\right\} \quad (5.9)$$

They stated that their correlation have a maximum difference of 5% from the numerical result. These authors also claimed that their correlation is better than other available expressions although they did not include a valuable parameter (soil thermal conductivity), i.e. they assumed a uniform temperature distribution on the borehole wall.In order to assess the equation produced by Sharaqawy et al. (2009), 2D steady state numerical simulation using Flex PDE software was conducted.

Table 5.7 below, present the values of borehole thermal resistance and their percentage of difference to the numerical borehole resistance as a function of the ratio k_g/k_s and different U-tube pipe configuration.

It is clear from Figure 5.8, that Sharaqawy et al. (2009) equation performed the best when minimum shank spacing applied, where BHE resistance values were overestimated by only 9%. In addition, it was noticed that when Along Outer wall configuration applied, the values of BHE resistance were underestimated by maximum of 58%. This is clearly far from the 5 % difference limits they claimed for their equation when compared to the numerical solution.

Therefore if Sharqawy 's et al.(2009), equation considered in estimating the value of BHE resistance , it will lead to under sizing the borehole depth, which may reduce the thermal performance of the entire system.

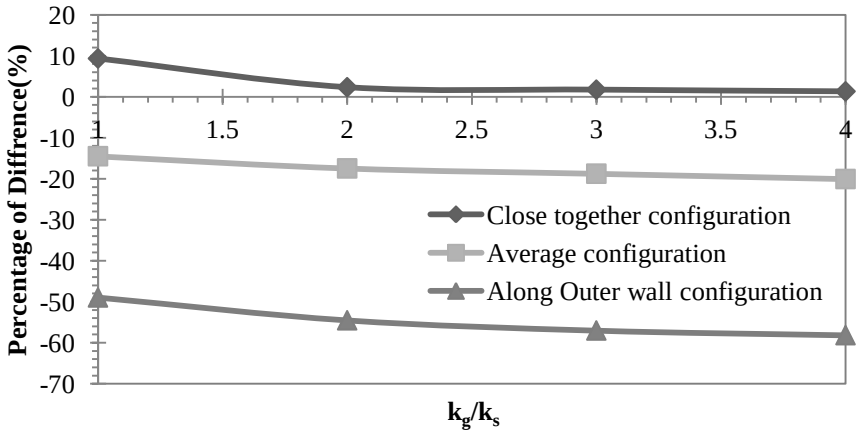

Figure 5.8: Borehole thermal resistance value as a function of soil thermal conductivity, using Flex PDE and Sharaqawy et al. (2009), and close, average and along the outer wall configurations, respectively.

Table 5.7:Borehole thermal resistance values (K.m/W) using Sharqawy et al. (2009) and numerical solutions as a function of k_g/k_s .

Borehole Thermal Resistance (K.m/W)				
Configuration	k_g/k_s	Flex PDE	Sharqawy et al. (2009)	ΔR_b
Close Together	1	0.120	0.124	+9.33
	2	0.0606	0.062	+2.31
	3	0.0406	0.0413	+1.72
	4	0.0306	0.031	+1.30
Average	1	0.0895	0.0765	-14.52
	2	0.0463	0.0382	-17.49
	3	0.0314	0.0255	-18.789
	4	0.0239	0.0191	-20.08
Along Outer Wall	1	0.0686	0.035	-48.97
	2	0.0385	0.0175	-54.54
	3	0.0270	0.0116	-57.03
	4	0.0208	0.0087	-58.17

5.8. Discussion

The sizing of GSHP, particularly the loop length of the BHE, depends on the value borehole thermal resistance R_b. Thus, calculating the correct value of the borehole resistance is quite crucial.

Therefore, the investigation in this chapter aimed to assess number of the available equations established to calculate the value of borehole thermal resistance, using numerical simulation.

However, the equation presented by Bennet et al., (1987), proved to produce almost the exact values of numerical resistance with a maximum value of difference that is less than 0.6%.

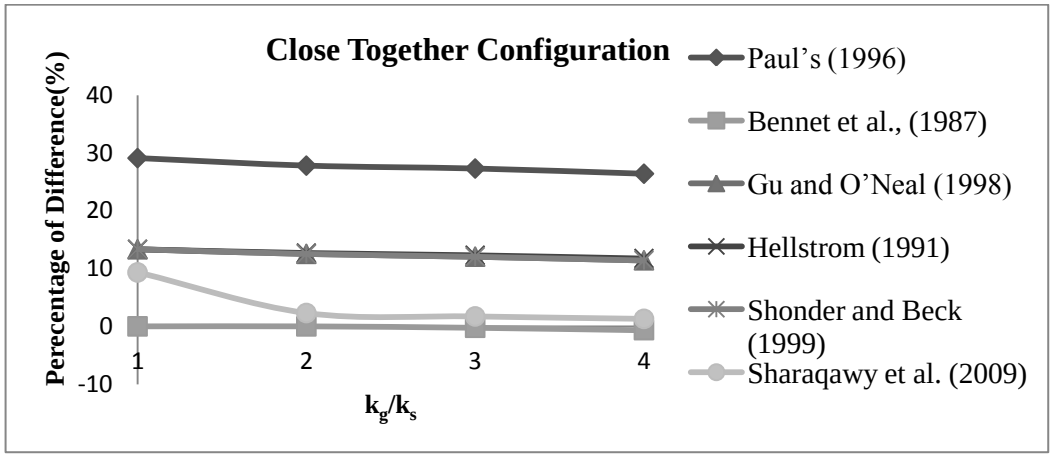

Figure 5.9: Borehole thermal resistance values as a function of k_g/k_s using different analytical and semi analytical equations with close together configuration.

As can be seen in Figure 5.9, for close together configuration, Bennet et al.(1987) and Sharaqawy et al.(2009), performed the best in estimating the values of borehole resistance as compare to the other equations. While Gu and O'Neal(1998), Shonder and Beck(1999),and Hellstrom(1991), estimation to the value of borehole thermal resistance was close to each other.

Using the average pipe configuration, the percentage of differences between the equations presented in this chapter and the numerical solutions are illustrated in

Figure 5.10 as a function of k_g/k_s. The results reveal that Bennet et al., (1987) once again produced highly accurate values, while Gu and O'Neal (1998) overestimated the borehole resistance by a only 7%.

However, Shonder and Beck's(1999) equation did not provide good result as their equation overestimated the borehole resistance by 50%.

Despite the fact that Gu and O'Neal's(1998) and Shonder and Beck's (1999)equations are based on equivalent diameter of the U-tube pipes, different equivalent theories have been employed, and Hellstrom (1991)equation was based on numerical simulations.

In Shonder and Beck (1999) it was ($\sqrt{2}$ d_p), whereas in Gu and O'Neal (1998) was ($\sqrt{2\ s\ d_p}$). Hence, the shank spacing was included in Gu and O'Neal's equivalent diameter theory. Adding shank spacing to Gu and O'Neal's equation led to create more flexible solution when changing the shank spacing.

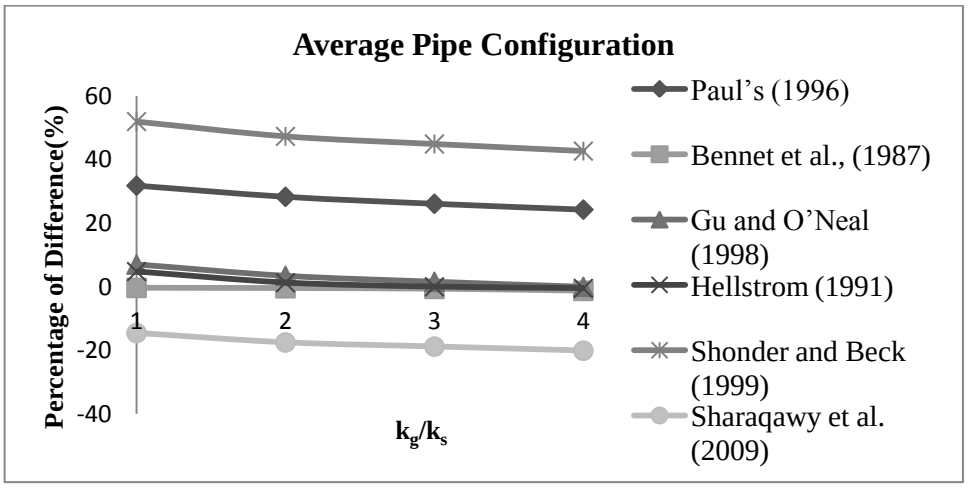

Figure 5.10: Borehole thermal resistance values as a function of k_g/k_s using different analytical and semi analytical equations with Average pipe configuration.

When Along Outer Wall configuration applied, Hellstrom(1991), Gu and O'Neal (1998), and Bennt's et al. equations (1987) proved to be the best fit to the numerical results, as shown in Figure 5.11.

Shonder and Beck (1999), gave the unaccepted results by over- estimating the BHE resistance by 95% respectively, whereas Sharaqawy et al. (2009)

underestimated the borehole resistance by 58 %. Therefore, the discrepancy in their solution worsens as shank spacing increased (Lamarche et al. 2010) .

Therefore, using Sharqawy et al.(2009) , Shonder and Beck(1999), to estimate the value of borehole thermal resistance will actually affect the sizing of the ground loop significantly and hence the efficiency of the system.

5.9. Summary and Conclusion

To summarise Table 5.8, presents all the equations discussed in the literature to calculate the borehole thermal resistance with their best and worse fit configurations to the numerical borehole resistance.

Table 5.9 shows that Bennet et al. (1987) equation is the best fit to the numerical solution in all the pipe configurations used. Therefore, it is recommended to use Bennet et al. (1987) equation in the determination of borehole thermal resistance in case of a single U-pipes configuration placed on the centre of the borehole.

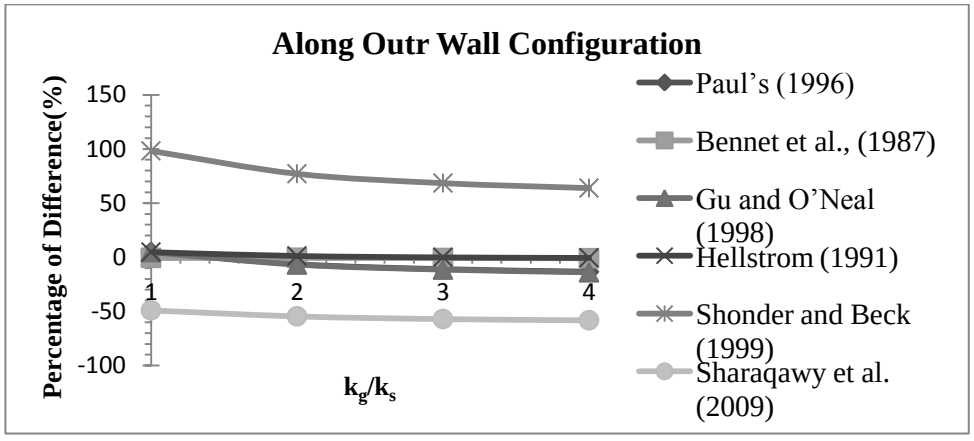

Figure 5.11: Borehole thermal resistance values as a function of k_g/k_s using different analytical and semi analytical equations with Along Outer Wall configuration.

Table 5.8: The best fit equation in determination of borehole thermal resistance when compared to numerical solution using Flex PDE.

Equation	Best Fit configuration	Worse Fit configuration	Parameters used
Paul (1996)	Along Outer Wall (4.95-13.46 %)	Average (31.0-24.27%)	β_o,β_i,d_p,d_b,k_g
Bennet et al., (1987)	All (0.0-1.255%)	N/A	s,d_p,d_b,k_g,k_s
Gu and O'Neal (1998)	Along Outer Wall (4.81-13.94%)	Close Together (13.33-11.43%)	s,d_p,d_b,k_g
Hellstrom (1991)	Along Outer Wall (0-4%)	Close Together (13.13-11.76%)	s,d_p,d_b,k_g,k_s
Shonder and Beck (1999)	Close Together (13.33-11.34%)	Along Outer Wall (98.25-63.91%)	d_p,d_b,k_g
Sharaqawy et al. (2009)	Close Together (9.33-1.3%)	Along Outer Wall (48.97-58.97%)	s,d_p,d_b,k_g

Chapter 6:Numerical Characterization for The Factors Influencing the Borehole Thermal Resistance.

6.0. Introduction

The previous chapter shows that the values of borehole thermal resistance depend on number of geometric configuration parameters such as: borehole diameter (m), pipe diameter(m), and the sank spacing(m). In addition, the values was found to be also influenced by thermal properties of the soil and the BH grout materials.

This chapter will present a thorough investigation involves all the parameters of the borehole heat exchanger that may affect the borehole thermal resistance values. The investigation will be performed using 2D steady state numerical simulation.

In addition, depending on the most influential factors influencing the values of borehole thermal resistance, Contour Charts will be developed based on numerical simulation.

6.1. Problem Configuration

Several parameters that have been shown in Figure 6.1,could influence the value of borehole thermal resistance value. These parameters are as follow:

1. The Standard Dimension Ratio(SDR).
2. The pipe thermal conductivity(k_p).
3. The shank spacing(s)
4. The ratio of the borehole diameter to the pipe diameter (d_b/d_p).
5. The grout thermal conductivity (k_g).

The study presented in this chapter will be based mainly on three geometric configurations: close together, average pipe, and along the outer wall, with shank spacing30mm,50mm,67.5mm shank spacings, respectively, as shown in Figure 6.2. The following section will present the influence SDR on the BHE resistance value.

It is important to mention that fluid flow rate is also curial in the resulted value of borehole thermal resistance, however it's effect has been ignored in this thesis. This is simply because of the assumption made earlier in calculating the borehole resistance in 2D steady state simulation, therefore the depth of the U-tube has not been considered. Furthermore, due to the limitation of the time, as studying the effect of the fluid flow rate will need 3D simulations.

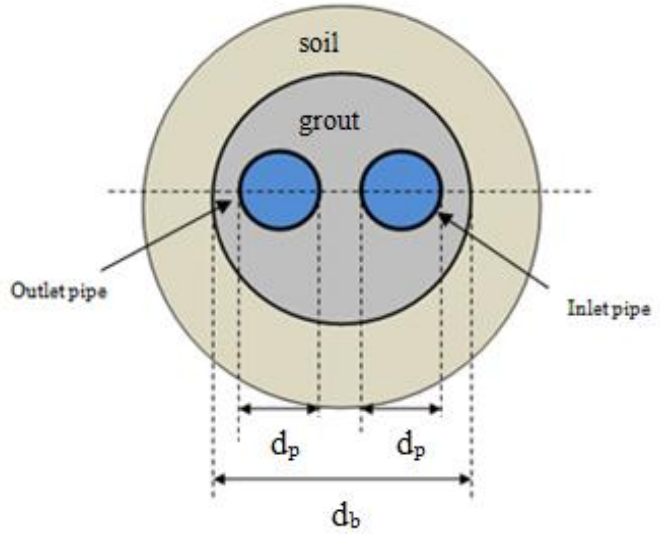

Figure 6.1: Cross section of the borehole heat exchanger system.

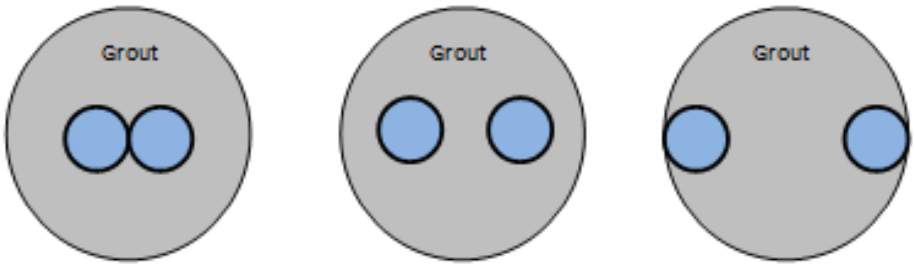

Figure 6.2: Pipe configurations. The inner circle corresponds to the two legs of the U-tube installed in the borehole (from left to right: close together configuration, average configuration, and along the outer wall configuration).

6.2. Standard Dimension Ratio(SDR)

The U-tube has a standard nominal diameter denoted by D_o. The ratio of the pipe's outer diameter, D_o, to the wall thickness is defined in the SDR is shown in Figure 6.3. It can be calculated using the following expression:

$$SDR = \frac{\text{Outer Diamter}}{\text{pipe wall thickness}} \tag{6.1}$$

Therefore, the internal pipe diameter D_i, varies according to the SDR. In order to examine the effect of the pipe wall thickness on the value of borehole thermal resistance, a numerical simulation using the Flex PDE program was carried out.

The values of borehole thermal resistance were estimated as a function of the SDR and pipe configuration, are illustrated in Table 6.1.

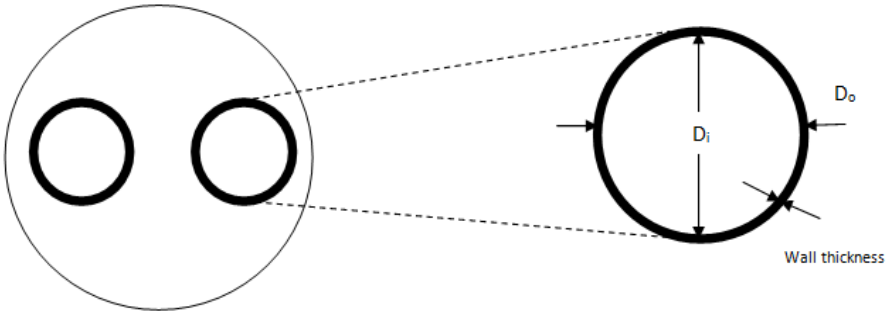

Figure 6.3: Definition of the pipes' standard ratio.

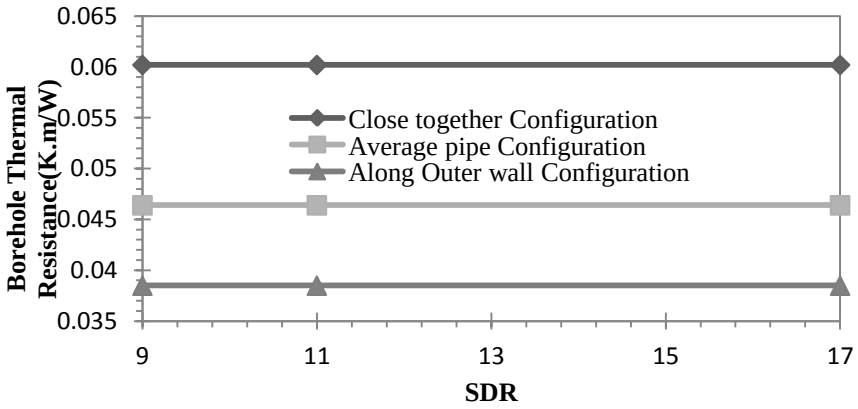

Figure 6.4: The borehole thermal resistance for a single U-tube borehole as a function of SDR for close together, average, and along the outer wall configurations.

The conducted results are presented in Figure 6.4, show that the effect of the pipe's wall thickness on borehole thermal resistance is insignificant. Hence, the effect of the thickness of the pipe wall will be not taken into consideration in the rest of the study.

The following analysis will study the influence of the pipe thermal conductivity on the borehole thermal resistance

Table 6.1: Parameters of the three cases employed to investigate the effect of U-tube wall thickness , when the U-tube pipes located on the borehole centre.

Configuration	SDR	s (mm)	s/d_b	d_b/d_p	k_g/k_s	k_g/k_p	R_b(K.m/W)
Close together	9	30	0.3	3.33	2.0	4.0	0.0602
	11						0.0602
	17						0.0602
Average pipe	9	50	0.5	3.33	2.0	4.0	0.0464
	11						0.0464
	17						0.0464
Along Outer wall	9	67.5	0.675	3.33	2.0	4.0	0.0385
	11						0.0385
	17						0.0385

Note that k_s used in all the cases above as 1 W/K, dp (Outer diameter) as 0.03m, d_b as 0.1m., and k_p as 0.5W/K.m.

6.3. The Effect of The Pipe Thermal Conductivity (k_p)

It was noticed from analysing the equations in the previous chapter, that they ignored the effect of U-pipe thermal conductivity when calculating the borehole thermal resistance. Therefore, this section will investigate the effect of pipe thermal

conductivity (k_p) on R_b, in a form of the dimensionless ratio k_g/k_p. The parameters used in this analysis along with the resulted borehole resistance, are displayed in Table 6.2.

From Table 6.2, it can be seen that the effect of the dimensionless ratio of k_g/k_p on the value of borehole thermal resistance K.m/W, is close to zero. This might explain the fact that all the equations founded to calculate the borehole thermal resistance , did not include this parameter.

Table 6.2: Parameters employed to investigate the value of borehole thermal resistance for three configurations as a function of dimensionless ratio of k_g/k_p, when the U-tube pipes positioned on the borehole centre.

Configuration	s (mm)	s/d_b	d_b/d_p	k_g/k_s	k_g/k_p	R_b (K.m/W)
Close Together	30	0.3		2.0	12	0.0606
					9	0.0606
					6	0.0606
					4	0.0606
Average Pipe	50	0.5	3.33	2.0	12	0.0463
					9	0.0463
					6	0.0463
					4	0.0463
Along Outer Wall	67.5	0.675	3.33	2.0	12	0.0385
					9	0.0385
					6	0.0385
					4	0.0385

Note :k_p values used in the table above are 0.17,0.23,0.33, and 0.5 W/K.m

6.4.The Effect of Shank Spacing(s)

The shank spacing is defined as centre to centre distance between the U-tube legs as shows in Figure 6.5.It is already known from Table 6.1, that the shank spacing could be a crucial parameter that influence the value of borehole thermal resistance, when the pipes are located on the borehole centre. In this section, however, the focus will be on applying different shank spacings while of setting the axis of U-tube position within the borehole.

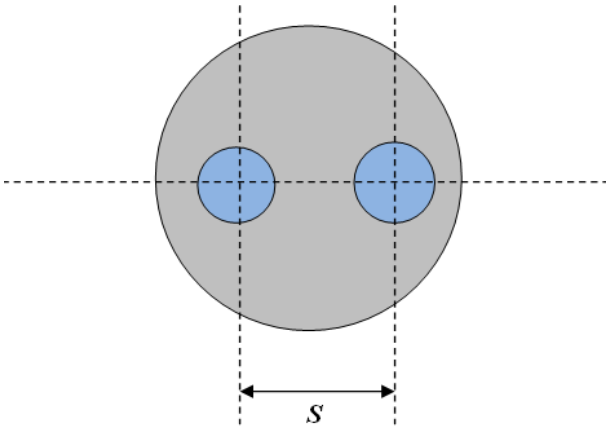

Figure 6.5:Shank spacing for a single U-tube pipe in the borehole.

The value of shank spacing in the heat exchanger system, has to be within the maximum and minimum limits of shank spacing. The limits of shank spacing(s) should be as follows:

$$s_{min} = d_p \tag{6.2}$$

$$s_{max} = d_b - d_p \tag{6.3}$$

where s_{max} and s_{min} are the maximum and minimum shank spacing respectively, d_b is the borehole diameter and d_p is the pipe diameter.

The present section will compare the values of borehole thermal resistance for three cases, where the U-tube is positioned on and above the centre. Each case will have

a number of hypothetical positions for the U-tube pipes, which will be modified according to the shank spacings that may occur during insulation. The exact values of the borehole resistance will be obtained from the 2D steady-state simulations using the Flex PDE software program.

Case One: U-tube pipes on the centre of the borehole

This case could have five different shank spacing between the U-tube pipes as illustrated in Figure 6.6. The resulted values of borehole resistance using the five above configurations are presented in Table 6.3.

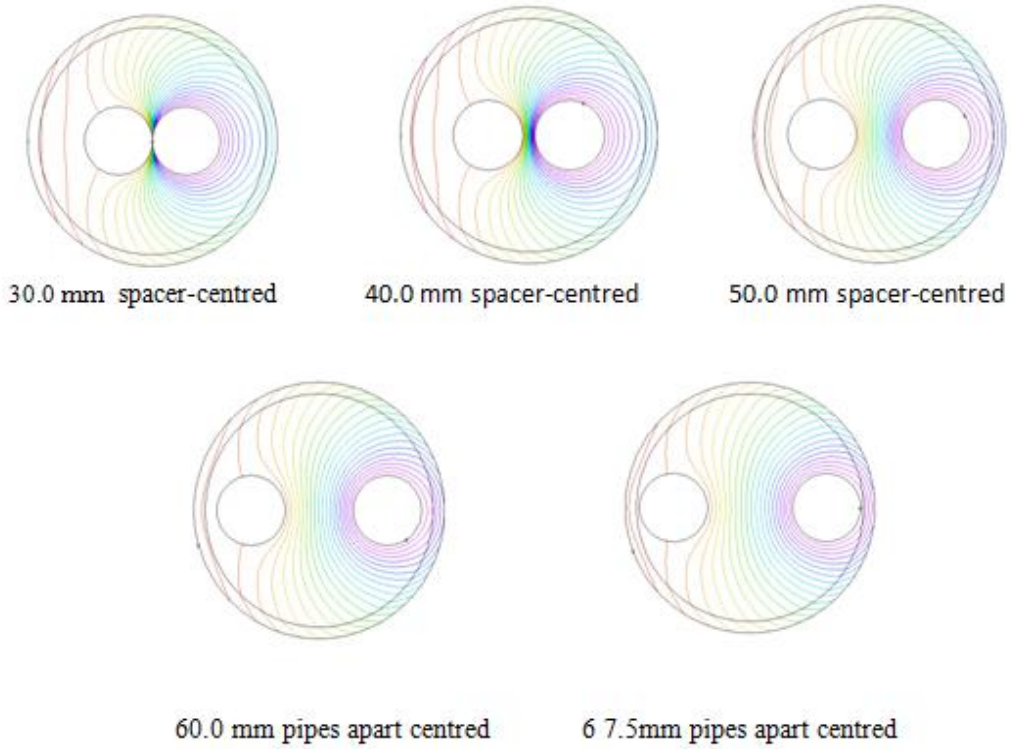

Figure 6.6: Heat flow inside borehole in different U-tube pipes positions around the horizontal centre of the borehole

Table 6.3: Borehole thermal resistance for five U-pipe configurations on the borehole centre modified according to their shank spacing(s), where k_g/k_s is 2 and d_b/d_p is 3.33.

No.	Pipes positions on the borehole centre	s/d_b	R_b(K.m/W)
1	Pipes with 30.0 mm spacer	0.3	0.0606
2	Pipes with 40.0 mm spacer	0.4	0.0528
3	Pipes with 50.0 mm spacer	0.5	0.0463
5	Pipes with 60.0 mm spacers	0.6	0.0413
7	Pipes with 67.5 mm spacers	0.675	0.0385

It is crucial to specify that the shank spacings were chosen so that the pipes would not catch each other and the borehole wall. Soil thermal conductivity was taken 1 W/K.m., and pipe diameter was fixed to the value 0.03m.

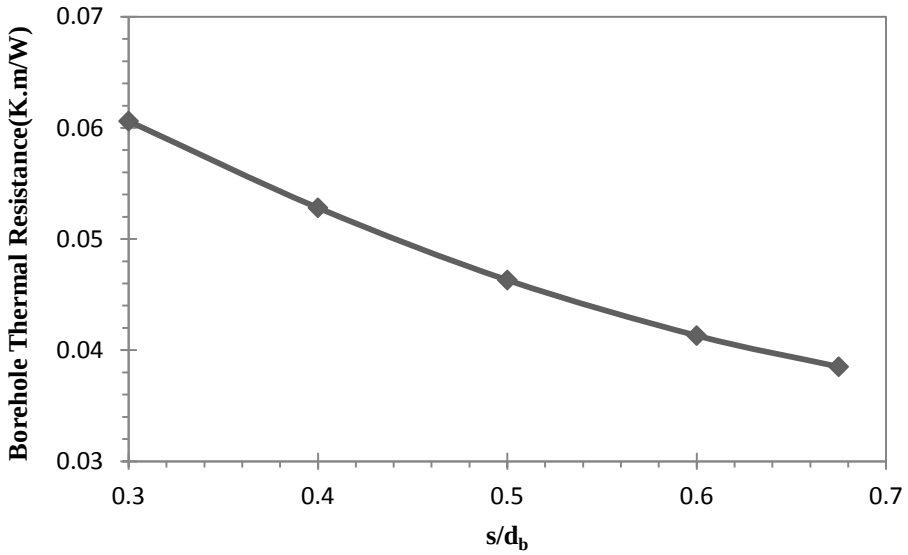

Figure 6.7: Borehole thermal resistance values as a function of the ratio s/d_b.

It is clear from Figure 6.7,that there is a significant linear decrease in borehole resistance when shank spacing increased. In fact, the values of borehole thermal resistance decreased to a maximum 36%, when a maximum shank spacing applied.

The question is whether the shank spacing impact on the borehole thermal resistance value will continue to be effective when changing the pipes' positions to above or below the horizontal central line. Therefore, the next analysis will compare the borehole thermal resistance when U-tube pipes are positioned above and on the centre of the borehole using the same shank spacings illustrated in the Table 6.3.

Case Two: U-tube pipes above the horizontal central line of the borehole

This case will have four different shank spacing, where U-pipes are positioned 15mm above the central line of the borehole ,as shown in Figure 6.8.Table 6.4, illustrate the impact of locating the U-tube pipes above the borehole centre as compared to the original geometry, i.e when the U-pipes located on the centre of the borehole.

It can be concluded from Figure 6.9, that there is a slight increase in value of borehole thermal resistance when positioning the U-tube pipe 15mm above the central horizontal line.

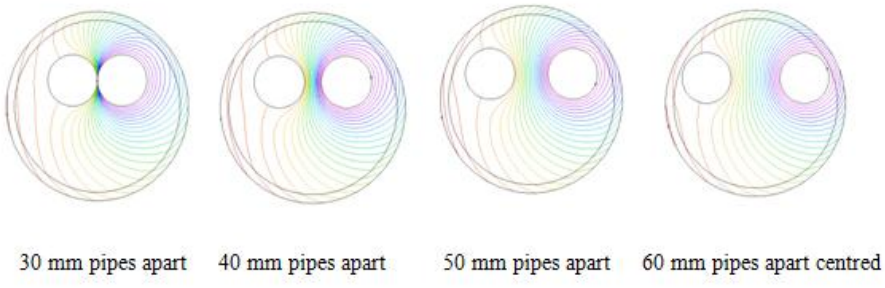

Figure 6.8: Heat flow inside the borehole in different U-tube pipes positioned 15mm above the horizontal centre of the borehole.

Table 6.4: Borehole thermal resistance for four pipe configurations above the horizontal centre of the borehole modified according to their shank spacing(s).

No.	Pipes positions at 15 mm above the centre	R_b(K.m/W)
1	Pipes with 30.0 mm spacer	0.0630
2	Pipes with 40.0 mm spacer	0.0549
3	Pipes with 50.0 mm spacer	0.0485
4	Pipes with 60.0 mm spacers	0.0436

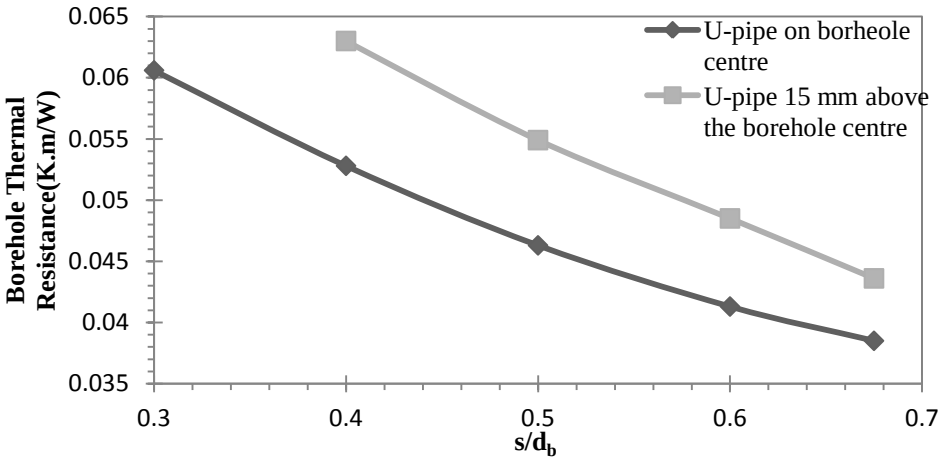

Figure 6.9: Borehole thermal resistance values(K.m/W), when U-tube located on the borehole centre and 15 mm above the centre respectively.

Case Three: U-tube pipes placed together at different positions within the borehole

In this case the U-tube pipe are placed together to create number of cases where the U-tube centre is offset from the borehole central axis as illustrated in Figure 6.10, and 6.11.

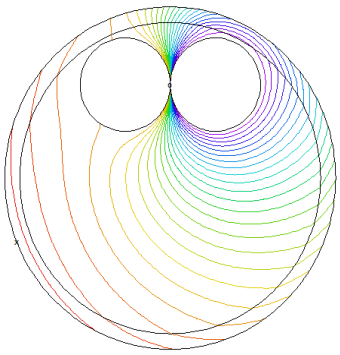

Figure 6.10: Heat flow inside the borehole when the U-tube pipes are positioned together, 30mm above the centre of the borehole.

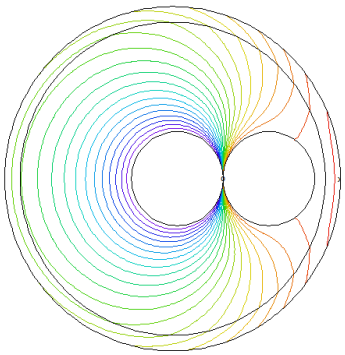

Figure 6.11: Heat flow inside the borehole for different U-tube pipes positioned together right of the borehole centre.

Table 6.5: Borehole thermal resistance for two pipe configurations located 30mm above the horizontal centre of the borehole and 15mm offset the borehole centre .

No.	Pipes positions	R_b (K.m/W)
1	Together at the top	0.0761
2	Together to right of centre	0.0559

The highest value of the borehole thermal resistance, recorded when the pipes are placed together at the top of the borehole, where the value of borehole thermal resistance was 0.0761 K.m/W.

All the cases presented demonstrate that by applying maximum shank spacing between the pipes, the values of borehole thermal resistance are significantly reduced, and in some cases up to 36 % when compared to the scenarios where pipes were in direct contact.

The scenarios presented in the third case study are probably the closest to real life installations. This is probably due to the fact that both BHE pipes are transferred in a way that they can be inserted into the borehole apparel (Acuna et al., 2010).

It can be seen from Figure 6.9, that changing the pipes' positions while keeping the same distance between them does not significantly affect borehole thermal resistance. In fact, a maximum difference of 5.56 % difference between the values of borehole thermal resistance when changing the pipes' positions within the same configuration.

6.5. The Ratio of Borehole Diameter to U-tube Pipe Diameter (d_b/d_p)

To elucidate the influence of the dimensionless ratio of borehole diameter (d_p) to the U-pipe diameter (d_b) on the values of R_b, a 2D steady-state analysis was performed to estimate the borehole thermal resistance for configurations shown in Figure 6.2. The parameters used for this analysis are presented below in Table 6.6.

From Figure 6.10, it is clear that the value of borehole thermal resistance increases with the increase of d_b/d_p. This is due to the fact that when decreasing the value of U-tube diameter, the heat flow is lower, hence less heat exchanged between the U-tube and surrounding. This leads to increase the difference extracted from the U-tube and borehole wall, resulting in higher values of borehole thermal resistance.

Table 6.6: Borehole thermal resistance as a function of dimensionless ratio of d_b/d_p, when U-pipes were positioned on the borehole centre.

Configuration	s (m)	s/d_b	d_b/d_p	k_g/k_s	k_g/k_p	R_b(K.m/W)
Close Together	0.03	0.3	3.33	2.0	4.0	0.0606
			5			0.080
			10			0.111
Average Pipe	0.05	0.5	3.33	2.0	4.0	0.0463
			5			0.064
			10			0.092
Along Outer Wall	0.0675	0.675	3.33	2.0	4.0	0.038
			5			0.0552
			10			0.083

Note: ks is used in all of the above cases as 1 W/K

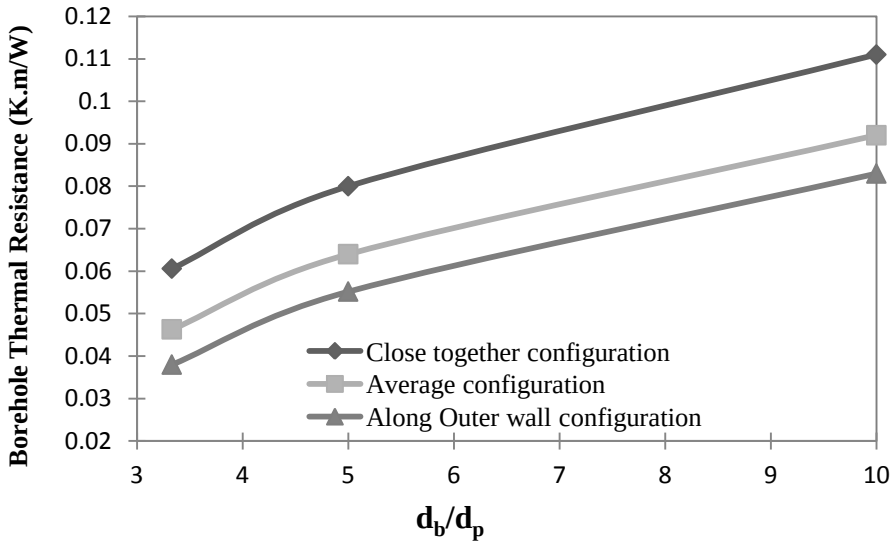

Figure 6.12: Numerical values of borehole thermal resistances for different pipe configurations as a function of the dimensionless ratios of d_b/d_p.

6.6. The Effect of The Grout Thermal Conductivity

In order to study the effect of grout materials on the value of borehole thermal resistance, three configurations were utilised ,as illustrated in Table 6.7.

The influence of the grout thermal conductivity in a single U-pipe is clearly demonstrated Figure 6.13. The higher the ratio of grout thermal conductivity to soil thermal conductivity, the less the thermal resistance of the borehole. In fact, Borehole thermal resistance was reduced to a maximum of 80 % from its initial value when the ratio of k_g/k_s was increased to 3 W/K.m.

It can also be noticed that although when grout thermal conductivity equalised the soil thermal conductivity around the borehole, i.e. no thermal resistance assumed, the thermal resistance still existed. This proves the fact that backfilling material is not the only the factor that influencing the borehole resistance value, but also the geometrical factors of the borehole might influence the value of borehole resistance.

Table 6.7: Numerical values to borehole thermal resistance (K.m/W) for a single U-pipe as a function of filling material thermal conductivity for three different shank spacing of the U-pipes ,where d_b/d_p is 3.33.

	Borehole Thermal Resistance (K.m./W)					
K_g/K_s	0.6	1	1.5	2	2.5	3
Close together configurations	0.199	0.12	0.081	0.0606	0.049	0.04
Average configurations	0.149	0.092	0.062	0.047	0.038	0.032
Along outer -wall configurations	0.114	0.075	0.052	0.041	0.033	0.028

Note that thermal conductivity of the soil for this analysis was take to be 1 W/K.m, and d_p is 0.03m.

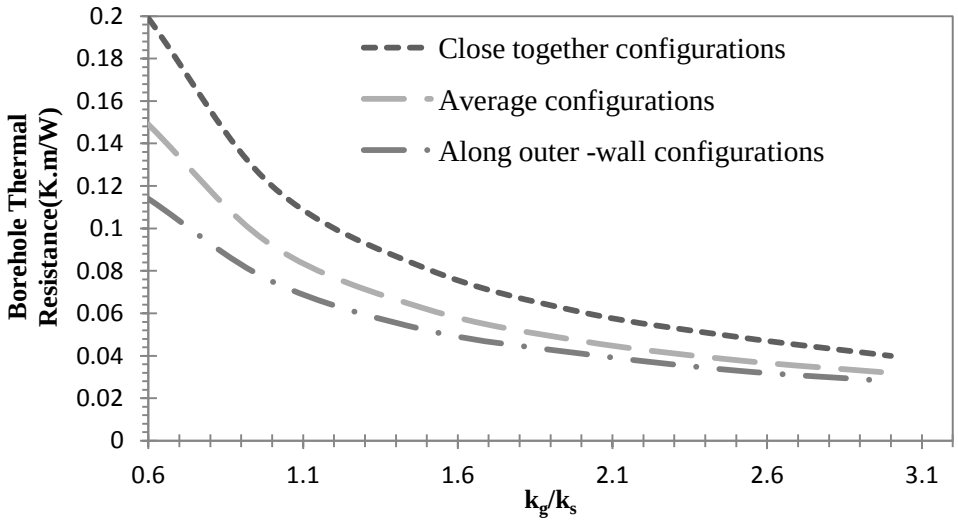

Figure 6.13: Numerical results for borehole thermal resistance (K.m/W) using Flex PDE for single U-pipe as a function of filling material thermal conductivity for three different shank spacing of the U-pipes.

6.7. Development of U-tube BH Thermal Resistance Charts

It is known now that estimating the value of borehole thermal resistance is curial to the sizing of the Borehole Heat Exchanger system. All the equations, except Bennet et al.(1987), presented in chapter five performed poorly in estimating the borehole resistance value. In addition the only one recommended as a better fit correlation, found to be very complicated and long equation.

Therefore in this thesis, charts to obtain the values of BHE thermal resistance will be introduced based on the results of series of numerical simulations at different geometric configuration and thermal materials. This will allow obtaining the value of borehole resistance without the urge to used long complicated equations.

These Contour Charts are based on shank spacing to borehole diameter(s/d_b), borehole diameter to U-pipe diameter(d_b/d_p), and grout thermal conductivity to the soil thermal conductivity(k_g/k_s).

The resulting borehole resistances were presented as ratios of the numerical borehole resistance to the analytical solution presented by Incropera and Dewitt (2002),

$$R_b^a = \frac{ln\left(d_b/d_p\right)}{2\,\pi k_g} \tag{6.2}$$

where d_b is the borehole diameter (m), d_p is the pipe diameter (m), and k_g is the thermal conductivity of the grout material (W/K.m).

The contour charts determines the borehole resistance based on parameters in the following ranges:

1. Maximum borehole diameter (d_b) = 0.2m

2. U-pipe diameter 0.03m $\leq d_p \leq$ 0.075m.

3. Shank spacing $0.075 \leq s \leq 0.12$ m.

4. Ratio of grout to soil thermal conductivity $3.5 \leq \frac{k_g}{k_s} \leq 1.0$.

The determination of the borehole thermal resistance using the Contour Charts illustrated in Figure 6.14below, could be done through the following equation:

$$R_b = R_b^a \times Fg \tag{6.3}$$

where R_b is the borehole thermal resistance (K.m/W), R_b^a is the analytical value of borehole thermal resistance determined from Equation 6.2, Fg is the geometric factor obtained from the Contour Charts presented in Figure 6.14.

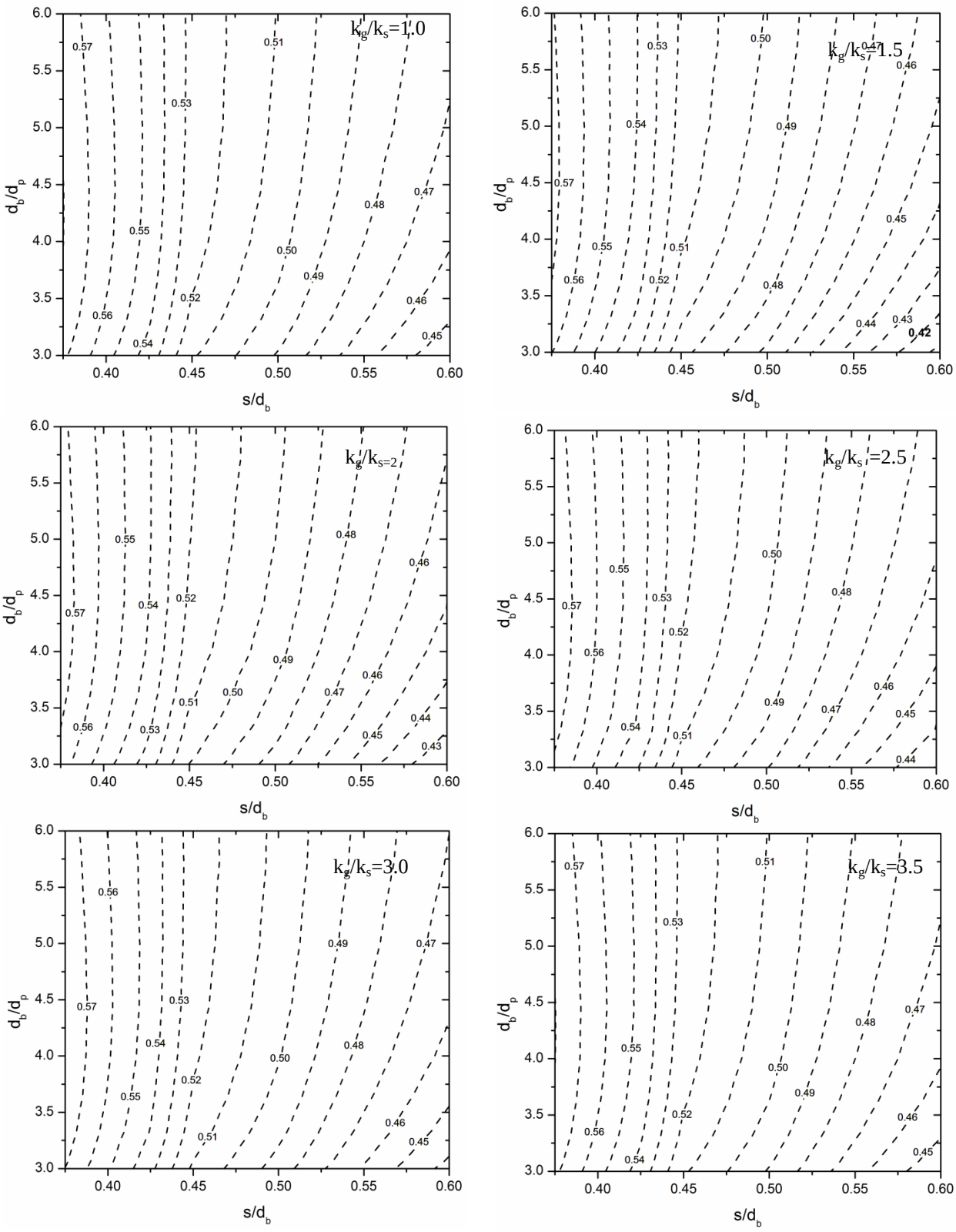

Figure 6.14: Geometric Factor as a function of d_b/d_p,s/d_b, and k_g/k_s.

For the sake of simplification, and since the values of normalised resistances are quiet close to each other, the average values for all the ratios are presented in single Contour Chart, as shown in Figure 6.13 below.

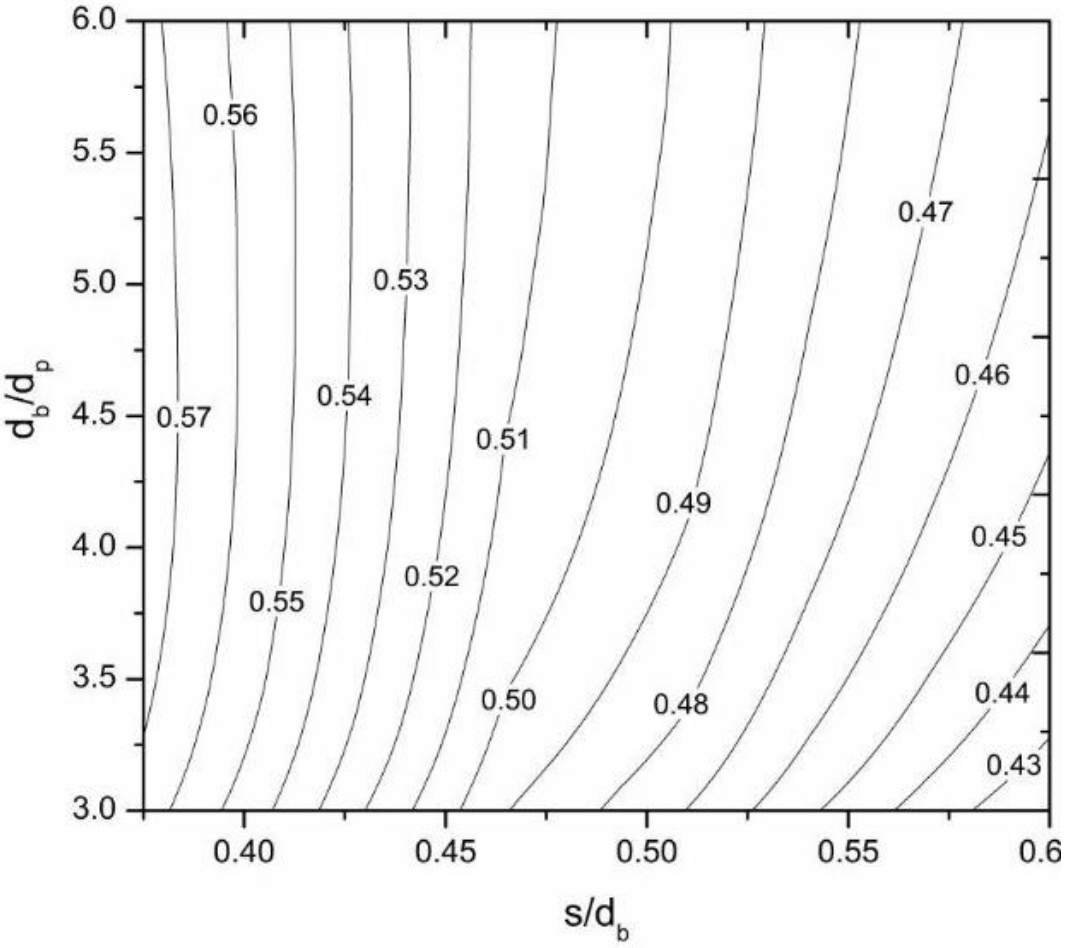

Figure 6.15:The Average Normalised Geometric Factor as a function of d_b/d_p, and s/d_b.

In order to assess the accuracy of this new method in calculating the value of borehole thermal resistance, 2 D numerical model is conducted. The assessment will be based on three configurations namely are: Close Together , Average , and Along Outer Wall. The results of

the investigation that are shown in Table 6.9, based on the percentage of difference to the numerical solution.

Table 6.8:Borehole thermal resistance values (K.m/W) using Contour Charts and numerical solutions as a function of k_g/k_s .

Borehole Thermal Resistance (K.m/W)				
Configuration	k_g/k_s	Flex PDE	Current work. (2013)	ΔR_b(%)
Close Together	1	0.0847	0.0843	0.472
	2	0.0431	0.0421	0.464
	3	0.0290	0.0281	0.689
Average	1	0.0778	0.0784	0.771
	2	0.0400	0.0398	0.500
	3	0.0271	0.0270	0.369
Along Outer Wall	1	0.06030	0.0609	0.995
	2	0.03055	0.0304	0.490
	3	0.02037	0.0203	0.343

We can see from Table 6.8, that the percentage of difference between the numerical and contour charts borehole resistance values for all the ratios of k_g/k_s are less than 1.0%.This results is better than all the solution discussed in chapter five to calculate the BHE resistance

6.8. Summary and Conclusion

Borehole thermal resistance values are not only influenced by the geometry of the borehole heat exchanger system, but also the thermal conductivity of the surrounding soils and backfilling materials.

The investigation into the geometry of the borehole, using a 2D steady-state simulation, includes: U-pipe wall thickness, shank spacing between the two legs of the U-tube, U-tube pipe positioning inside the borehole, borehole diameter, pipe diameter, pipe thermal conductivity, grout thermal conductivity, and soil thermal conductivity.

The numerical results revealed that the thickness of the U-tube wall dose not significantly change the value of borehole thermal resistance. Pipe thermal conductivity was one parameter studied. Using a variety of pipe thermal conductivity values for the U-pipes, the BHE resistance did not change at all. This may be due to the thin pipe wall thickness, which makes the effect of the pipe's wall thickness extremely limited.

However, the effect of shank spacing(s) between the two legs of the U-pipe is found to be more significant on the BHE resistance. In fact, reducing the shank spacing led to increase in borehole thermal resistance by 37%. Thus, controlling the shank spacing might be crucial to control the value of borehole resistance. On the other hand, changing the U-pipe positions while keeping the same shank spacing did not really affect BHE resistance.

It was also found that with the decrease of U-pipe diameter, borehole thermal resistance values increased. This is due to the fact that when decreasing the value of U-tube diameter, the heat flow is lower, hence less heat exchanged between the U-tube and surrounding. This leads to increase the difference extracted from the U-tube and borehole wall, leading to increase the borehole thermal resistance values

Therefore, it was concluded that the higher thermal conductivity of the grout, the less BHE thermal resistance of the exchanger system. In fact, it was found that when increasing the ratio of k_g/k_s to 3, the resistance of the borehole decreased to 80%. Hence, it is curial to use thermally enhanced grout inside the borehole in order to reduce the length of the ground loop, and thus enhance the efficiency of the ground source heat pump.

Due to the difficulty in the determining the value of borehole thermal resistance, Contour Charts were introduced based on the results of series of numerical

simulations at different geometric configuration and thermal materials, to calculate borehole resistance.

After assessing the resulted values of borehole thermal resistance from the Contour Charts, it was found that the percentage of difference yields good results. In fact the percentage of difference found to be less than 1.0%. The results refer that this solution is better than all of the solution introduced in chapter five as well as it is easy to us.

Chapter 7: Design Optimisation of Ground Heat Exchanger System

7.0 Introduction

The design optimisation in this research is attempted through the reduction of the borehole thermal resistance value. This reduction will lead to lower the required loop depth, and therefore enhance the thermal efficiency of the system and decrease the installation cost.

The optimisation strategy is based on the most influential factors found on the values of BHE resistance in the previous chapter. These factors namely are: the shank spacing between the U-tube legs, pipe diameter (d_p), borehole diameter(d_b)the grout thermal conductivity (k_g)and the soil thermal conductivity (k_s).

The investigation in this chapter will be accomplished by reviewing the previous methods proposed to reduce the value of borehole thermal resistance , followed by presentation to the new methods suggested in this field.
The next section will examine the effect of reducing borehole thermal resistance on the total loop length of the system.

7.1. Borehole Length Reduction Rate (BLRR) as a Function of Borehole Thermal Resistance

Borehole Length Reduction Rate (BLRR) was introduced by Lee et al. (2009). The borehole loop length is a function of borehole thermal resistance (R_b)and ground thermal resistance (R_g). Therefore, the reduction rate in the borehole length can be estimated using the steady-state line source model as follows:

$$T_{bhw} = T_o - \frac{q/_L}{4\pi k_s} \left(\ln \frac{4\alpha t}{r_b^2} - \gamma\right) \quad (7.1)$$

where T_{bhw} is the temperature of the borehole wall (°C), T_o is the undisturbed ground temperature (°C), α is thermal diffusivity – commonly ranging between 0.005×10^{-4} to 0.02×10^{-4} m^2/s and will be taken as 0.005×10^{-4} m^2/s – r_b is the borehole radius(m), k_s is soil thermal conductivity (W/K.m), and γ is Euler's constant value which is equal to (0.577).

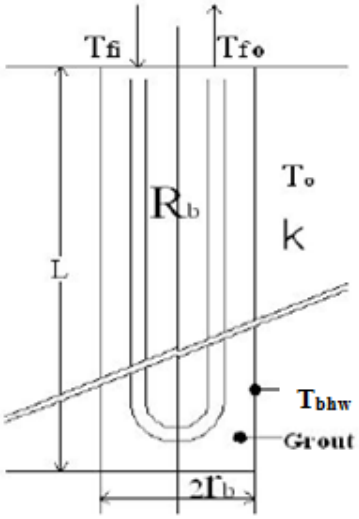

Figure 7.1: Section in the ground heat exchanger system (Lee et al., 2009).

The borehole thermal resistance is estimated by:

$$R_b = \frac{T_{bhw} - T_f}{q/_L} \tag{7.2}$$

where L is the length of the U-tube pipes (m) and q is the heat flow rate (W/m), T_f is calculated using the equation below.

$$T_f = \frac{T_{fi} + T_{fo}}{2} \tag{7.3}$$

Then

$$\frac{L}{q} = \frac{R_b + \frac{1}{4\pi k_s}\left(ln\frac{4\alpha t}{r_b^2} - 0.5772\right)}{T_o - T_f} \tag{7.4}$$

where the term $\frac{1}{4\pi k_s}(ln\frac{4\alpha}{r_b^2} - 0.5772)$ defines the value of ground thermal resistance(R_g).

Hence

$$BLRR = \frac{(L/q)_{R_b} - (L/q)_{reduced\ R_b}}{(L/q)_{R_b}} \quad (7.5)$$

In order to assess the impact of reducing the borehole resistance on the borehole loop depth, an investigation will be conducted using 100m diameter borehole contains single U-tube pipes of 30mm diameter separated by 30mm shank spacing. This configuration was specifically chosen, as it is the most likely to occur during real life application (Acuña, 2010).

The value of BLRR therefore is calculated by dividing the sum of the numerical borehole resistance and numerical ground thermal resistance over the sum of the undisturbed temperature of the ground and the mean temperatures of the inlet and outlet pipes.

The values of grout and soil thermal conductivity used through the this analysis are 1,2,and 3 W/K.m., respectively. The resulted ratios of BLRR are presented in Tables 7.1, 7.2, and 7.3 as a function of borehole thermal resistances and the ratios of k_g/k_s.

Figure 7.2 indicates that for k_g/k_s=1, 16% reduction rate in the loop depth could be obtained, if R_b=0.0.This conclusion was also mentioned by Kavanaugh in the ASHRAE journal (2010).Various methods to reduce BHE resistance were introduced in the literature and will be discussed in the following section.

Table 7.1: BLRR as a function of borehole thermal resistance value when k_g/k_s is 3.

	R_b	R_g	L/q	BLRR
1 R_b	0.0406	0.613	0.163	-
0.9 R_b	0.0365	0.613	0.162	0.85
0.7R_b	0.0284	0.613	0.160	2.8
0.5R_b	0.0203	0.613	0.158	3.3
0.3 R_b	0.0121	0.613	0.156	4.5
0.1 R_b	0.004	0.613	0.1542	5.7
0 R_b	0	0.613	0.153	6.3

able 7.2: BLRR as a function of borehole thermal resistance value when k_g/k_s is 2.

	R_b	R_g	L/q	BLRR
1 R_b	0.0606	0.613	0.168	-
0.9 R_b	0.0545	0.613	0.166	1.2
0.7R_b	0.0424	0.613	0.163	3.0
0.5R_b	0.0303	0.613	0.160	4.7
0.3 R_b	0.0182	0.613	0.157	6.5
0.1 R_b	0.0060	0.613	0.154	8.3
0 R_b	0	0.613	0.153	9.0

Table 7.3: BLRR as a function of borehole thermal resistance value when k_g/k_s is 1.

	R_b	R_g	L/q	BLRR
1 R_b	0.120	0.613	0.183	-
0.9 R_b	0.108	0.613	0.180	1.6
0.7R_b	0.084	0.613	0.174	4.9
0.5R_b	0.06	0.613	0.168	8.1
0.3 R_b	0.036	0.613	0.162	11.2
0.1 R_b	0.012	0.613	0.156	15.0
0 R_b	0	0.613	153	16.4

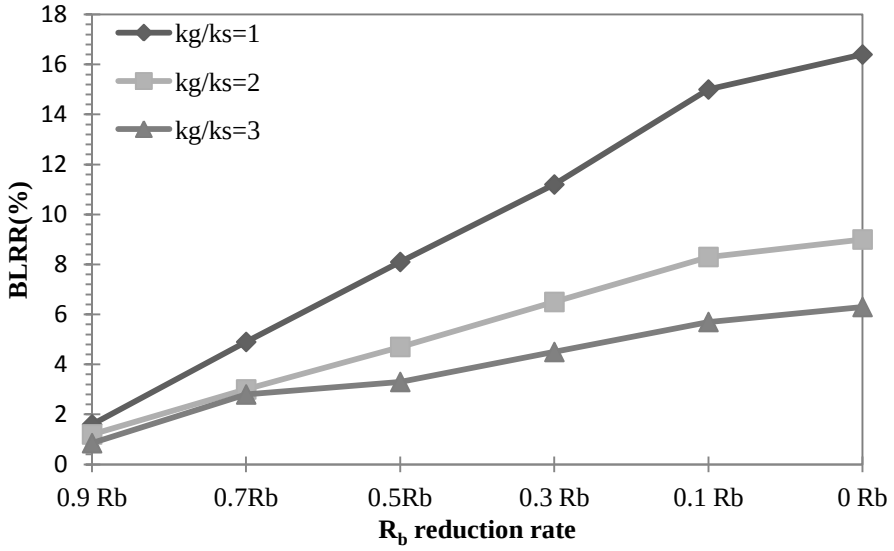

Figure 7.2: BLRR as a function of borehole thermal conductivity for different ratios of k_g/k_s.

7.2. Previous Methods

7.2.1 Double U-pipe system,

The contribution of the grout to total borehole thermal resistance is quite large for single U-pipes of polyethylene, but usually decreases with a number pipes in the borehole. According to the study by Heya et al. (2003) on double and single U-pipe systems, shown in Figure 7.3,the double U-tube boreholes are superior to those of the single U-tube with reduction in borehole resistance of 30 to 90 %. However, the cost of a double U-pipe system is significantly higher than a conventional single pipe.

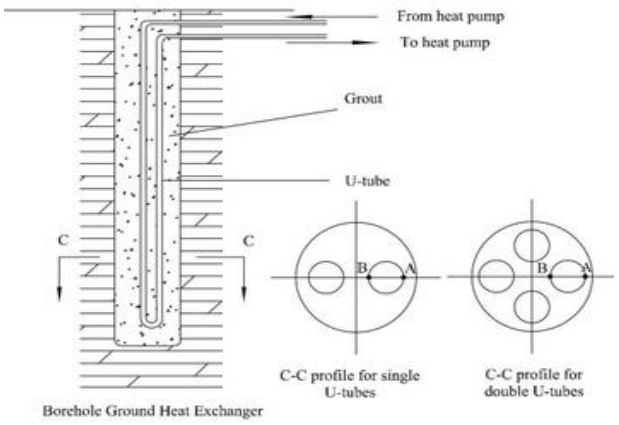

Figure 7.3: Schematic diagram of boreholes in the vertical GHE: (a) double U-tube and (b)single U-tube (Heya et al. 2003)

7.2.2. GEOCLIP

In Sweden, an attempt to reduce the borehole thermal resistance value was proposed by J. Acuna (2010). The attempt basically suggested that by increasing the shank spacing between the U- pipes within the borehole ,the value of BHE resistance will decrease(this was also proven in chapter six). Nevertheless, controlling the spacing between the U-tube legs during installation might not be possible to be achieved in reality, unless GEOCLIPS are employed.

GEOCLIPS, as shown in Figure 7.4, is designed to improve the vertical heat exchanger (VHE) performance through controlling the shank spacing between the U-tube pipes (Jeppesen, 2010). However the U-tube pipe position within the borehole is not controlled.

Figure 7.4: Typical vertical heat exchanger installation on the left, compared to a GEOCLIP installation on the right (www.geoclip.com).

7.2.3. Air Insulator Zone(Lee et al. ,2010)

In Korea, Lee et al. (2010) conducted an attempt to lower the value of the BHE resistance by reducing the thermal interference between the inlet and outlet pipes. An insulation zone was added between the U-tube pipes for this purpose using air, as shown in Figure 7.5.

Lee et al. (2010) claimed that thermal interference between the inlet and outlet pipes was achieved. However, the question is whether this method achieved its aim of reducing BHE resistance. In order to investigate this solution, 2D steady-state numerical analysis was conducted using the Flex PDE software program.

The air insulation zone effectiveness will be examined using different shank spacings and ratios of k_g/k_s. The borehole and U-tube diameter used in this investigation are 100mm and 30mm, respectively.

As can be seen in Figure 7.6, the isothermal lines between the U-tube legs dispersed when compared to the original geometry. This indicates that there is no

heat being exchanged between the U-tube legs. Tables 7.4, 7.5,and 7.6, present the influence of this insulation zone on the value of BHE resistance , when k_g/k_s are 1 , 2, and 3, respectively.

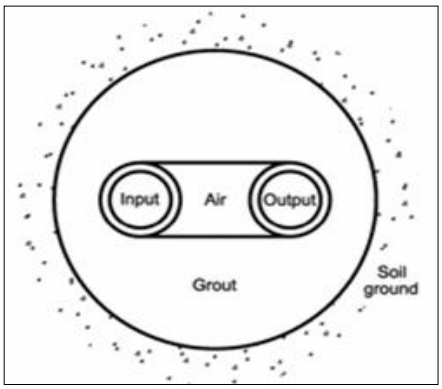

Figure 7.5: Cross section of ground source heat exchanger showing latticed pipe system (Lee et al. 2010).

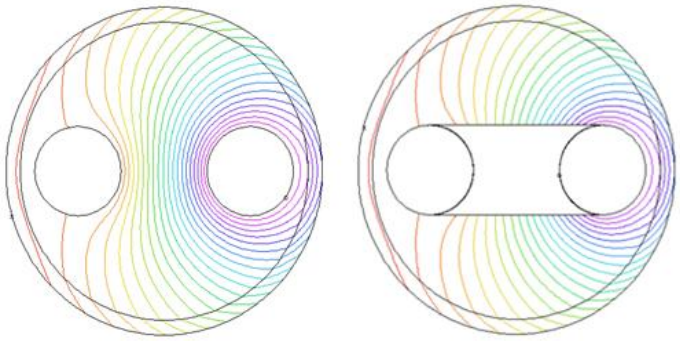

Figure 7.6: Air insulation zone located between the U-tube legs to the right and to the left side is the original geometry, when the 60mm spacing used

Tables 7.4, 7.5 and 7.6, disclose that this solution did not reduce the BHE resistance value, in fact, in most cases the borehole resistance values increased. This may be due to the fact that that the insulation zone reduced the area of thermal exchange between the U-pipe and the surrounding. The reduction in the area of thermal exchange leads to an increase in the difference between the inlet and borehole wall temperatures, hence high values of BHE resistance value resulted.

This investigation proves that the area of heat exchange is crucial to the value of BHE resistance. Therefore, to resolve the problem associated with this method, next section will present number of new solutions.

Table 7.4: Borehole thermal resistance as a function of shank spacing when the ratio of k_g/k_s is 1.

Borehole Thermal Resistance (K.m/W)			
s/d_b	Without Insulation Zone	With Insulation Zone	POR (%)
0.4	0.1030	0.1030	0%
0.5	0.0895	0.0895	0%
0.6	0.0770	0.0770	0%
0.0675	0.0686	0.0686	0%

Table 7.5: Borehole thermal resistance as a function of shank spacing when the ratio of k_g/k_s is 2.

Borehole Thermal Resistance (K.m/W)			
s/d_b	Without Insulation Zone	With Insulation Zone	POR (%)
0.4	0.0528	0.0539	+2.08
0.5	0.0463	0.0479	+3.40
0.6	0.0413	0.0435	+5.30
0.675	0.0385	0.0421	+9.30

Table 7.6: Borehole thermal resistance as a function of shank spacing when the ratio of k_g/k_s is 3.

	Borehole Thermal Resistance (K.m/W)		
s/d_b	Without Insulation Zone	With Insulation Zone	POR (%)
0.4	0.0355	0.0368	+3.6
0.5	0.0314	0.0334	+6.3
0.6	0.0284	0.0311	+9.5
0.675	0.0270	0.0304	+12.5

7.3. New Methods To Reduce Borehole Thermal Resistance

The key solution is to add a barrier located in between the inlet and outlet pipes. The barrier is supposed to reduce BHE thermal resistance by reducing the thermal circuit between the U-tube legs impacting the area of thermal exchange between the inlet pipe and the surrounding.

7.3.1. Dummy Pipe

Adding a single pipe between the inlet and outlet pipes, called a "dummy pipe", is one of proposed solutions that aimed to reduce BHE resistance value. This solution suggests to use two inlet pipes instead of one inlet pipe and one outlet pipe.

The outlet pipes' diameter is $\sqrt{2}$ ×diameter of the inlet pipe (d_p), hence the area of the outlet pipe should accommodate the fluid velocity circulated from the two inlet pipes. Since the sum of the areas of heat exchange in the inlet pipes is higher than the area of heat exchange in the outlet pipe, thermal exchange between the inlet pipes and the surrounding should exceed the heat exchange in the normal U-pipe configuration. Therefore, the value of BHE resistance should be reduced. A

diagram of this solution is shown in Figure 7.7, while the numerical; simulation for this model is presented in Figure 7.8.

The influence of using two inlet pipes on the BHE resistance values is presented in Tables 7.7,7.8 and 7.9 using borehole of 0.16 m diameter, inlet pipe diameter of 0.02m, and outlet pipe diameter of 0.028m, respectively.

Figure 7.8 shows that the maximum reduction to the borehole resistance value achieved when the spacing between the dummy pipe and outlet pipe was at its minimum value, where the reduction rate reached a value of 68%. This result indicates that inserting material between the inlet and outlet pipe that have low thermal resistance helps in reducing effectively the thermal circuit between the U-tube pipes and hence leads to lower the BHE resistance value.

According to Figure 7.2, the BLRR is approximately only 5%. This reduction rate is small and will not make a huge difference to the system's thermal efficiency or to the installation costs.

Therefore, in order to achieve the highest reduction rate in the borehole, complete elimination to the value of borehole resistance must be achieved. For this reason, the following analysis will present the new types of barriers that may be inserted between the single U-tube pipes .

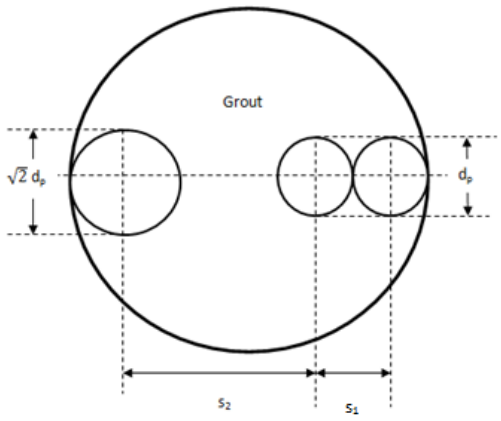

Figure 7.7: Geothermal heat exchanger geometry with two inlet pipes and one outlet pipe.

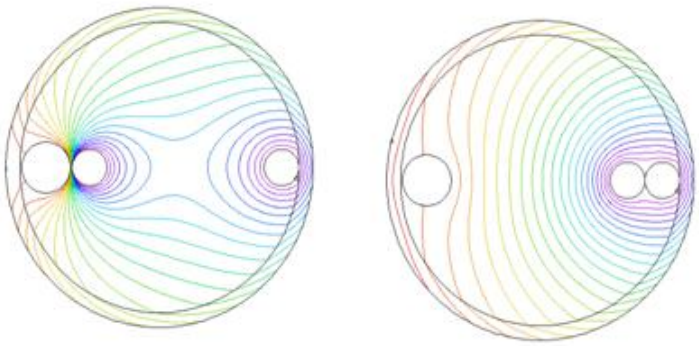

Figure 7.8: Isothermal lines in the borehole when two inlet pipes and one outlet pipe are used.

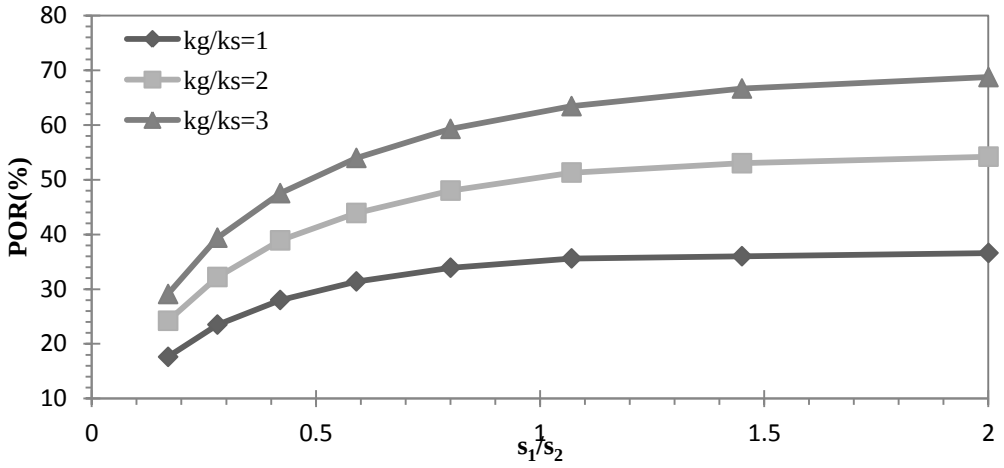

Figure 7.9: Percentage of reduction in the borehole thermal resistance value as a function of dimensionless s_1/s_2 ratio.

Table 7.7: Borehole thermal resistance as a function of spacing between the outlet pipe and dummy pipe(S_2), and between dummy pipe and the inlet pipe(S_1) with a ratio of k_g/k_s is 1.

S_1	S_2	R_b	POR (%)
0.02	0.115	0.0955	17.6
0.03	0.105	0.0887	23.5
0.04	0.095	0.0835	28.0
0.05	0.085	0.0795	31.4
0.06	0.075	0.0766	33.9
0.07	0.065	0.0747	35.6
0.08	0.055	0.0736	36.0
0.09	0.045	0.0735	36.6

Note: original geometry without the dummy pipe recorded is 0.116 K.m/W and BHE resistance when k_g/k_s is 1. This value has been used to find the POR.

Table 7.8: Borehole thermal resistance as a function of spacing between the outlet pipe and dummy pipe(S_2), and between dummy pipe and the inlet pipe(S_1) with a ratio of k_g/k_s is 2.

S_1	S_2	R_b	POR (%)
0.02	0.115	0.0539	24.2
0.03	0.105	0.0482	32.2
0.04	0.095	0.0435	38.9
0.05	0.085	0.0399	43.9
0.06	0.075	0.0370	48.0
0.07	0.065	0.0349	51.3
0.08	0.055	0.0334	53.0
0.09	0.045	0.0326	54.2

Note: original geometry without the dummy pipe is recorded as 0.0712 K.m/W and BHE resistance when k_g/k_s is 2. This value is used to find the POR.

Table 7.9: Borehole thermal resistance as a function of spacing between the outlet pipe and dummy pipe(S_2), and between dummy pipe and the inlet pipe(S_1) with a ratio of k_g/k_s is 3.

S_1	S_2	R_b	POR (%)
0.02	0.115	0.0370	29.09
0.03	0.105	0.0320	39.39
0.04	0.095	0.0277	47.53
0.05	0.085	0.0243	53.97
0.06	0.075	0.0215	59.28
0.07	0.065	0.0193	63.44
0.08	0.055	0.0176	66.66
0.09	0.045	0.0165	68.75

Note: original geometry without the dummy pipe is recorded as 0.0526 K.m/W and BHE resistance when k_g/k_s is 3. This value is used to find the POR.

7.3.2. Barrier Between The U-tube Pipes

Adding a barrier between the inlet and outlet pipes is another solution that aims to reduce the borehole thermal resistance effect from the borehole heat exchanger system. Two types of materials will be used to form this barrier, namely are: plastic and brass. The barrier materials will be added at different configurations for maximum reduction in BHE resistance.

Plastic was selected as the insulator because of the following features (Productive Plastic (PP) Inc., 2013):

1. Resistance to corrosion and chemicals.
2. High strength-to-weight ratio.
3. Good durability.
4. Low cost.
5. Ease of manufacture.
6. Resistance to water.

7. Plastic materials have different low thermal conductive values ,as illustrated in Table 7.10.

Brass is the generic term for a range of copper-zinc alloys with differing combinations of properties, including strength, wear-resistance, hardness, colour, and corrosion-resistance (Smith, 1982).However, brass was chosen simply because:

1. It does not become brittle at low temperatures.
2. It has an excellent thermal conductivity of 109 W/K.m, making it a first choice for heat exchangers.
3. Almost 100% of brass is made from recycled materials.

The first step in this investigation, will present the original borehole geometries and their borehole resistance values ,as shown in Figure 7.10.The subsequent steps will take place by adding plastic and brass layers between the U-tube pies.

Table 7.10: Different plastic material thermal conductivity (Engineering tool box, 2013)

Plastic	Thermal Conductivity W/K.m
Epoxy	0.17
Epoxy glass fibre	0.23
Polyethylene, low density (PEL)	0.33
Polyethylene, high density (PEH)	0.50

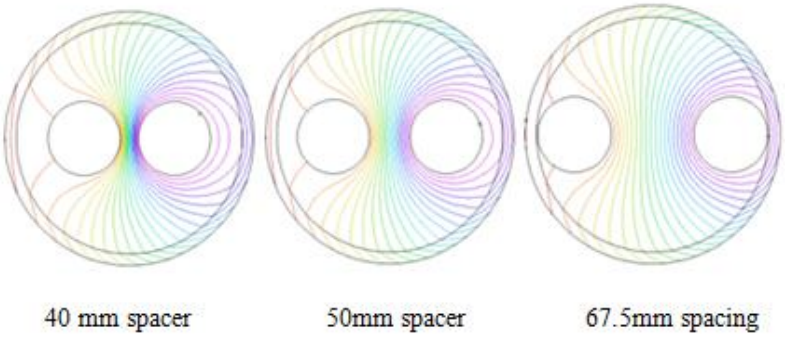

Figure 7.10: U-tube pipe configuration.

Figure 7.10 presents the isothermal lines inside the borehole for three pipe configurations employed in this investigation, while Table 7.11, presents the original values of borehole thermal resistance. Two types of barriers will be investigated in this chapter, where both will be located between the inlet and outlet pipes. The next section will investigate the effect of the I-shaped barrier formed by plastic and/or brass materials.

Table 7.11: Borehole thermal resistance values using original geometry without a plastic barrier, when k_g/k_s is 2.

Case Number	Pipe Configuration	Borehole Thermal Resistance (K.m/W)
1	40mm spacer centred	0.0528
2	50mm spacer centred	0.0463
3	67.5mm spacer centred	0.0385

Note: the configurations were specifically chosen so that they did not cut into the barrier wall.

7.3.2.1. The I-Shaped Barrier

An I-shaped barrier of 80mm width and 3mm thickness is located exactly between the U-shaped pipes. The main target for this barrier is to reduce the short circuit between the U-tube legs without affecting the area of thermal interference between the inlet pipes and the borehole surrounding.

The mid plastic I-shaped barrier will be added to the three geometric configurations that modified according to the shank spacings, as shown in Figure 7.10. The barrier will be located within the borehole geometry as shown in Figure 7.11. The isothermal lines resulted from the numerical simulation are presented in Figure 7.12.

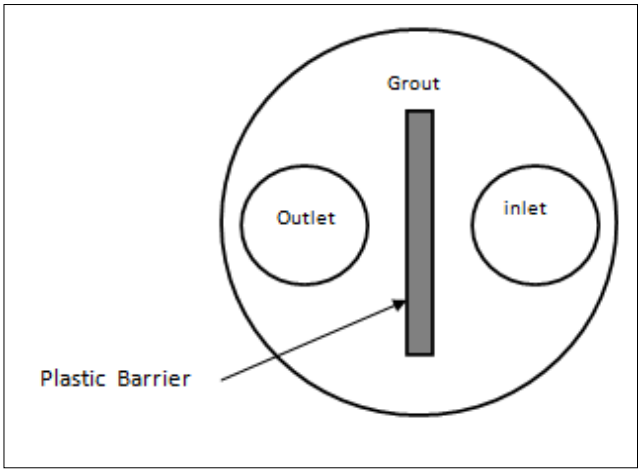

Figure 7.11: Diagram to the borehole geometry with the I-shaped plastic barrier located between the U-tube legs.

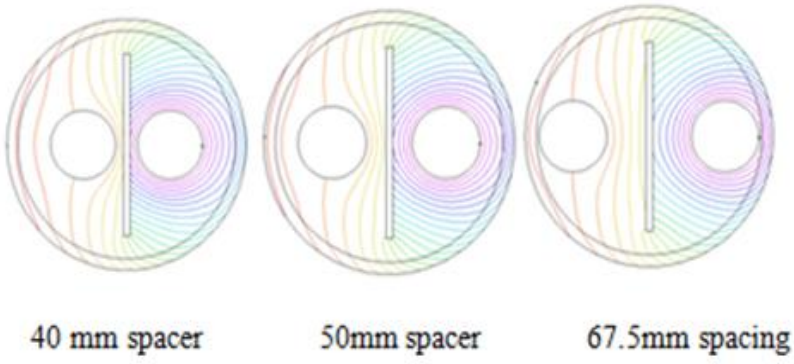

Figure 7.12: Numerical simulation for the borehole located between the U-shaped pipes and separated by 40mm, 50mm and 67.5mm, respectively.

As can be seen from Figure 7.12, the isothermal lines' configuration is different as compared to the original geometry in Figure 7.10, where the isothermal lines more steep near the borehole centre after adding the plastic barrier.

A diagram to the temperature distribution on the plastic barrier is illustrated in Figure 7.13, where higher temperatures are located around the top and bottom of the plastic barrier. The resulted borehole thermal resistance, after adding the barrier and the percentage of reduction, are presented in Table 7.8.

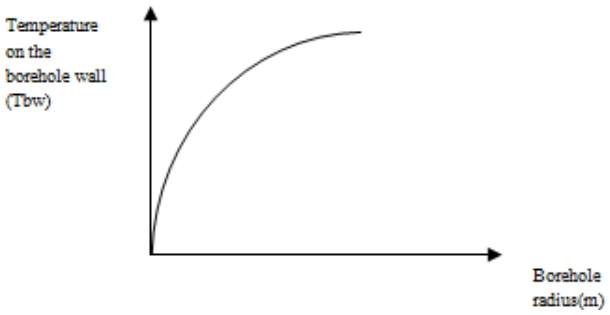

Figure 7.13 Diagram for the temperature distribution after adding plastic I-shaped barrier.

Table 7.12: Borehole thermal resistance values using the I-shaped plastic barrier as a function of plastic thermal conductivity when kg/ks is 2, where kg is 2 W/K.m.

Plastic Material W/K.m	40mm spacer		50mm spacer		67.5mm spacer	
	R_b	POR (%)	R_b	POR (%)	R_b	POR (%)
0.17	0.0536	+15	0.047	+15	0.0389	+10.2
0.23	0.0536	+15	0.047	+15	0.0389	+10.2
0.33	0.0535	+13	0.0469	+13	0.0389	+10.2
0.5	0.0534	+11	0.0469	+13	0.0389	+10.2

As can been seen in Table 7.12, all the percentage of reduction are positive values. This indicates that adding the plastic I-shaped barrier leads to an increase, instead of decrease, in the values of BHE resistance. This may be due to the fact that the mid barrier has low thermal conductivity, which means that the temperature is

distributed unevenly between the inlet pipe and the barrier. Therefore, a reflector layer made of 3mm thickness of brass is added to the plastic layer next to the inlet pipe ,as shown in Figure 7.15.

The fact that the main aim is for the inlet pipe to exchange a maximum amount of heat and for the outlet pipe to maintain the gained heat, this step might produce better results in terms of reducing borehole resistance. The results of the numerical steady-state simulation are presented in Figure 7.14.

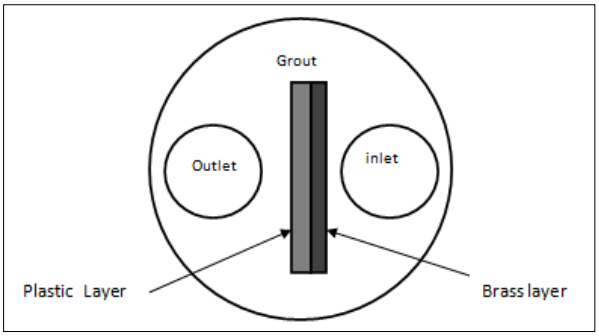

Figure 7.14: Diagram of the plastic I-shaped barrier with a reflector (brass layer) added next to the inlet pipe.

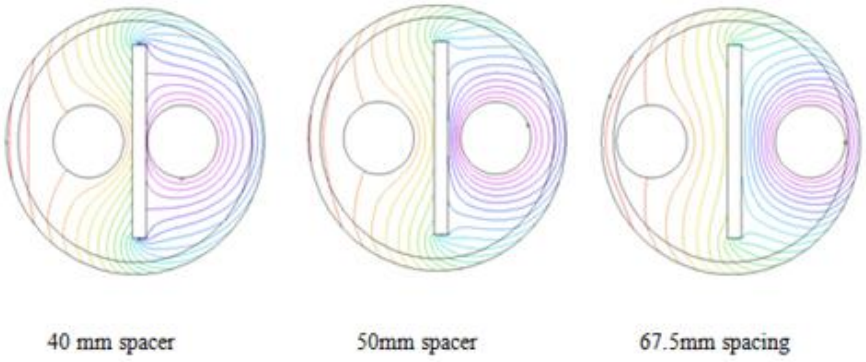

Figure 7.15: Numerical simulation for the borehole when the I-shaped plastic barrier, with a right layer of brass, is located between the U-shaped pipes and separated by 40mm, 50mm and 67.5mm, respectively.

It can be seen from Figure 7.15, that the isothermal lines are distributed more evenly along the reflector layer when minimum shank spacing was applied. This might indicate achieving lower BHE resistance value as compared to the other U-

pipe configuration. The impact of the addition of a reflector layer on borehole thermal resistance is illustrated in Table 7.13.

It is clear from Table 7.13, that borehole thermal resistance values were reduced when the right layer of brass was added to the plastic barrier. In fact, the percentage of reduction in BHE resistance reached a maximum of 45% when 40 mm shank spacing applied. This is the highest percentage of reduction recorded since adding the mid I-shaped barrier. However, according to Table 7.2, this will only led to 8%reduction on the borehole loop length near perfect borehole conditions. Therefore, a complete elimination of the value of borehole resistance is crucial to achieve significant decrease in the depth of the borehole.

Table 7.13: Borehole thermal resistance values as a function of plastic thermal conductivity, using an I-shaped plastic barrier with the right layer of brass located between the U-shaped pipes and separated by 40mm, 50mm and 67.5mm, respectively, when k_g/k_s is 2.

Plastic Material W/K.m	40mm spacer		50mm spacer		67.5mm spacer	
	R_b	POR (%)	R_b	POR (%)	R_b	POR (%)
0.17	0.0298	-44.0	0.0336	-36.0	0.0318	-39.7
0.23	0.0295	-44.1	0.0340	-35.6	0.0322	-39.0
0.33	0.0293	-44.5	0.0344	-34.8	0.0325	-38.4
0.5	0.0290	-45.0	0.0349	-33.9	0.0328	-37.8

Note: the original values of R_b were 0.0528, 0.0463 and 0.0385 K.m/W for 40mm, 50mm and 67.5mm spacing, respectively.

7.3.2.2 The U-Shaped Barrier

It is known now that the plastic barrier on its own, does not reduce the value of borehole resistance, and adding a reflector layer assessed in reducing the BHE

value to almost half. Therefore next step will investigate the effect of adding U-shaped barrier made of plastic layer with outer layer brass placed around the outlet pipe on BHE resistance.

The new solution composed of 3mm thickness of U-shaped plastic layer with 3 mm thickness of outer reflector layer made of Brass, to be placed around the outlet pipe ,as shown in Figure 7.16.

Two configurations were chosen for this analysis so that they would not cut into the U-shaped barrier, where shank spacing(s) are 40 mm and 50 mm. The results of the numerical steady-state simulation are presented in Figure 7.17. The influence of this barrier on the value of borehole resistance is presented in Table 7.14.

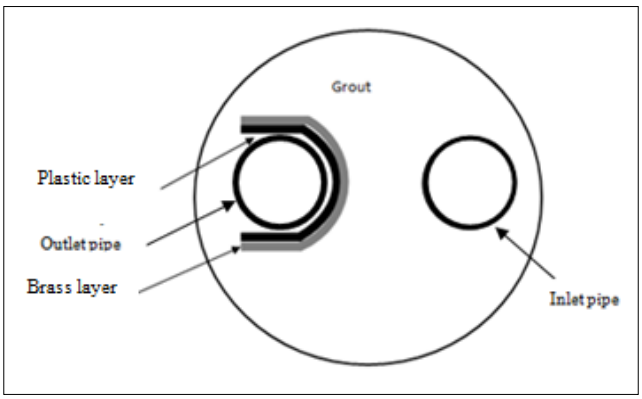

Figure 7.16: Diagram for the plastic U-shaped barrier, consisting of plastic and brass material surrounding the outlet pipe.

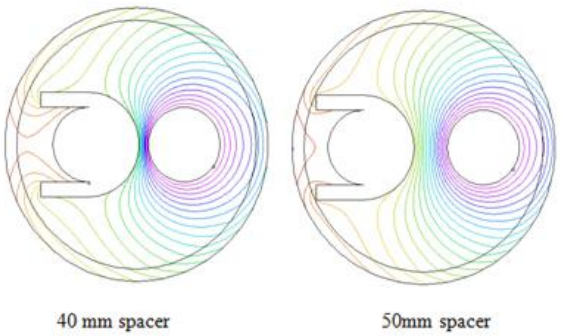

Figure 7.17: Numerical simulation for the borehole when the U-shaped plastic barrier, with an outer layer of brass, is located between the U-shaped pipes and separated by 40mm and 50mm, respectively.

Table 7.14 clearly indicates that a significant decrease in the value of borehole thermal resistance is achieved when adding a single layer of brass to the outer surface of the U-shaped plastic layer. In fact, BHE resistance decreased to 77 %when compared to the resistance obtained from the original geometry. This may be due to the fact that the brass layer has high thermal conductivity, which is assessed in increasing the thermal heat exchange between the inlet pipe and grout, i.e. the difference between the borehole wall temperature and the average inlet and outlet pipes temperature has decreased, leading to a decrease the value of BHE resistance.

The following investigation will examine the influence of using 6mm thickness of the plastic layer instead of 3mm with 3 mm reflector layer to the outer side of the barrier, on the value of borehole thermal resistance. The resulting numerical isothermal lines in the borehole are presented in Figure 7.18.The influence of the above barrier on the BHE resistance is presented in Table 7.15.

Table 7.14: Borehole thermal resistance values using the U-shaped plastic barrier with the outer layer of brass located between the U-shaped pipes, and separated by 40 and 50mm, respectively, as a function of plastic thermal conductivity when k_g/k_s is 2.

Plastic Material W/K.m	40mm spacer		50mm spacer	
	R_b	POR (%)	R_b	POR (%)
0.17	0.0122	-77.00	0.0215	-53.56
0.23	0.0154	-70.83	0.0244	-47.30
0.33	0.0198	-62.5	0.0280	-39.52
0.5	0.0254	-51.89	0.0322	-30.45

Note: the original values of R_b were 0.0528 and 0.0463 K.m/W for 40mm and 50mm spacing, respectively.

In Table 7.11, the borehole thermal resistance impact on BHE was eliminated. This indicates that the temperatures inside the borehole are equal or higher to the assumed average value of the undisturbed temperatures, i.e. there is no resistance to the temperatures inside the borehole ,as illustrated in Figure 7.19.

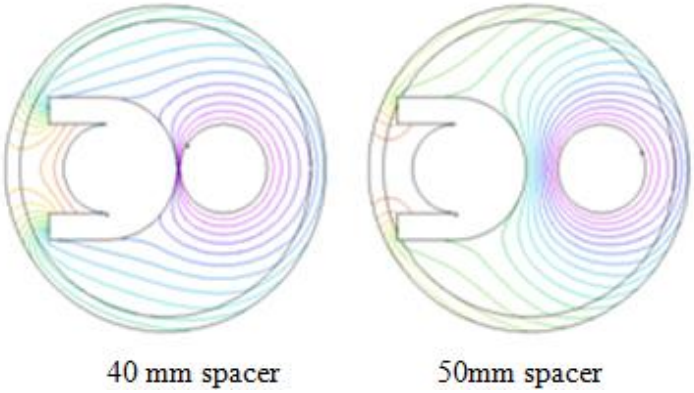

Figure 7.18: Numerical simulation for the borehole when the barrier consists of a U-shaped 6mm plastic barrier and a 3mm thick outer layer of brass, which is located between the U-shaped pipes and separated by 40mm and 50mm, respectively.

Table 7.15: Percentages of reduction to the values of borehole resistance using a 6mm inner layer U-shaped plastic barrier with a 3mm outer layer of brass, located between the U-shaped pipes but separated by 40mm and 50 mm, respectively, as a function of plastic thermal conductivity, when k_g/k_s is 2.

Plastic Material W/K.m	40mm spacer		50mm spacer	
	R_b	POR (%)	R_b	POR (%)
0.17	0.0005	-100	0.0008	-98.3
0.23	0.0003	-100	0.0030	-93.5
0.33	0.0004	-100	0.0060	-87
0.5	0.0037	-93	0.0105	-77.3

Note: the original values of R_b were 0.0528 and 0.0463 K.m/W for 40mm and 50mm spacing, respectively.

As can be seen from Figure 7.20, the distribution of the temperature around the borehole wall is better after adding U-shaped plastic barrier with an outer layer of brass. This may be because of the fact that brass assess in transferring heat to the inlet pipe leading to increase the heat exchanged, as illustrated in Figure 7.21.

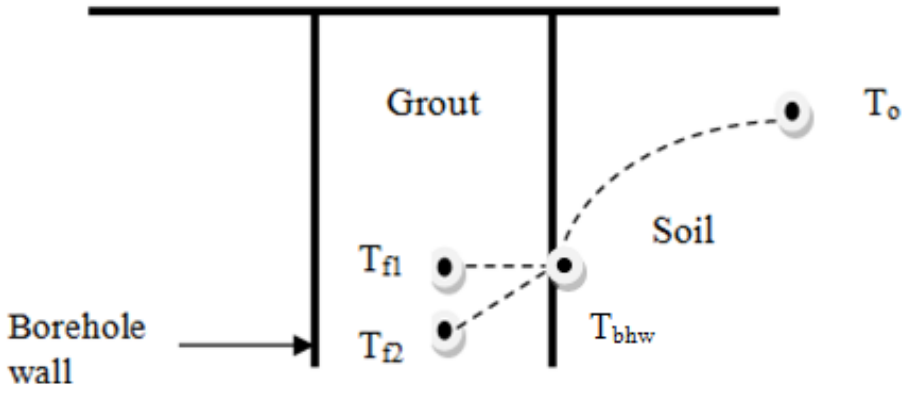

Figure 7.19: Diagram to clarify the undisturbed temperature (T_o), temperatures around the borehole wall (T_{bhw}), and average temperatures of the inlet and outlet pipes (T_f) when BHE resistance existed (T_{f2}), and when BHE resistance eliminated from the system (T_{f1}).

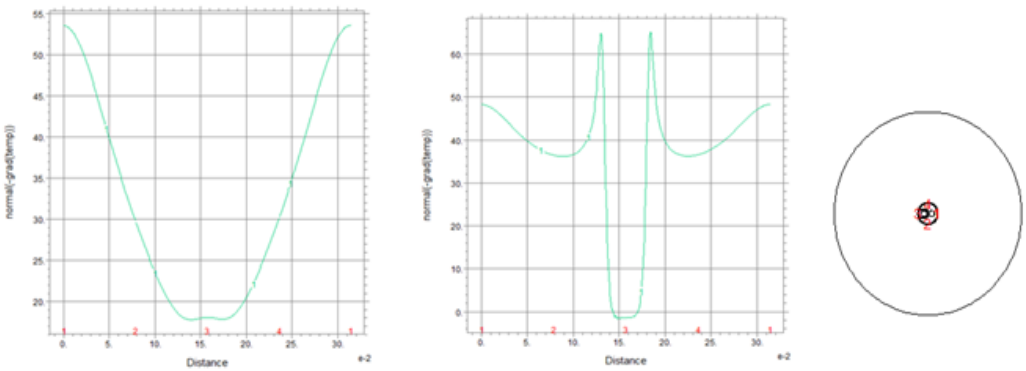

Case 1 Case 2

Figure 7.20: Temperature around the borehole wall before (case 1) and after (case 2) adding the U-tube barrier which consists of an outer layer of brass and an inner plastic that have thicknesses of 3mm and 6mm, respectively.

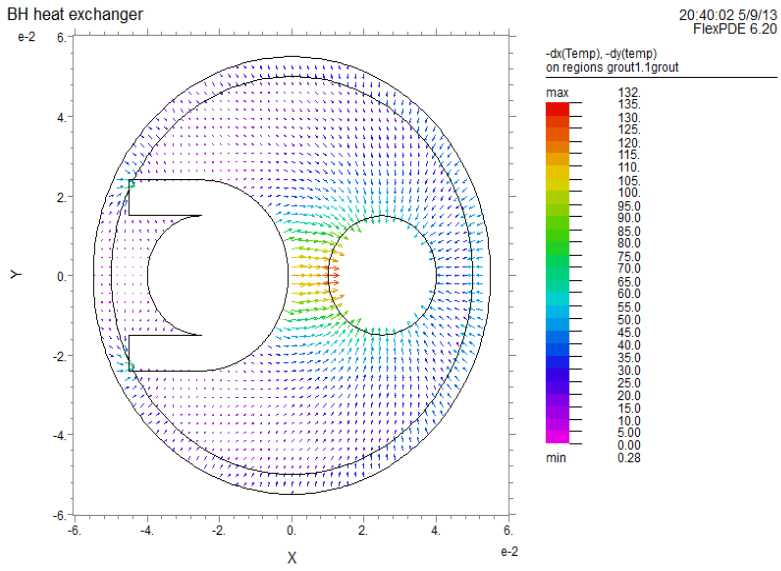

Figure 7.21: The diagram shows the direction of heat transfer in a single U-tube borehole when the U-shaped barrier consists of plastic, and an outer brass layer located around the outlet pipe.

A complete elimination to the BHE resistance in perfect ground conditions leads to a reduction in the borehole depth to 16% as illustrated in Figure 7.2. A 16% reduction in the borehole depth is a defiant mark of improvement in the solutions presented in this chapter. However, this indicates that even by eliminating the borehole resistance, a reduction in the is not significant. This is due to the fact that the borehole thermal resistance is only 15 to 25 % from the total resistance, and the rest is attributed to the ground around the borehole (Kavanaugh, 2010). Hence, reducing the total resistance is crucial to optimising the BHE system, therefore, deep mixing technique is explained in the following section.

7.4 Deep Mixing

Deep Soil Mixing (DSM) is one of the successful ground improvement techniques to stabilize soft and problematic soils. It treats the soil by mixing it with cementitious and/or other reagent materials. The reagent is injected through the hollow rotating Kelly bars, with some type of cutting tool at the bottom, as shown in Figure 7.22 (Madhyannapu, 2007).

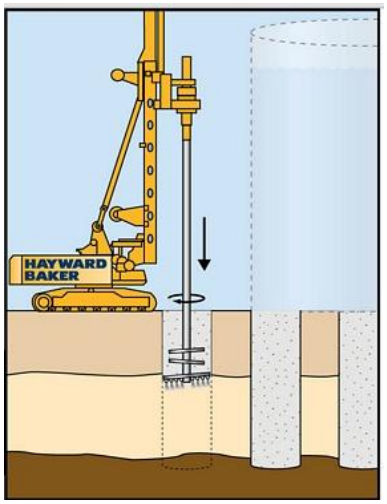

Figure 7.22: Wet soil deep mixing (Madhyannapu, 2007).

In this study, the deep mixing approach is proposed to improve the thermal properties of the soil. In order to examine the impact of deep mixing on the total thermal resistance value, a 2D numerical simulation analysis, using the Flex PDE program, will be carried out.

The first step in this investigation is conducted to assess the influence of soil diameter on ground thermal resistance, before commencing the deep mixing, as illustrated in Table7.12.

The total thermal resistance values increase with a increase in soil diameter, until 20m diameter when the soil diameter's effect on the total thermal resistance becomes negligible. The borehole resistance value was constant for each ratio.

Since the results shows that the R_g is responsible for 85 to 75 % of the total resistance (Kavanaugh, 2010), its increase leads to a significant rise in the values

of R_t. However, the influence of soil diameter started to insignificant after 20m , as shown in Table 7.16.

Reducing the total thermal resistance may be achieved by increasing the soil thermal conductivity. Natural graphite (NG) is well known as highly anisotropic forms of carbon with low density and is abundantly available in nature, can be used for this purpose by mixing it with the soil.(Zheng W. G. et al. 2002; Chen G. H. et al, 2001).

Natural graphite has good thermal conductivity (k=2000W/m/K in a-direction) and is highly temperature dependent (Kelly B.T., 1981). The superior thermal property along two directions makes it one of the potential candidates to combat thermal management problems. Natural graphite has high chemical and thermal stability over a range of temperatures with a very high melting point, high thermal and electrical conductivity and is resistant to attack by most chemical reagents. Hence, graphite has attracted researchers to enhance thermal conductivity in various applications.

In fact the maximum diameter of deep mixing is about 0.5 m, the deep mixing radius employed will be 0.25m. The analysis will aim to estimate the total thermal reduction as a function of the ratio between deep mixing thermal conductivity to soil thermal conductivity. The total reduction in the value of loop length can be calculated by subtracting the original total resistance from the reduced one, followed by a division of the answer on the original value of R_t ,as illustrated in Appendix C Tables C.1 to C.9.

Figure 7.23, proves that the higher thermal conductivity of the soil, the lower total resistance of the whole GBH system. The ground thermal resistance values were found to be constant during the deep mixing. This is due to the fact that the ground resistance is a function of undisturbed ground temperature and the temperature around borehole wall. Since there is no change in these temperatures during the analysis, the R_g values did not change.

The maximum reduction to the total thermal resistance was found to be 31%. Therefore, a reduction in the total borehole depth if deep mixing is applied can

reach 31%. However, if the U-shape barrier is applied (inner plastic and outer layer of brass) next to the outlet pipe, the borehole thermal resistance can be eliminated from the total resistance value. Therefore, the reduction rate can reach a value of 34%. This reduction can make significant reductions on GSHP installation costs.

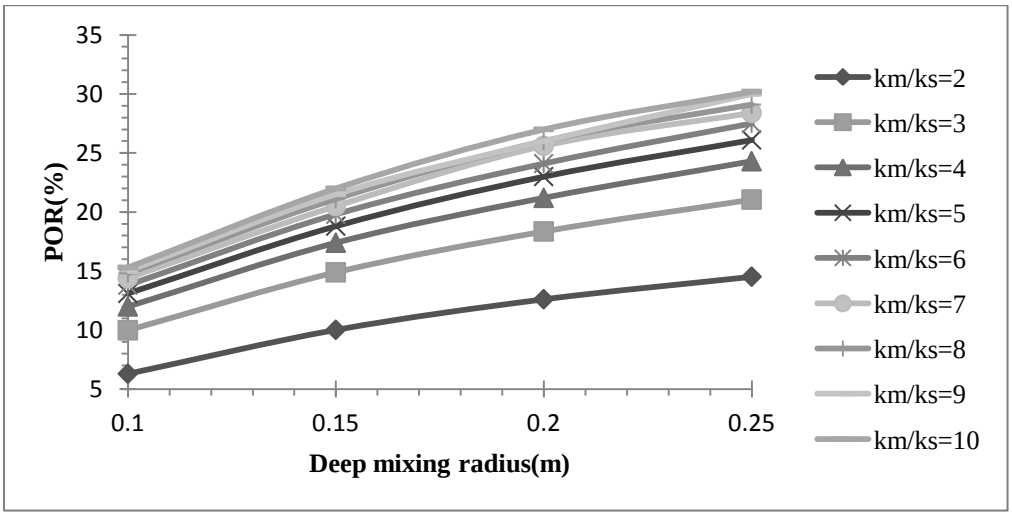

Figure 7.23: The Percentage of Reduction in the total thermal resistance as a functioned deep mixing radius and the ratio of k_m/k_s.

Table 7.16: Total thermal resistance as a function of soil diameter around the borehole when shank spacing is 50mm and k_g/k_s is 2.

Soil Diameter (m)	**Ground Thermal Resistance (R_g) (K.m/W)**	**Borehole Thermal Resistance (R_b) (K.m/W)**	**Total Thermal Resistance (R_t) (K.m/W)**
1	0.366	0.0464	0.4124
2	0.476	0.0465	0.5225
3	0.541	0.0465	0.5875
4	0.586	0.0465	0.6325
5	0.622	0.0465	0.6685
6	0.0651	0.0466	0.1117
7	0.675	0.0466	0.7216
8	0.696	0.0467	0.7427
9	0.715	0.0467	0.7617
10	0.732	0.0467	0.7787
11	0.747	0.0467	0.7937
12	0.761	0.0467	0.8077
13	0.774	0.0467	0.8207
14	0.785	0.0467	0.8317
15	0.796	0.0468	0.8428
16	0.807	0.0468	0.8538
17	0.816	0.0468	0.8628
18	0.826	0.0468	0.8728
19	0.834	0.0468	0.8808
20	0.842	0.0468	0.8888

7.5. Summary and Conclusion

Reducing borehole thermal resistance to optimize the use of ground source heat pump systems was the main aim of this chapter, and a variety of methods were investigated. 2D finite element analyses, using the Flex PDE analysis, were established to find the best method in terms of BHE resistance reduction.

As concluded from chapter six, the shank spacing is considered vital to achieving this goal, hence GEOCLIPS was introduced to this field. These GEOCLIPS assess control of the shank spacing between the U-tube legs throughout the entire borehole depth. Hence, these clips aim to reduce thermal interference between the U-tube legs.

Another solution was introduced to assess limiting thermal interference between the U-tube legs (suggested by Lee et al., 2010). The solution was mainly based on adding a low thermal conductivity zone between the U-pipes, and in this case air was used. After applying this solution using Flex PDE, it was found that borehole resistance values did not change after adding the air zone. In fact they increased. This was mainly because the solution reduced the thermal interference between the two pipes, leading to a higher difference between the undisturbed ground temperature and the surrounding.

Therefore, other solutions were presented such as the dummy pipe. This solution intended to use W-shaped pipes instead of U shaped pipes, where two inlet pipes and one outlet pipe are used. This solution resulted in a dramatic reduction in the value of BHE resistance when enhanced grout was used. However, the question is whether this solution is applicable in a real life installation.

Other solutions include adding an I-shaped barrier and a U-shaped barrier between the U-shape pipes. It was found that a U-shaped barrier, consisting of a plastic barrier of 6mm in thickness and a layer of brass to the outer side, achieved outstanding results in completely eliminating BHE resistance values from the GSHP system. However, even with eliminating borehole thermal resistance the total reduction in borehole length, in near perfect ground conditions, was found to be only 16 %.

The deep mixing technique was then presented to reduce the total thermal resistance of GSHP systems. The results of the investigation point to the fact that the higher the thermal conductivity, the lower the total resistance.

If both the deep mixing technique and the application of the U-shaped barrier are used, which will reduce the total thermal resistance by deep mixing, this leads to a 34 % reduction in the total loop length. This reduction will significantly enhance the thermal performance of the GSHP and reduce the installation costs associated with drilling and materials. Therefore, the research's aim to optimise the GSHP system was achieved.

Chapter 8: Summary and Conclusion

8.0. Introduction

The primary aim of this study was to develop a two-dimensional numerical model for borehole heat exchangers (BHEs) in order to calculate the value of borehole thermal resistance and purpose methods to reduce it, to encourage the economic feasibility of the GSHP system.
In this chapter, a summary of the main findings, with respect to the aims and objectives, are presented. This is followed by a discussion to the potential areas for further research.

8.1. Summary and Conclusion

GSHP has low impact on the environment, therefore it is recommended choice in energy supply, especially for large buildings where the upfront cost is not a pressure for the owners.

Sensible sizing to ground loop length is crucial, since the efficiency of vertical loops (defined by loop length and the amount of heat extracted from the soil) varies significantly depending on the rate at which the heat transfers through the soil to the U-tube pipes. This rate is mainly controlled by the thermal resistance between the U-tube pipes and the borehole wall (borehole thermal resistance) and between the borehole wall and surrounding ground(ground thermal resistance).
The ground thermal resistance found to be influenced by the thermal properties of the soil around the vertical closed loop system. The soil thermal properties includes the thermal conductivity, heat capacity, and thermal diffusivity.

The soil thermal conductivity is significantly influenced by the saturation and dry density. Therefore, an increase in either the saturation or dry density of a soil will result in an increase in its thermal conductivity.

The higher the thermal conductivity of the soil, the less ground resistance, and hence more heat is transferred per unit of piping. This will reduce the installation costs because of shorter U- tubes being required. Therefore, it can be concluded that the soil thermal impacts the sizing of the total system.

In all design methods for sizing of the borehole depth in GSHP systems, the borehole resistance is also quite crucial parameter in the estimation of the required borehole length. This resistance can be obtained using theoretical expressions or can be measured experimentally.

This research assessed number of methods established mainly to calculate the value of borehole resistance. These methods include Paul(1996);Sharqawy et al.(2009); Bennet et al.(1987); Shonder and Beck(1999); Gu and O'Neal(1998); and Hellstrom(1991).

Paul's (1996) equation depends on coefficients that have been derived based on three configurations: close together, average pipe, and along outer wall. Therefore, this equation is only suitable for specific parameters. Changing pipes' positions or spacing between the U-tube pipes, without being categorized under the three main configurations, is not considered an option. However, even after following the same configurations the results were far from the numerical results obtained using Flex PDE.

In addition, Shonder and Beck(1999) overestimated the values of borehole thermal resistance by 98% and 85%, respectively. Overestimating the value of borehole thermal resistance will lead to overestimating the required depth of the borehole, and hence the installation cost. However, Bennet et al. (1987) and Hellstrom (1991)equations produced the most accurate results with regards to the values of borehole resistance, with a maximum difference to the numerical resistance of 1.225% and 13.13 % respectively.

A thorough analysis using the Flex PDE software was a constructive first step to narrow down the most influential parameters in the design of BHE. The results

revealed that the borehole diameter greatly influence the values of the borehole thermal resistance.

In addition, the thermal conductivity of the surrounding soils and the backfilling materials were found to greatly affect the value of BHE resistance. It was found that the higher the thermal conductivity of the grout, the less BHE thermal resistance of the heat exchanger system. In another word, when the borehole and pipe diameters assumed to be 0.1m, and 0.03m respectively, the increase in the ratio of k_g/k_s to from 0.6 to 3, led to decrease the value of borehole resistance to 80%. Hence, it is important to use thermally enhanced grout inside the borehole in order to reduce the length of the ground loop, and thus enhance the efficiency of the GSHP.

Moreover, the effect of shank spacing(s) between the two legs of the U-pipe were found to significantly affect BHE resistance. Using the original parameters utilized in this research proved that reducing the shank spacing led to an increase in the borehole thermal resistance by 37%.

However, the thickness of the U-tube wall found to have no influence on the value of borehole thermal resistance, and therefore the pipe wall thermal conductivity did not affect BHE resistance.

Due to the difficulty found in determining the value of borehole thermal resistance, Contour Charts were introduced to calculate the borehole thermal resistance as a ratio between of numerical to analytical resistances. These ratios were calculated as a function of the most influential parameters on BHE thermal resistance, i.e. the borehole and U-tube diameter and shank spacing. After assessing the borehole thermal resistance values obtained from the Contour Charts, a maximum difference of 1% was found, when compared to the numerical borehole resistance. This percentage proved that the new Contour Charts are better than all the equation explained earlier including Bennet et al. (1987).

Reducing borehole thermal resistance to optimize the use of borehole heat exchanger systems was the main aim of conducting this thesis. Therefore, variety

of methods were investigated. A 2D numerical analysis, using Flex PDE program, was conducted to find the best method in terms of BHE resistance reduction.

Solutions, such as adding the dummy pipe, have been presented in chapter seven to reduce the value of borehole resistance. This solution resulted in a dramatic reduction in the value of BHE resistance when enhanced grout was used. However, the question is whether this solution is applicable in real life installations.

Other methods were suggested in this thesis to include adding either an I-shaped barrier or a U-shaped barrier between the U-shape pipes. These barriers were composed of brass and plastic materials. In both barriers, when placing a plastic barrier in the middle with a layer of brass material to the right side in cases of the I-shaped barrier, and the outer layer in cases of the U-shaped barrier, these processes achieved outstanding results in reducing BHE resistance.

However, the best result was obtained from the U-shaped barrier when maximum shank spacing applied. Nevertheless, even when eliminating borehole thermal resistance the total reduction in borehole length in near perfect ground conditions was found to be only 16 %.

Therefore, the deep mixing technique was presented in this study to further reduce the total thermal resistance of GSHP systems. The results of the investigation point to the fact that the higher thermal conductivity of the soil around BHE, the total lower resistance.

If both the deep mixing technique and the application of a U-shaped barrier are used, this will reduce the total thermal resistance by deep mixing and lead to a 34 % reduction in the total loop length. This reduction will significantly enhance the thermal performance of the GSHP and help to reduce installation costs associated with drilling and materials.

8.2. Future Work

The calculations of the value of borehole thermal resistance in both Flex PDE and the equations proposed in the literature are based on the fact that the U-tube pipes are located on the borehole centre. Therefore, the lack of equations to calculate R_b in different U-tube pipe positions within borehole, suggests to develop equation that is suitable for any U-pipe position.

Elimination of the borehole resistance was found in the steady-state analysis, which meant the effect of time was not counted. Therefore, applying an unsteady-state analysis is crucial to identifying the effect of the barrier in the longer term.

Also all the results in this thesis are based on the fact that there is no water movement under the ground. So, the question is whether the ground movement influences the total thermal resistance of the GSHP system.

In this research, it was concluded that changing the pipes' positions within the borehole will not have great influence on thermal resistance values; however, this conclusion might change if ground water movement existed. Future analyses of ground water movement, therefore, should investigate the portions of U-tube pipes and whether less resistance will occur when placing U-tube pipes perpendicular and parallel to water movement.

Appendix A : Borehole thermal resistance values as a function of k_g/k_s and s/d_b.

Tables A.1 to Table A.6 summarise the effect of ratios of k_g/k_s and s/d_b on the borehole thermal resistance. To normalise the resistance values, they are given as a ratio of the analytical value for resistance for concentric single pipe in borehole given by Incropera and Dewitt(2002).

The values of borehole resistance obtained in Table A.1 to A.6, are quiet close , however the closest values for all the ratios of k_g/k_s are presented in Table A.5.

Table A.1: Summary of results demonstrating the effect of ratio s/d_b on the borehole resistance, when k_g/k_s is 1.0.

K_g/k_s = 1.0 W/K.m					
No.	s/d_b	d_b/d_p	$R_{numerical}$	$R_{analytical}$	$R_{numerical}/R_{analytical}$
1	(0.075/0.2)0.375	(0.2/0.075)2.67	0.084772	0.156183	0.542774
2	0.375	2.86	0.092055	0.167169	0.55067
3	0.375	3.07	0.099708	0.17897	0.557121
4	0.375	3.33	0.107793	0.191715	0.562256
5	0.375	3.64	0.116370	0.205571	0.566082
6	0.375	4	0.125540	0.220748	0.568703
7	0.375	4.44	0.135412	0.237525	0.570096
8	0.375	5	0.146151	0.25628	0.570279
9	0.375	5.71	0.158024	0.277543	0.569368
10	0.375	6.67	0.171394	0.302089	0.567363
11	(0.08/0.2)0.4	(0.2/0.075)2.67	0.081311	0.156183	0.520614
12	0.4	2.86	0.088436	0.167169	0.529022
13	0.4	3.07	0.095950	0.17897	0.536123
14	0.4	3.33	0.103893	0.191715	0.541914

15	0.4	3.64	0.112317	0.205571	0.546366
16	0.4	4	0.121332	0.220748	0.54964
17	0.4	4.44	0.131050	0.237525	0.551731
18	0.4	5	0.141641	0.25628	0.552681
19	0.4	5.71	0.153375	0.277543	0.552617
20	0.4	6.67	0.166623	0.302089	0.551569
21	(0.085/0.2)0.425	(0.2/0.075)2.67	0.077925	0.156183	0.498934
22	0.425	2.86	0.084929	0.167169	0.508043
23	0.425	3.07	0.092317	0.17897	0.515824
24	0.425	3.33	0.100125	0.191715	0.52226
25	0.425	3.64	0.108411	0.205571	0.527365
26	0.425	4	0.117290	0.220748	0.53133
27	0.425	4.44	0.126874	0.237525	0.53415
28	0.425	5	0.137339	0.25628	0.535894
29	0.425	5.71	0.148957	0.277543	0.536699
30	0.425	6.67	0.162097	0.302089	0.536587
31	(0.09/0.2)0.45	(0.2/0.075)2.67	0.074635	0.156183	0.477869
32	0.45	2.86	0.081525	0.167169	0.48768
33	0.45	3.07	0.088797	0.17897	0.496156
34	0.45	3.33	0.096484	0.191715	0.503268
35	0.45	3.64	0.104648	0.205571	0.50906
36	0.45	4	0.113407	0.220748	0.51374
37	0.45	4.44	0.122876	0.237525	0.517318
38	0.45	5	0.133232	0.25628	0.519869
39	0.45	5.71	0.144750	0.277543	0.521541
40	0.45	6.67	0.157801	0.302089	0.522366
41	(0.095/0.2)0.475	(0.2/0.075)2.67	0.071426	0.156183	0.457322
42	0.475	2.86	0.078222	0.167169	0.467922
43	0.475	3.07	0.085387	0.17897	0.477102

44	0.475	3.33	0.092964	0.191715	0.484907
45	0.475	3.64	0.101019	0.205571	0.491407
46	0.475	4	0.109674	0.220748	0.496829
47	0.475	4.44	0.119042	0.237525	0.501177
48	0.475	5	0.129304	0.25628	0.504542
49	0.475	5.71	0.140739	0.277543	0.507089
50	0.475	6.67	0.153711	0.302089	0.508827
51	(0.1/0.2)0.5	(0.2/0.075)2.67	0.068309	0.156183	0.437365
52	0.5	2.86	0.075015	0.167169	0.448738
53	0.5	3.07	0.082083	0.17897	0.458641
54	0.5	3.33	0.089561	0.191715	0.467157
55	0.5	3.64	0.097519	0.205571	0.474381
56	0.5	4	0.106083	0.220748	0.480562
57	0.5	4.44	0.115362	0.237525	0.485684
58	0.5	5	0.125544	0.25628	0.48987
59	0.5	5.71	0.136903	0.277543	0.493268
60	0.5	6.67	0.149812	0.302089	0.49592
61	(0.105/0.2)0.525	(0.2/0.075)2.67	0.065280	0.156183	0.417971
62	0.525	2.86	0.071900	0.167169	0.430104
63	0.525	3.07	0.078880	0.17897	0.440744
64	0.525	3.33	0.086259	0.191715	0.449933
65	0.525	3.64	0.094142	0.205571	0.457954
66	0.525	4	0.102626	0.220748	0.464901
67	0.525	4.44	0.111828	0.237525	0.470805
68	0.525	5	0.121939	0.25628	0.475804
69	0.525	5.71	0.133234	0.277543	0.480048
70	0.525	6.67	0.146086	0.302089	0.483586
71	(0.11/0.2)0.55	(0.2/0.075)2.67	0.062335	0.156183	0.399115
72	0.55	2.86	0.068875	0.167169	0.412008

73	0.55	3.07	0.075775	0.17897	0.423395
74	0.55	3.33	0.083085	0.191715	0.433378
75	0.55	3.64	0.090879	0.205571	0.442081
76	0.55	4	0.099294	0.220748	0.449807
77	0.55	4.44	0.108429	0.237525	0.456495
78	0.55	5	0.118478	0.25628	0.462299
79	0.55	5.71	0.129717	0.277543	0.467376
80	0.55	6.67	0.142519	0.302089	0.471778
81	(0.115/0.2)0.575	(0.2/0.075)2.67	0.059452	0.156183	0.380656
82	0.575	2.86	0.065934	0.167169	0.394415
83	0.575	3.07	0.072764	0.17897	0.406571
84	0.575	3.33	0.080003	0.191715	0.417302
85	0.575	3.64	0.087732	0.205571	0.426772
86	0.575	4	0.096081	0.220748	0.435252
87	0.575	4.44	0.105156	0.237525	0.442716
88	0.575	5	0.115150	0.25628	0.449313
89	0.575	5.71	0.126341	0.277543	0.455212
90	0.575	6.67	0.139099	0.302089	0.460457
91	(0.12/0.2)0.6	(0.2/0.075)2.67	0.056661	0.156183	0.362786
92	0.6	2.86	0.063074	0.167169	0.377307
93	0.6	3.07	0.069840	0.17897	0.390233
94	0.6	3.33	0.077019	0.191715	0.401737
95	0.6	3.64	0.084687	0.205571	0.41196
96	0.6	4	0.092980	0.220748	0.421204
97	0.6	4.44	0.102002	0.237525	0.429437
98	0.6	5	0.111984	0.25628	0.43696
99	0.6	5.71	0.123095	0.277543	0.443517
100	0.6	6.67	0.135816	0.302089	0.449589
101	(0.125/0.2)0.625	(0.2/0.075)2.67	0.0538	0.156183	0.344468

102	0.625	2.86	0.0601	0.167169	0.359516
103	0.625	3.07	0.0668	0.17897	0.373247
104	0.625	3.33	0.0739	0.191715	0.385468
105	0.625	3.64	0.0816	0.205571	0.396943
106	0.625	4	0.0898	0.220748	0.406799
107	0.625	4.44	0.0988	0.237525	0.415956
108	0.625	5	0.1087	0.25628	0.424145
109	0.625	5.71	0.1198	0.277543	0.431645
110	0.625	6.67	0.1325	0.302089	0.438612

Table A.2: Summary of results demonstrating the effect of ratio s/d_b on the borehole resistance, when k_g/k_s is 1.5.

K_g/k_s = 1.5W/K.m					
No.	s/d_b	d_b/d_p	$R_{numerical}$	$R_{analytical}$	$R_{numerical}/R_{analytical}$
1	(0.075/0.2)0.375	(0.2/0.075)2.67	0.057201	0.104122	0.549365
2	0.375	2.86	0.062022	0.111446	0.556521
3	0.375	3.07	0.067087	0.119313	0.562277
4	0.375	3.33	0.072443	0.12781	0.566802
5	0.375	3.64	0.078127	0.137047	0.570074
6	0.375	4	0.084207	0.147165	0.572194
7	0.375	4.44	0.090758	0.158353	0.573137
8	0.375	5	0.097887	0.170853	0.572931
9	0.375	5.71	0.105776	0.185029	0.571673
10	0.375	6.67	0.114666	0.201393	0.569364
11	(0.08/0.2)0.4	(0.2/0.075)2.67	0.054994	0.104122	0.528169
12	0.4	2.86	0.059723	0.111446	0.535892
13	0.4	3.07	0.064689	0.119313	0.542179
14	0.4	3.33	0.069944	0.12781	0.54725

15	0.4	3.64	0.075520	0.137047	0.551052
16	0.4	4	0.081491	0.147165	0.553739
17	0.4	4.44	0.087934	0.158353	0.555304
18	0.4	5	0.094961	0.170853	0.555805
19	0.4	5.71	0.102753	0.185029	0.555335
20	0.4	6.67	0.111559	0.201393	0.553937
21	(0.085/0.2)0.425	(0.2/0.075)2.67	0.052873	0.104122	0.507799
22	0.425	2.86	0.057516	0.111446	0.516089
23	0.425	3.07	0.062391	0.119313	0.522919
24	0.425	3.33	0.067550	0.12781	0.528519
25	0.425	3.64	0.073028	0.137047	0.532868
26	0.425	4	0.078903	0.147165	0.536153
27	0.425	4.44	0.085251	0.158353	0.53836
28	0.425	5	0.092189	0.170853	0.539581
29	0.425	5.71	0.099899	0.185029	0.53991
30	0.425	6.67	0.108628	0.201393	0.539383
31	(0.09/0.2)0.45	(0.2/0.075)2.67	0.050840	0.104122	0.488273
32	0.45	2.86	0.055398	0.111446	0.497084
33	0.45	3.07	0.060188	0.119313	0.504455
34	0.45	3.33	0.065259	0.12781	0.510594
35	0.45	3.64	0.070649	0.137047	0.515509
36	0.45	4	0.076437	0.147165	0.519397
37	0.45	4.44	0.082703	0.158353	0.52227
38	0.45	5	0.089563	0.170853	0.524211
39	0.45	5.71	0.097202	0.185029	0.525334
40	0.45	6.67	0.105868	0.201393	0.525679
41	(0.095/0.2)0.475	(0.2/0.075)2.67	0.048908	0.104122	0.469718
42	0.475	2.86	0.053368	0.111446	0.478869
43	0.475	3.07	0.058079	0.119313	0.486778

44	0.475	3.33	0.063069	0.12781	0.493459
45	0.475	3.64	0.068379	0.137047	0.498946
46	0.475	4	0.074091	0.147165	0.503455
47	0.475	4.44	0.080284	0.158353	0.506994
48	0.475	5	0.087076	0.170853	0.509654
49	0.475	5.71	0.094655	0.185029	0.511568
50	0.475	6.67	0.103264	0.201393	0.512749
51	(0.1/0.2)0.5	(0.2/0.075)2.67	0.047037	0.104122	0.451749
52	0.5	2.86	0.051427	0.111446	0.461452
53	0.5	3.07	0.056065	0.119313	0.469899
54	0.5	3.33	0.060980	0.12781	0.477114
55	0.5	3.64	0.066219	0.137047	0.483185
56	0.5	4	0.071862	0.147165	0.488309
57	0.5	4.44	0.077989	0.158353	0.492501
58	0.5	5	0.084722	0.170853	0.495877
59	0.5	5.71	0.092245	0.185029	0.498543
60	0.5	6.67	0.100807	0.201393	0.500549
61	(0.105/0.2)0.525	(0.2/0.075)2.67	0.045245	0.104122	0.434538
62	0.525	2.86	0.049573	0.111446	0.444816
63	0.525	3.07	0.054144	0.119313	0.453798
64	0.525	3.33	0.058992	0.12781	0.46156
65	0.525	3.64	0.064166	0.137047	0.468204
66	0.525	4	0.069748	0.147165	0.473944
67	0.525	4.44	0.075817	0.158353	0.478785
68	0.525	5	0.082496	0.170853	0.482848
69	0.525	5.71	0.089971	0.185029	0.486254
70	0.525	6.67	0.098491	0.201393	0.489049
71	(0.11/0.2)0.55	(0.2/0.075)2.67	0.043540	0.104122	0.418163
72	0.55	2.86	0.047809	0.111446	0.428988

73	0.55	3.07	0.052318	0.119313	0.438494
74	0.55	3.33	0.057105	0.12781	0.446796
75	0.55	3.64	0.062219	0.137047	0.453998
76	0.55	4	0.067747	0.147165	0.460347
77	0.55	4.44	0.073763	0.158353	0.465814
78	0.55	5	0.080395	0.170853	0.470551
79	0.55	5.71	0.087826	0.185029	0.474661
80	0.55	6.67	0.096308	0.201393	0.478209
81	(0.115/0.2)0.575	(0.2/0.075)2.67	0.041924	0.104122	0.402643
82	0.575	2.86	0.046136	0.111446	0.413976
83	0.575	3.07	0.050588	0.119313	0.423994
84	0.575	3.33	0.055391	0.12781	0.433385
85	0.575	3.64	0.060379	0.137047	0.440571
86	0.575	4	0.065857	0.147165	0.447505
87	0.575	4.44	0.071826	0.158353	0.453582
88	0.575	5	0.078414	0.170853	0.458956
89	0.575	5.71	0.085807	0.185029	0.463749
90	0.575	6.67	0.094254	0.201393	0.46801
91	(0.12/0.2)0.6	(0.2/0.075)2.67	0.040396	0.104122	0.387968
92	0.6	2.86	0.044555	0.111446	0.39979
93	0.6	3.07	0.048955	0.119313	0.410307
94	0.6	3.33	0.053635	0.12781	0.419646
95	0.6	3.64	0.058647	0.137047	0.427933
96	0.6	4	0.064078	0.147165	0.435416
97	0.6	4.44	0.070004	0.158353	0.442076
98	0.6	5	0.076553	0.170853	0.448064
99	0.6	5.71	0.083911	0.185029	0.453502
100	0.6	6.67	0.092326	0.201393	0.458437
101	(0.125/0.2)0.625	(0.2/0.075)2.67	0.03884	0.104122	0.373024

102	0.625	2.86	0.0429	0.111446	0.38494
103	0.625	3.07	0.0472	0.119313	0.395598
104	0.625	3.33	0.0519	0.12781	0.406072
105	0.625	3.64	0.0568	0.137047	0.414456
106	0.625	4	0.0622	0.147165	0.422655
107	0.625	4.44	0.0681	0.158353	0.430052
108	0.625	5	0.0746	0.170853	0.436633
109	0.625	5.71	0.0820	0.185029	0.443174
110	0.625	6.67	0.0904	0.201393	0.448874

Table A.3: Summary of results demonstrating the effect of ratio s/d_b on the borehole resistance, when k_g/k_s is 2.0.

K_g/k_s = 2.0W/K.m					
No.	s/d_b	d_b/d_p	$R_{numerical}$	$R_{analytical}$	$R_{numerical}/R_{analytical}$
1	(0.075/0.2)0.375	(0.2/0.075)2.67	0.043264	0.078092	0.554013
2	0.375	2.86	0.046865	0.083585	0.560687
3	0.375	3.07	0.050648	0.089485	0.565994
4	0.375	3.33	0.054648	0.095858	0.570093
5	0.375	3.64	0.058896	0.102785	0.573002
6	0.375	4	0.063440	0.110374	0.574773
7	0.375	4.44	0.068339	0.118762	0.575428
8	0.375	5	0.073672	0.12814	0.574934
9	0.375	5.71	0.079576	0.138771	0.573434
10	0.375	6.67	0.086232	0.151045	0.570903
11	(0.08/0.2)0.4	(0.2/0.075)2.67	0.041681	0.078092	0.533742
12	0.4	2.86	0.045195	0.083585	0.540707
13	0.4	3.07	0.048901	0.089485	0.546471
14	0.4	3.33	0.052824	0.095858	0.551065

15	0.4	3.64	0.056987	0.102785	0.554429
16	0.4	4	0.061447	0.110374	0.556716
17	0.4	4.44	0.066263	0.118762	0.557948
18	0.4	5	0.071517	0.12814	0.558116
19	0.4	5.71	0.077346	0.138771	0.557364
20	0.4	6.67	0.083937	0.151045	0.555709
21	(0.085/0.2)0.425	(0.2/0.075)2.67	0.040155	0.078092	0.514201
22	0.425	2.86	0.043602	0.083585	0.521649
23	0.425	3.07	0.047236	0.089485	0.527865
24	0.425	3.33	0.051085	0.095858	0.532924
25	0.425	3.64	0.055172	0.102785	0.536771
26	0.425	4	0.059557	0.110374	0.539593
27	0.425	4.44	0.064300	0.118762	0.541419
28	0.425	5	0.069485	0.12814	0.542258
29	0.425	5.71	0.075250	0.138771	0.54226
30	0.425	6.67	0.081783	0.151045	0.541448
31	(0.09/0.2)0.45	(0.2/0.075)2.67	0.038687	0.078092	0.495403
32	0.45	2.86	0.042084	0.083585	0.503487
33	0.45	3.07	0.045652	0.089485	0.510164
34	0.45	3.33	0.04931	0.095858	0.514407
35	0.45	3.64	0.053450	0.102785	0.520018
36	0.45	4	0.057768	0.110374	0.523384
37	0.45	4.44	0.062445	0.118762	0.525799
38	0.45	5	0.067570	0.12814	0.527314
39	0.45	5.71	0.073280	0.138771	0.528064
40	0.45	6.67	0.079763	0.151045	0.528074
41	(0.095/0.2)0.475	(0.2/0.075)2.67	0.037306	0.078092	0.477719
42	0.475	2.86	0.040641	0.083585	0.486224
43	0.475	3.07	0.044147	0.089485	0.493345

44	0.475	3.33	0.047863	0.095858	0.499311
45	0.475	3.64	0.051820	0.102785	0.504159
46	0.475	4	0.056077	0.110374	0.508063
47	0.475	4.44	0.060698	0.118762	0.511089
48	0.475	5	0.065769	0.12814	0.513259
49	0.475	5.71	0.071432	0.138771	0.514747
50	0.475	6.67	0.077871	0.151045	0.515548
51	(0.1/0.2)0.5	(0.2/0.075)2.67	0.036011	0.078092	0.461136
52	0.5	2.86	0.039274	0.083585	0.469869
53	0.5	3.07	0.042723	0.089485	0.477432
54	0.5	3.33	0.046381	0.095858	0.483851
55	0.5	3.64	0.0502081	0.102785	0.488477
56	0.5	4	0.054485	0.110374	0.49364
57	0.5	4.44	0.059054	0.118762	0.497247
58	0.5	5	0.064078	0.12814	0.500062
59	0.5	5.71	0.069698	0.138771	0.502252
60	0.5	6.67	0.076099	0.151045	0.503817
61	(0.105/0.2)0.525	(0.2/0.075)2.67	0.034773	0.078092	0.445282
62	0.525	2.86	0.037985	0.083585	0.454448
63	0.525	3.07	0.041381	0.089485	0.462435
64	0.525	3.33	0.044984	0.095858	0.469277
65	0.525	3.64	0.048835	0.102785	0.475118
66	0.525	4	0.052991	0.110374	0.480104
67	0.525	4.44	0.057514	0.118762	0.484279
68	0.525	5	0.062496	0.12814	0.487717
69	0.525	5.71	0.068077	0.138771	0.490571
70	0.525	6.67	0.074444	0.151045	0.49286
71	(0.11/0.2)0.55	(0.2/0.075)2.67	0.033608	0.078092	0.430364
72	0.55	2.86	0.036774	0.083585	0.439959

73	0.55	3.07	0.040123	0.089485	0.448377
74	0.55	3.33	0.043676	0.095858	0.455632
75	0.55	3.64	0.047482	0.102785	0.461955
76	0.55	4	0.051594	0.110374	0.467447
77	0.55	4.44	0.056075	0.118762	0.472163
78	0.55	5	0.061019	0.12814	0.47619
79	0.55	5.71	0.066560	0.138771	0.479639
80	0.55	6.67	0.072903	0.151045	0.482657
81	(0.115/0.2)0.575	(0.2/0.075)2.67	0.032521	0.078092	0.416445
82	0.575	2.86	0.035645	0.083585	0.426452
83	0.575	3.07	0.038949	0.089485	0.435257
84	0.575	3.33	0.042458	0.095858	0.442926
85	0.575	3.64	0.046223	0.102785	0.449706
86	0.575	4	0.050295	0.110374	0.455678
87	0.575	4.44	0.054739	0.118762	0.460913
88	0.575	5	0.059648	0.12814	0.465491
89	0.575	5.71	0.065164	0.138771	0.469579
90	0.575	6.67	0.071473	0.151045	0.47319
91	(0.12/0.2)0.6	(0.2/0.075)2.67	0.031514	0.078092	0.40355
92	0.6	2.86	0.034599	0.083585	0.413938
93	0.6	3.07	0.037863	0.089485	0.423121
94	0.6	3.33	0.041337	0.095858	0.431232
95	0.6	3.64	0.045059	0.102785	0.438381
96	0.6	4	0.049096	0.110374	0.444815
97	0.6	4.44	0.053506	0.118762	0.450531
98	0.6	5	0.058384	0.12814	0.455627
99	0.6	5.71	0.387206	0.138771	2.790252
100	0.6	6.67	0.070156	0.151045	0.464471
101	(0.125/0.2)0.625	(0.2/0.075)2.67	0.0305	0.078092	0.390565

102	0.625	2.86	0.0355	0.083585	0.424717
103	0.625	3.07	0.0367	0.089485	0.410125
104	0.625	3.33	0.0401	0.095858	0.418327
105	0.625	3.64	0.0438	0.102785	0.426132
106	0.625	4	0.0478	0.110374	0.433073
107	0.625	4.44	0.0522	0.118762	0.439535
108	0.625	5	0.0571	0.12814	0.445606
109	0.625	5.71	0.0625	0.138771	0.450382
110	0.625	6.67	0.0688	0.151045	0.455493

Table A.4: Summary of results demonstrating the effect of ratio s/d_b on the borehole resistance, when k_g/k_s is 2.5.

K_g/k_s = 2.5W/K.m					
No.	s/d_b	d_b/d_p	$R_{numerical}$	$R_{analytical}$	$R_{numerical}/R_{analytical}$
1	(0.075/0.2)0.375	(0.2/0.075)2.67	0.034837	0.062473	0.557633
2	0.375	2.86	0.037709	0.066868	0.563932
3	0.375	3.07	0.040727	0.071588	0.568908
4	0.375	3.33	0.043919	0.076686	0.572712
5	0.375	3.64	0.047308	0.082228	0.575327
6	0.375	4	0.050935	0.088299	0.576847
7	0.375	4.44	0.054846	0.09501	0.577266
8	0.375	5	0.059105	0.102512	0.576567
9	0.375	5.71	0.063820	0.111017	0.574867
10	0.375	6.67	0.069139	0.120836	0.572172
11	(0.08/0.2)0.4	(0.2/0.075)2.67	0.033601	0.062473	0.537848
12	0.4	2.86	0.036403	0.066868	0.544401
13	0.4	3.07	0.039358	0.071588	0.549785
14	0.4	3.33	0.042486	0.076686	0.554026

15	0.4	3.64	0.045808	0.082228	0.557085
16	0.4	4	0.049366	0.088299	0.559078
17	0.4	4.44	0.053209	0.09501	0.560036
18	0.4	5	0.057403	0.102512	0.559964
19	0.4	5.71	0.062058	0.111017	0.558995
20	0.4	6.67	0.067324	0.120836	0.557152
21	(0.085/0.2)0.425	(0.2/0.075)2.67	0.032403	0.062473	0.518672
22	0.425	2.86	0.035162	0.066868	0.525842
23	0.425	3.07	0.038059	0.071588	0.531639
24	0.425	3.33	0.041270	0.076686	0.538169
25	0.425	3.64	0.044386	0.082228	0.539792
26	0.425	4	0.047882	0.088299	0.542271
27	0.425	4.44	0.051666	0.09501	0.543795
28	0.425	5	0.055804	0.102512	0.544366
29	0.425	5.71	0.060407	0.111017	0.544124
30	0.425	6.67	0.065625	0.120836	0.543091
31	(0.09/0.2)0.45	(0.2/0.075)2.67	0.031292	0.062473	0.500888
32	0.45	2.86	0.033986	0.066868	0.508255
33	0.45	3.07	0.036828	0.071588	0.514444
34	0.45	3.33	0.039840	0.076686	0.519521
35	0.45	3.64	0.043043	0.082228	0.523459
36	0.45	4	0.046484	0.088299	0.526439
37	0.45	4.44	0.050215	0.09501	0.528523
38	0.45	5	0.054303	0.102512	0.529723
39	0.45	5.71	0.058861	0.111017	0.530198
40	0.45	6.67	0.064039	0.120836	0.529966
41	(0.095/0.2)0.475	(0.2/0.075)2.67	0.030219	0.062473	0.483713
42	0.475	2.86	0.032875	0.066868	0.49164
43	0.475	3.07	0.035667	0.071588	0.498226

44	0.475	3.33	0.038626	0.076686	0.50369
45	0.475	3.64	0.041778	0.082228	0.508075
46	0.475	4	0.045170	0.088299	0.511557
47	0.475	4.44	0.048854	0.09501	0.514199
48	0.475	5	0.052899	0.102512	0.516027
49	0.475	5.71	0.057418	0.111017	0.5172
50	0.475	6.67	0.062559	0.120836	0.517718
51	(0.1/0.2)0.5	(0.2/0.075)2.67	0.029221	0.062473	0.467738
52	0.5	2.86	0.031830	0.066868	0.476012
53	0.5	3.07	0.034575	0.071588	0.482972
54	0.5	3.33	0.037487	0.076686	0.488838
55	0.5	3.64	0.040593	0.082228	0.493664
56	0.5	4	0.043941	0.088299	0.497639
57	0.5	4.44	0.047582	0.09501	0.50081
58	0.5	5	0.051588	0.102512	0.503239
59	0.5	5.71	0.056071	0.111017	0.505067
60	0.5	6.67	0.061182	0.120836	0.506323
61	(0.105/0.2)0.525	(0.2/0.075)2.67	0.028298	0.062473	0.452964
62	0.525	2.86	0.030853	0.066868	0.461402
63	0.525	3.07	0.033555	0.071588	0.468724
64	0.525	3.33	0.036424	0.076686	0.474976
65	0.525	3.64	0.039487	0.082228	0.480214
66	0.525	4	0.042796	0.088299	0.484671
67	0.525	4.44	0.046399	0.09501	0.488359
68	0.525	5	0.050370	0.102512	0.491357
69	0.525	5.71	0.054822	0.111017	0.493816
70	0.525	6.67	0.059904	0.120836	0.495746
71	(0.11/0.2)0.55	(0.2/0.075)2.67	0.027429	0.062473	0.439054
72	0.55	2.86	0.029944	0.066868	0.447808

73	0.55	3.07	0.032607	0.071588	0.455481
74	0.55	3.33	0.035437	0.076686	0.462105
75	0.55	3.64	0.038462	0.082228	0.467748
76	0.55	4	0.041735	0.088299	0.472655
77	0.55	4.44	0.045305	0.09501	0.476845
78	0.55	5	0.049245	0.102512	0.480383
79	0.55	5.71	0.053668	0.111017	0.483421
80	0.55	6.67	0.058725	0.120836	0.485989
81	(0.115/0.2)0.575	(0.2/0.075)2.67	0.026626	0.062473	0.4262
82	0.575	2.86	0.029107	0.066868	0.43529
83	0.575	3.07	0.031735	0.071588	0.443301
84	0.575	3.33	0.034529	0.076686	0.450265
85	0.575	3.64	0.037521	0.082228	0.456304
86	0.575	4	0.040762	0.088299	0.461636
87	0.575	4.44	0.044301	0.09501	0.466277
88	0.575	5	0.048212	0.102512	0.470306
89	0.575	5.71	0.052610	0.111017	0.473891
90	0.575	6.67	0.057644	0.120836	0.477043
91	(0.12/0.2)0.6	(0.2/0.075)2.67	0.025889	0.062473	0.414403
92	0.6	2.86	0.028342	0.066868	0.42385
93	0.6	3.07	0.030939	0.071588	0.432181
94	0.6	3.33	0.033703	0.076686	0.439494
95	0.6	3.64	0.036663	0.082228	0.44587
96	0.6	4	0.039876	0.088299	0.451602
97	0.6	4.44	0.043388	0.09501	0.456668
98	0.6	5	0.047274	0.102512	0.461156
99	0.6	5.71	0.051648	0.111017	0.465226
100	0.6	6.67	0.056662	0.120836	0.468917
101	(0.125/0.2)0.625	(0.2/0.075)2.67	0.0251	0.062473	0.401774

102	0.625	2.86	0.0275	0.066868	0.411258
103	0.625	3.07	0.0300	0.071588	0.419065
104	0.625	3.33	0.0328	0.076686	0.427718
105	0.625	3.64	0.03577	0.082228	0.43501
106	0.625	4	0.0389	0.088299	0.440549
107	0.625	4.44	0.0424	0.09501	0.446269
108	0.625	5	0.0463	0.102512	0.451654
109	0.625	5.71	0.0506	0.111017	0.455786
110	0.625	6.67	0.0566	0.120836	0.468403

Table A.5: Summary of results demonstrating the effect of ratio s/d_b on the borehole resistance, when k_g/k_s is 3.0.

K_g/k_s = 3.0W/K.m					
No.	s/d_b	d_b/d_p	$R_{numerical}$	$R_{analytical}$	$R_{numerical}/R_{analytical}$
1	(0.075/0.2)0.375	(0.2/0.075)2.67	0.029195	0.052061	0.560784
2	0.375	2.86	0.031574	0.055723	0.566624
3	0.375	3.07	0.034084	0.059657	0.571333
4	0.375	3.33	0.036739	0.063905	0.5749
5	0.375	3.64	0.039558	0.068524	0.577287
6	0.375	4	0.042575	0.073583	0.578598
7	0.375	4.44	0.045829	0.079175	0.578832
8	0.375	5	0.049374	0.085427	0.577967
9	0.375	5.71	0.053299	0.092514	0.576118
10	0.375	6.67	0.057727	0.100696	0.57328
11	(0.08/0.2)0.4	(0.2/0.075)2.67	0.028174	0.052061	0.541173
12	0.4	2.86	0.030504	0.055723	0.547422
13	0.4	3.07	0.032960	0.059657	0.552492
14	0.4	3.33	0.035562	0.063905	0.556482

15	0.4	3.64	0.038324	0.068524	0.559279
16	0.4	4	0.041283	0.073583	0.56104
17	0.4	4.44	0.044480	0.079175	0.561793
18	0.4	5	0.047970	0.085427	0.561532
19	0.4	5.71	0.051844	0.092514	0.560391
20	0.4	6.67	0.056227	0.100696	0.558384
21	(0.085/0.2)0.425	(0.2/0.075)2.67	0.027207	0.052061	0.522598
22	0.425	2.86	0.029491	0.055723	0.529243
23	0.425	3.07	0.032898	0.059657	0.551452
24	0.425	3.33	0.03448	0.063905	0.539551
25	0.425	3.64	0.037157	0.068524	0.542248
26	0.425	4	0.040064	0.073583	0.544474
27	0.425	4.44	0.043211	0.079175	0.545766
28	0.425	5	0.046653	0.085427	0.546115
29	0.425	5.71	0.050484	0.092514	0.54569
30	0.425	6.67	0.054827	0.100696	0.54448
31	(0.09/0.2)0.45	(0.2/0.075)2.67	0.026295	0.052061	0.505081
32	0.45	2.86	0.028534	0.055723	0.512069
33	0.45	3.07	0.030895	0.059657	0.517877
34	0.45	3.33	0.033397	0.063905	0.522604
35	0.45	3.64	0.036059	0.068524	0.526224
36	0.45	4	0.038920	0.073583	0.528927
37	0.45	4.44	0.042022	0.079175	0.530748
38	0.45	5	0.045422	0.085427	0.531705
39	0.45	5.71	0.049214	0.092514	0.531963
40	0.45	6.67	0.053523	0.100696	0.531531
41	(0.095/0.2)0.475	(0.2/0.075)2.67	0.025437	0.052061	0.4886
42	0.475	2.86	0.027634	0.055723	0.495917
43	0.475	3.07	0.029953	0.059657	0.502087

44	0.475	3.33	0.032411	0.063905	0.507175
45	0.475	3.64	0.035030	0.068524	0.511208
46	0.475	4	0.037849	0.073583	0.514372
47	0.475	4.44	0.040911	0.079175	0.516716
48	0.475	5	0.044274	0.085427	0.518267
49	0.475	5.71	0.048033	0.092514	0.519197
50	0.475	6.67	0.052311	0.100696	0.519494
51	(0.1/0.2)0.5	(0.2/0.075)2.67	0.024634	0.052061	0.473176
52	0.5	2.86	0.026792	0.055723	0.480807
53	0.5	3.07	0.029072	0.059657	0.487319
54	0.5	3.33	0.031490	0.063905	0.492763
55	0.5	3.64	0.034069	0.068524	0.497183
56	0.5	4	0.036851	0.073583	0.500809
57	0.5	4.44	0.039877	0.079175	0.503656
58	0.5	5	0.043208	0.085427	0.505789
59	0.5	5.71	0.046936	0.092514	0.507339
60	0.5	6.67	0.051188	0.100696	0.508342
61	(0.105/0.2)0.525	(0.2/0.075)2.67	0.023878	0.052061	0.458654
62	0.525	2.86	0.026010	0.055723	0.466773
63	0.525	3.07	0.028253	0.059657	0.473591
64	0.525	3.33	0.030636	0.063905	0.479399
65	0.525	3.64	0.033179	0.068524	0.484195
66	0.525	4	0.035928	0.073583	0.488265
67	0.525	4.44	0.038922	0.079175	0.491595
68	0.525	5	0.042223	0.085427	0.494258
69	0.525	5.71	0.045925	0.092514	0.496411
70	0.525	6.67	0.050153	0.100696	0.498063
71	(0.11/0.2)0.55	(0.2/0.075)2.67	0.023199	0.052061	0.445612
72	0.55	2.86	0.025288	0.055723	0.453816

73	0.55	3.07	0.027499	0.059657	0.460952
74	0.55	3.33	0.029849	0.063905	0.467084
75	0.55	3.64	0.032361	0.068524	0.472258
76	0.55	4	0.035079	0.073583	0.476727
77	0.55	4.44	0.038045	0.079175	0.480518
78	0.55	5	0.041319	0.085427	0.483676
79	0.55	5.71	0.044997	0.092514	0.48638
80	0.55	6.67	0.049204	0.100696	0.488639
81	(0.115/0.2)0.575	(0.2/0.075)2.67	0.022569	0.052061	0.433511
82	0.575	2.86	0.024629	0.055723	0.44199
83	0.575	3.07	0.026811	0.059657	0.449419
84	0.575	3.33	0.029132	0.063905	0.455864
85	0.575	3.64	0.031616	0.068524	0.461386
86	0.575	4	0.034307	0.073583	0.466235
87	0.575	4.44	0.037247	0.079175	0.470439
88	0.575	5	0.040498	0.085427	0.474066
89	0.575	5.71	0.044154	0.092514	0.477268
90	0.575	6.67	0.048342	0.100696	0.480079
91	(0.12/0.2)0.6	(0.2/0.075)2.67	0.021998	0.052061	0.422543
92	0.6	2.86	0.024035	0.055723	0.43133
93	0.6	3.07	0.026192	0.059657	0.439043
94	0.6	3.33	0.028487	0.063905	0.445771
95	0.6	3.64	0.030946	0.068524	0.451608
96	0.6	4	0.033614	0.073583	0.456817
97	0.6	4.44	0.036531	0.079175	0.461396
98	0.6	5	0.039761	0.085427	0.465438
99	0.6	5.71	0.043398	0.092514	0.469097
100	0.6	6.67	0.047568	0.100696	0.472392
101	(0.125/0.2)0.625	(0.2/0.075)2.67	0.0213	0.052061	0.409135

102	0.625	2.86	0.0233	0.055723	0.41814
103	0.625	3.07	0.0255	0.059657	0.427444
104	0.625	3.33	0.0277	0.063905	0.433456
105	0.625	3.64	0.0302	0.068524	0.440721
106	0.625	4	0.0328	0.073583	0.445755
107	0.625	4.44	0.0357	0.079175	0.45090
108	0.625	5	0.0389	0.085427	0.45536
109	0.625	5.71	0.0426	0.092514	0.460471
110	0.625	6.67	0.0467	0.100696	0.463772

Table A.6: Summary of results demonstrating the effect of ratio s/d_b on the borehole resistance, when k_g/k_s is 3.5.

K_g/k_s = 3.5W/K.m					
No.	s/d_b	d_b/d_p	$R_{numerical}$	$R_{analytical}$	$R_{numerical}/R_{analytical}$
1	(0.075/0.2)0.375	(0.2/0.075)2.67	0.025138	0.044624	0.563329
2	0.375	2.86	0.027175	0.047763	0.568955
3	0.375	3.07	0.029323	0.051134	0.573454
4	0.375	3.33	0.031595	0.054776	0.576804
5	0.375	3.64	0.034008	0.058734	0.579017
6	0.375	4	0.036591	0.063071	0.580156
7	0.375	4.44	0.039377	0.067864	0.580234
8	0.375	5	0.042412	0.073223	0.579217
9	0.375	5.71	0.045773	0.079298	0.577228
10	0.375	6.67	0.049567	0.086311	0.574284
11	(0.08/0.2)0.4	(0.2/0.075)2.67	0.024275	0.044624	0.54399
12	0.4	2.86	0.026269	0.047763	0.549986
13	0.4	3.07	0.028371	0.051134	0.554836
14	0.4	3.33	0.030597	0.054776	0.558584

15	0.4	3.64	0.032961	0.058734	0.561191
16	0.4	4	0.035493	0.063071	0.562747
17	0.4	4.44	0.038230	0.067864	0.563333
18	0.4	5	0.041218	0.073223	0.562911
19	0.4	5.71	0.044535	0.079298	0.561616
20	0.4	6.67	0.048289	0.086311	0.559477
21	(0.085/0.2)0.425	(0.2/0.075)2.67	0.023460	0.044624	0.525726
22	0.425	2.86	0.025414	0.047763	0.532086
23	0.425	3.07	0.027473	0.051134	0.537275
24	0.425	3.33	0.029655	0.054776	0.541387
25	0.425	3.64	0.031973	0.058734	0.54437
26	0.425	4	0.034461	0.063071	0.546384
27	0.425	4.44	0.037154	0.067864	0.547477
28	0.425	5	0.040100	0.073223	0.547642
29	0.425	5.71	0.043380	0.079298	0.54705
30	0.425	6.67	0.047099	0.086311	0.545689
31	(0.09/0.2)0.45	(0.2/0.075)2.67	0.022693	0.044624	0.508538
32	0.45	2.86	0.024609	0.047763	0.515231
33	0.45	3.07	0.026629	0.051134	0.520769
34	0.45	3.33	0.028769	0.054776	0.525212
35	0.45	3.64	0.031046	0.058734	0.528587
36	0.45	4	0.033493	0.063071	0.531036
37	0.45	4.44	0.036147	0.067864	0.532639
38	0.45	5	0.039057	0.073223	0.533398
39	0.45	5.71	0.042304	0.079298	0.533481
40	0.45	6.67	0.045994	0.086311	0.532887
41	(0.095/0.2)0.475	(0.2/0.075)2.67	0.021975	0.044624	0.492448
42	0.475	2.86	0.023855	0.047763	0.499445
43	0.475	3.07	0.025838	0.051134	0.5053

44	0.475	3.33	0.027940	0.054776	0.510077
45	0.475	3.64	0.030179	0.058734	0.513825
46	0.475	4	0.032590	0.063071	0.516719
47	0.475	4.44	0.035210	0.067864	0.518832
48	0.475	5	0.038088	0.073223	0.520164
49	0.475	5.71	0.041306	0.079298	0.520896
50	0.475	6.67	0.044969	0.086311	0.521011
51	(0.1/0.2)0.5	(0.2/0.075)2.67	0.021306	0.044624	0.477456
52	0.5	2.86	0.023152	0.047763	0.484727
53	0.5	3.07	0.025101	0.051134	0.490887
54	0.5	3.33	0.027169	0.054776	0.496002
55	0.5	3.64	0.029375	0.058734	0.500136
56	0.5	4	0.031753	0.063071	0.503448
57	0.5	4.44	0.034342	0.067864	0.506041
58	0.5	5	0.037192	0.073223	0.507928
59	0.5	5.71	0.040383	0.079298	0.509256
60	0.5	6.67	0.044023	0.086311	0.510051
61	(0.105/0.2)0.525	(0.2/0.075)2.67	0.020687	0.044624	0.463585
62	0.525	2.86	0.022502	0.047763	0.471118
63	0.525	3.07	0.024420	0.051134	0.477569
64	0.525	3.33	0.026457	0.054776	0.483004
65	0.525	3.64	0.028632	0.058734	0.487486
66	0.525	4	0.030982	0.063071	0.491224
67	0.525	4.44	0.033543	0.067864	0.494268
68	0.525	5	0.036367	0.073223	0.496661
69	0.525	5.71	0.039535	0.079298	0.498562
70	0.525	6.67	0.043155	0.086311	0.499994
71	(0.11/0.2)0.55	(0.2/0.075)2.67	0.020111	0.044624	0.450677
72	0.55	2.86	0.021906	0.047763	0.45864

73	0.55	3.07	0.023797	0.051134	0.465385
74	0.55	3.33	0.025806	0.054776	0.471119
75	0.55	3.64	0.027953	0.058734	0.475925
76	0.55	4	0.030277	0.063071	0.480046
77	0.55	4.44	0.032814	0.067864	0.483526
78	0.55	5	0.035615	0.073223	0.486391
79	0.55	5.71	0.038762	0.079298	0.488814
80	0.55	6.67	0.042363	0.086311	0.490818
81	(0.115/0.2)0.575	(0.2/0.075)2.67	0.019604	0.044624	0.439315
82	0.575	2.86	0.021367	0.047763	0.447355
83	0.575	3.07	0.023232	0.051134	0.454336
84	0.575	3.33	0.025217	0.054776	0.460366
85	0.575	3.64	0.027341	0.058734	0.465505
86	0.575	4	0.029642	0.063071	0.469978
87	0.575	4.44	0.032126	0.067864	0.473388
88	0.575	5	0.034937	0.073223	0.477132
89	0.575	5.71	0.038066	0.079298	0.480037
90	0.575	6.67	0.041650	0.086311	0.482557
91	(0.12/0.2)0.6	(0.2/0.075)2.67	0.019141	0.044624	0.42894
92	0.6	2.86	0.020884	0.047763	0.437242
93	0.6	3.07	0.022729	0.051134	0.444499
94	0.6	3.33	0.024692	0.054776	0.450781
95	0.6	3.64	0.026795	0.058734	0.456209
96	0.6	4	0.029076	0.063071	0.461004
97	0.6	4.44	0.031571	0.067864	0.46521
98	0.6	5	0.034335	0.073223	0.46891
99	0.6	5.71	0.037447	0.079298	0.472231
100	0.6	6.67	0.041016	0.086311	0.475212
101	(0.125/0.2)0.625	(0.2/0.075)2.67	0.0186	0.044624	0.416816

102	0.625	2.86	0.0203	0.047763	0.425015
103	0.625	3.07	0.0221	0.051134	0.432198
104	0.625	3.33	0.0241	0.054776	0.439974
105	0.625	3.64	0.0262	0.058734	0.446079
106	0.625	4	0.0284	0.063071	0.450286
107	0.625	4.44	0.0309	0.067864	0.455322
108	0.625	5	0.0336	0.073223	0.458872
109	0.625	5.71	0.0367	0.079298	0.462811
110	0.625	6.67	0.0403	0.086311	0.466916

Appendix B: Sample to the problem description scrip in Flex PDE program.

Sample to the problem description scrip in Flex PDE, to simulate the borehole heat exchanger system and the surrounding soil.

The model consists of a borehole with a single U-shape pipe. The borehole and U-tube diameter are assumed to be 0.1m and 0.03m, respectively. The borehole is assumed to be filled with grout with 2 W/K.m thermal conductivity and surrounded by soil that have 1 W/K.m thermal conductivity.

```
TITLE "BH heat exchanger"
VARIABLES
Temp (threshold = 0.01) (temperature)
SELECT
stages = 3
ERRLIM = staged (1e-3, 1e-4, 1e-5)
DEFINITIONS     {all units based on grams, days and m3}
rw = 0.015 {radius of the pipe, m}
rs = 0.05  {radius of the grout, m}
kr = 2 {thermal conductivity ratio between soil and grout}
s = 0.04 {distance between two centre points of the pipes}
ks = 1 {thermal conductivity of soil}
qgt = line_INTEGRAL (normal(-grad(temp)*k), 'ogt')
Tbww = line_INTEGRAL ((temp), 'gt')
Tbw = Tbww/(2*3.14*rs)
Tf = 8
INITIAL VALUES
Temp = 12
EQUATIONS
Temp: k*(dxx(Temp)+dyy(Temp))=0
BOUNDARIES      {Drawn inwards from the outside -- subsequent layers overlap}
REGION  'Soil'
k = ks {thermal conductivity of soil}
START(re,0)
value (Temp) = 12
ARC (CENTER = 0,0) ANGLE = -360
REGION  'Grout'
k = ks*kr {thermal conductivity of grout}
mesh_spacing = rw/5
START 'gt' (rs,0)
ARC (CENTER = 0,0) ANGLE = -360
Region 'inlet pipes'
k = 0.5
START 'inlet' ((0.5*s + rw),0) value(Temp) = 7
ARC (CENTER = 0.5*s,0) ANGLE = -360
close
Region 'outlet pipes'
k = 0.5
START 'outlet' (-(0.5*s + rw),0)  value(Temp) = 9
ARC (CENTER = -0.5*s,0) ANGLE = -360
CLOSE
PLOTS
contour(Temp)
Summary as "heat Flux Report"
report(qgt) as "qgt"
report (tbw) as "Tbhw"
report (-(Tf-tbw)/qgt) as "rb"
END
```

Appendix C: Deep mixing influence on thermal resistance

The influence of Deep mixing on the total thermal resistance of borehole with single U-tube pipe as a function of the thermal conductivity of the deep mixing area to soil thermal conductivity (k_m/k_s), when soil diameter around the borehole assumed to be 20m and the shank spacing between the U-tube pipes is 50mm.
The percentage of Reduction is calculated using the following equation:

$$POR = \frac{R_t - R_{t-new}}{R_t}$$

where R_t taken to be 0.8888 K.m/W, which is the maximum total resistance found when soil diameter assumed to be 20m, $R_{t\text{-}new}$, is the total thermal resistance after deep mixing.

Table C.1: Total thermal diameter as a function of total thermal resistance when thermal conductivity of the deep mixing area to soil thermal conductivity (k_m/k_s) is 2.

Deep Mixing Radius	**Ground Thermal Resistance (R_g) (K.m/W)**	**Borehole Thermal Resistance (R_b) (K.m/W)**	**Total Thermal Resistance (R_t) (K.m/W)**	**ROR (%)**
0.1	0.732	0.100	0.832	6.30
0.15	0.667	0.132	0.799	10.02
0.2	0.621	0.155	0.776	12.61
0.25	0.586	0.173	0.759	14.52

Table C.2: Total thermal diameter as a function of total thermal resistance when thermal conductivity of the deep mixing area to soil thermal conductivity (km/ks) is 3.

Deep Mixing Radius	**Ground Thermal Resistance (R_g) (K.m/W)**	**Borehole Thermal Resistance (R_b) (K.m/W)**	**Total Thermal Resistance (R_t) (K.m/W)**	**POR (%)**
0.1	0.732	0.0673	0.7993	9.98
0.15	0.667	0.0887	0.7557	14.89
0.2	0.621	0.104	0.725	18.35
0.25	0.586	0.115	0.701	21.05

Table C.3: Total thermal diameter as a function of total thermal resistance when thermal conductivity of the deep mixing area to soil thermal conductivity (km/ks) is 4.

Deep Mixing Radius	**Ground Thermal Resistance (R_g) (K.m/W)**	**Borehole Thermal Resistance (R_b) (K.m/W)**	**Total Thermal Resistance (R_t) (K.m/W)**	**POR (%)**
0.1	0.732	0.0507	0.782	12.0
0.15	0.667	0.0660	0.734	17.4
0.2	0.621	0.0781	0.700	21.2
0.25	0.586	0.0870	0.673	24.3

Table C.4: Total thermal diameter as a function of total thermal resistance when thermal conductivity of the deep mixing area to soil thermal conductivity (k_m/k_s) is 5.

Deep Mixing Radius	Ground Thermal Resistance (R_g) (K.m/W)	Borehole Thermal Resistance (R_b) (K.m/W)	Total Thermal Resistance (R_t) (K.m/W)	POR (%)
0.1	0.732	0.0407	0.772	13.1
0.15	0.667	0.0535	0.721	18.8
0.2	0.621	0.0626	0.684	23.0
0.25	0.586	0.097	0.656	26.1

Table C.5: Total thermal diameter as a function of total thermal resistance when thermal conductivity of the deep mixing area to soil thermal conductivity (k_m/k_s) is 6.

Deep Mixing Radius	Ground Thermal Resistance (R_g) (K.m/W)	Borehole Thermal Resistance (R_b) (K.m/W)	Total Thermal Resistance (R_t) (K.m/W)	POR (%)
0.1	0.732	0.0340	0.766	13.8
0.15	0.667	0.0447	0.712	19.8
0.2	0.621	0.0523	0.674	24.1
0.25	0.586	0.0582	0.644	27.5

Table C.6: Total thermal diameter as a function of total thermal resistance when thermal conductivity of the deep mixing area to soil thermal conductivity (k_m/k_s) is 7.

Deep Mixing Radius	Ground Thermal Resistance (R_g) (K.m/W)	Borehole Thermal Resistance (R_b) (K.m/W)	Total Thermal Resistance (R_t) (K.m/W)	POR (%)
0.1	0.732	0.0293	0.761	14.4
0.15	0.667	0.0384	0.706	20.5
0.2	0.621	0.0449	0.666	25.6
0.25	0.586	0.0499	0.636	28.4

Table C.7: Total thermal diameter as a function of total thermal resistance when thermal conductivity of the deep mixing area to soil thermal conductivity (k_m/k_s) is 8.

Deep Mixing Radius	Ground Thermal Resistance (R_g) (K.m/W)	Borehole Thermal Resistance (R_b) (K.m/W)	Total Thermal Resistance (R_t) (K.m/W)	POR (%)
0.1	0.732	0.0257	0.757	14.8
0.15	0.667	0.0337	0.701	21.1
0.2	0.621	0.0394	0.661	26.0
0.25	0.586	0.0438	0.630	29.1

Table C.8: Total thermal diameter as a function of total thermal resistance when thermal conductivity of the deep mixing area to soil thermal conductivity (k_m/k_s) is 9.

Deep Mixing Radius	Ground Thermal Resistance (R_g) (K.m/W)	Borehole Thermal Resistance (R_b) (K.m/W)	Total Thermal Resistance (R_t) (K.m/W)	POR (%)
0.1	0.732	0.0229	0.755	15.0
0.15	0.667	0.0300	0.697	21.5
0.2	0.621	0.0350	0.657	26.0
0.25	0.586	0.0390	0.625	30.0

Table C.9: Total thermal diameter as a function of total thermal resistance when thermal conductivity of the deep mixing area to soil thermal conductivity (k_m/k_s) is 10.

Deep Mixing Radius	Ground Thermal Resistance (R_g) (K.m/W)	Borehole Thermal Resistance (R_b) (K.m/W)	Total Thermal Resistance (R_t) (K.m/W)	POR (%)
0.1	0.732	0.0207	0.752	15.3
0.15	0.667	0.0271	0.694	22.0
0.2	0.621	0.0316	0.653	27.0
0.25	0.586	0.0351	0.621	30.2

References

Abdeen Mustafa Omer, 2006.Ground- Source Heat Pumps systems and applications. published by Since Direct, Renewable and Sustainable Energy reviews.

Acuña, J.; Palm, B(2010). Local Conduction Heat Transfer in U-pipe Borehole Heat Exchangers. Excerpt from the Proceedings of the COMSOL Conference 2009 Milan. The Royal Institute of Technology KTH.

Al-Khoury Rafid , 2012. The book of Computational Modelling of Shallow Geothermal Systems, Chapter 8.

Allan ML, Philipp acopoulos AJ, 1998. Ground water protection issues with geothermal heat pumps. Vol. 23, pp. 101–205.

Andrew D. Chiasson, 1992. Advances In Modelling Of Ground-Source Heat pump Systems. Master of Applied Science University of Windsor, Windsor, Ontario, Canada.

ASHRAE Handbook, 2003. HVAC Applications. SI ed. Atlanta, Ga: American Society of Heating, Refrigerating and Air Conditioning Engineers.

B. Hanumantha Rao and D. N. Singh, 2010. Application of Thermal Flux for Establishing Soil-water Characteristic Curve of Kaolin", Geomechanics and Geo-engineering: An International Journal, 5(4), pp. 259-266.

Banks, D. , 2008. An introduction to Thermo geology: ground source heating and cooling. Blackwell Publishing Ltd, Oxford, UK.

Becker, B.R., A. Misra, and B.A. Fricke ,1992. Development of correlations for soil thermal properties. (available at :http://web.ornl.gov/sci/buildings/2012/1992%20B5/021.pdf)

Bennet, J., Claesson, J., Hellstrom, G. (1987). Multipole Method to Compute the Conductive Heat Transfer to and between Pipes in a Composite Cylinder. Department of Building Physics, Lund Institute of Technology, Lund, Sweden.

Bernier, M. (2006). Closed loop -ground coupled heat pump systems. ASHRAE Journal Vol. 48(9), pp. 12-19.

Bi, Y., Chen, L., Wu, C., 2002. Ground heat exchanger temperature distribution analysis and experimental verification. Applied Thermal Engineering Vol. 22,pp. 183–189.

Birch, Francis and Clark, Harry, 1940. The Thermal Conductivity of Rocks and its Dependence upon Temperature and Composition. American Journal of Science, Vol. 288, No. 8, pp. 529-634.

Bose, J.E., Parker, J.D., McQuiston, F.C., 1985. Design/Data Manual for Closed-Loop Ground-Coupled Heat Pump Systems. American Society of Heating, Refrigeration and Air Conditioning Engineers (ASHRAE), Atlanta, GA, USA, 312 pp.

Brandl, H. (2006). Energy foundations and other thermo-active ground structure, Géotechnique 56, Vol. 2, pp. 81-122.

Brandon, T.L., and J.K. Mitchell (1989). Factors influencing thermal resistivity of sands. Geotech. Energy., 115(12), 1683–1698. Technical Papers.

British Eco Renewable Energy Solutions.(used on August,2012).

Busby, Jon; Lewis, Melinda; Reeves, Helen; Lawley, Russell (2009). Initial geological considerations before installing ground source heat pump systems. Quarterly Journal of Engineering Geology and Hydrogeology. Vol.42 (3), pp. 295-306.

Carslaw, H.S., J.C. Jaeger. 1947. Conduction of Heat in Solids. Oxford, UK: Oxford University Press, pp. 510.

Çengel Y.A. and Boles M.A. ,1994.Thermodynamics: An Engineering Approach. McGraw-Hill, Inc., New York.

Cenk Yavuzturk,1999. Modelling Of Vertical Ground Loop Heat Exchangers For Ground Source Heat Pump Systems. Diplom Ingenieur Technical University of Berlin,Germany.

Chi H, Lee C, Choi H-P (2008). A study on physical characteristics of grout material for backfilling ground heat exchange (in Korean). J Korean Geotech Soc. Vol. 24(1), pp. 37-49.

Chiasson, A.C. , S.J. Rees, J.D. Spitler. 2000. A Preliminary Assessment Of The Effects Of Ground-Water Flow On Closed-Loop Ground-Source Heat Pump Systems.

Climate Change Act Policy 2008.Chapter 27.

David D. Vanderburg ,2002.Comparative Energy And Cost Analysis Between Conventional Hvac Systems And Geothermal Heat Pump Systems Thesis.

De Vries, D.A. (1963) Thermal properties of soils. Physics of Plant Environment , North-Holland, Amsterdam, pp. 210-235.

De Vries, D.A.(2002). The thermal conductivity of soil. Mededelingen van de ,demonstration projects, Final project report.

Deerman, J. D.; Kavanaugh, S.P ,1991. Simulation of vertical U-tube ground coupled heat pump systems using the cylindrical heat source solution.

Eckhart, F., 1991. Grouting Procedures for Ground-Source Heat Pump System.Oklahoma State University, Ground Source Heat Pump Publications.

Eskilson, P., Claesson, J., 1988. Simulation model for thermally interacting heat extraction boreholes. Numerical Heat Transfer Vol. 13, pp. 149–165.

Gale, I. ,2004. GSHP Site Characterisation. Carbon Trust research, development and Gemant, A. 1952. How to compute thermal soil conductivities. Heating, Piping, and Air Geotechnical Engineering, ASCE. Vol. 115(12), pp.1683-1698.

Gehlin, S. , 2002. Thermal Response Test - Method Development and Evaluation. Doctoral, Lulea University of Technology.

Gori F.(1983). A theoretical model for predicting the effective thermal conductivity of saturated frozen soils XVI International Congress of Refrigeration , Paris BI-26. pp. 525-535.

Grant, M.A., I.G. Donaldson, and P.F. Bixley (1982). Geothermal Reservoir Engineering. Academic Press, New York, NY, USA.

Gu, Y., O'Neal, D.L., 1998. Development of an equivalent diameter expression for vertical U-tubes used in ground-coupled heat pumps. ASHRAE Transactions Vol. 104, pp. 347–355.

Gustafsson, A.-M., Westerlund, L., Hellstrom, G. ,2010. CFD-modelling of natural convection in a groundwater-filled borehole heat exchanger, Applied Thermal Engineering, 30, 683-691.

Hart, D. P. & Couvillion, 1986. Earth Coupled Heat Transfer: Publication of the National Water Well Association.

Hellström G. ,2001. Numerical evaluation of thermal response test. Numerical 2D axisymmetric model used for evaluation of Swedish thermal response test measurements.

Hellstrom, G., 1991. Ground Heat Storage; Thermal Analysis of Duct Storage Systems. Doctoral Thesis. Department of Mathematical Physics, University of Lund, Lund, Sweden.pp.310.

Hellström, G., Tsang, C.F., and Claesson., J., 1988. Buoyancy Flow at a Two-Fluid Interface in a Porous Medium: Analytical Studies, Water Resources Research. Vol. 24, No.4, pp. 493-506.

Hiromi Mori ,2010. Enhancement Of Heat Transfer For Ground Source Heat Pump Systems. PhD thesis for Nottingham University.

Hooper, F. C., and F. R. Leper ,1950. Transient heat flow apparatus for the determination of thermal conductivity. J. Amer. Soc. Heating and Ventilating Engineers. Vol. 22,pp.129-135.

Incropera F.P. and D.P. DeWitt , 2002. The book called "Fundamentals of Heat and Mass Transfer". 5th ed., J. Wiley, New York.

Incropera, F. P., Dewitt, D. P., Bergman, T. L. & Lavine, A. S. 2007. The book called "Fundamentals of Heat and Mass Transfer", 6th ed., J. Wiley, New York.

Ingersoll, L.R., Plass H.J. 1948. Theory of Ground Pipe Heat Source for the Heat pump. Heating, Piping & Air Conditioning 20(7), pp. 119-122.

Jason S. Pentland, Graduate Student, Gilson de F. N. Graduate Student, Delwyn G. Fredlund ,2001. Use of a General Partial Differential Equation Solver for Solution of Mass and Heat Transfer Problems in Geotechnical Engineering. University of Saskatchewan, Saskatoon, SK, Canada,.

Jenkins, D.P.,Tuker,R. And Rawlings, R., 2009. Modelling the Carbon-saving Performance of Domestic Ground-Source Heat Pump. Energy and Buildings.

Johansen, O. ,1975. Thermal conductivity of soils. Ph.D. thesis. Trondheim, Norway (CRREL Draft Translation 637)

Jon Busby ,Melinda Lewis ,Helen Reeves and Russell Lawley, 2010. Initial geological considerations before installing ground source heat pump systems.

Kannan, R.and Strachan, N. ,2009.Modelling the UK residential energy sector under long-term decarbonisation scenarios: Comparison between energy system and sectoral modelling approaches. Applied Energy Vol.86, pp.416-428.

Kasuda, T. & Archenbach, P. R. , 1965. Earth temperature and thermal diffusivity at selected stations in the United States. ASHRAE Transactions, 71**,** Part 1.

Kavanaugh, (2010). Design of Geothermal Systems .American Society of Heating Refrigerating and Air-Conditioning Engineers (ASHRAE), Atlanta, GA, USA, pp. 167.

Kavanaugh, S. P., 1985. Simulation and experimental verification of vertical ground-coupled heat pump systems. PhD, Oklahoma State University.

Kavanaugh, S.P.,K. Rafferty.1997. Ground-Source Heat Pumps; design of geothermal Systems for commercial and institutional Buildings. Chapter 3. Atlanta; ASHRAE.2007 ASHRAE Handbook-HVAC Applications, Chapter 32.

Kelly,B.T. ,1981. Physics of Graphite, Applied Science, London, pp. 477.

Kersten, M.S. ,1949. Thermal properties of soils. Engineering Experiment Station, University of Minnesota.

L. Lamarche, ,Stanislaw Kajl, Benoit Beauchamp, 2010.A review of methods to evaluate borehole thermal resistances in geothermal heat-pump systems. Geothermics Journal, Vol. 39 ,pp. 187–200.

Lawrence John Schwankl,1979. Law Calibration of the Neutron Soil Moisture Probe for Selected California Soils.

Lee Y., Sungho Park ,Jongchan Kim , Hyoung Chan Kim , Min-Ho Koo, 2010.Geothermal resource assessment in Korea. Available at Science Direct Renewable and Sustainable Energy Reviews, Vol(14).pp. 2392–2400.

Lee, Se-Kyoun Woo, Joung-son., 2009. A Study of the Effect of Borehole Thermal Resistance on the Borehole Length.

Li Xinguo , Zhihao Chen, Jun Zhao, 2006. The simulation and experiment on the thermal performance of U-vertical ground coupled heat exchanger. Available in Journal of Science Direct, Vol. 26, pp. 1564–1571.

Lu Aye and W. W. S. Charters. ,2003. Electrical and engine driven heat pumps for effective utilisation of renewable energy resources" Applied Thermal Engineering Volume 23, Issue 10, pp.1295-1300.

Lund, J.W.; Sanner, B.; Rybach, L.; Curtis, R. & Hellström G. ,2007. Geothermal Energy Uses. Geo-Heat Centre Quarterly Bulletin. Klamath Falls, Oregon. Oregon Institute of Technology, Vol. 28.

McGaw, R. ,1969. Heat conduction in saturated granular materials. special Rept. Army corps Engineering, Coki Region research and engineering laboratory.

Miaomiao He ,2012. Numerical Modelling of Geothermal Borehole Heat Exchanger Systems. PhD thesis for De Montfort University, Leicester, UK.

Mikael Philippe; Michel Bernier, 2010. Sizing Calculation Spreadsheet for the Vertical Geothermal Bore fields. This article was published in ASHRAE Journal, July 2010.

Miles, L. ,1994. Heat pumps Theory and services. Delmar Publishers Inc., pp. 397.

Mitchell, J.K. ,1991. Conduction phenomena: From theory to geotechnical practice. Geotechnique. Vol. 41(3), pp. 299-340.

Nakshabandi, G.A. and Kohnke, H. (1965), "Thermal conductivity and diffusivity of soils as related to water tension and other physical properties", Agricultural Meteorology, Vol. 2, pp.271-279.

Nippon Steel Corporation, 2005.The Company website was used on the April,2013.

Ochsner, T.E., R. Horton, and T. Ren. 2001. Simultaneous water content, bulk density, and air-filled porosity measurements with thermo-time domain reflectometry. Soil Sci. Soc. Am. J. 65,pp. 1618-1622.

Paul R. Intemann,1982. Towards Solving The Conflict Between Geothermal Resource Uses. Master thesis for the Energy Division in Oak Ridge National Laboratory,Tennessee.

Flex PDE Solutions Inc.,1999 Manual.

Phetteplace, G., 2007. Geothermal Heat Pump Technology, Journal of Energy Engineering, Vol. 133, No. 1, pgs. 32-38, American Society of Civil Engineers. Physics of plant environment. Amsterdam: North-Holland Publ. Co. pp. 210–235.

Rees, S. W., Adjali, M. H., Zhou, Z., Davies, M, & Thomas, H. R. ,2000. Ground heat transfer effects on the thermal performance earth-contact structures. Renewable and sustainable energy. Vol. 4, No. 3, pp. 213-265.

Remund and Lund, J.T. ,1993. Thermal Enhancement of Bentonite Grouts for vertical GSHP Systems, in Heat Pump and Refrigeration Systems, American Society of Mechanical Engineers, University of Missouri-Kansas City. Vol. 29, pp. 95-106.

Reynolds, W. C., and Perkins, H. C. ,1977. Engineering Thermodynamics, published by McGraw-Hill, New York.

Robin C. ,1999. Integrated building design BSRIA, Interactive CD.

Ruqun Wu 2009. Energy Efficiency Technologies-Air Source Heat pump vs. Ground Source Heat Pump. Journal of Sustainable Development. Australia.

Salomone, L.A., W.D. Kovacs, and T. Kusuda. 1984. Thermal performance of fine-grained soils. Journal of Geotechnical Engineering. Volume 3, pp. 359-374.

Sankaranarayanan K. P., 2004 .Study Of Frost Growth On Heat Exchangers Used.

Sass, J. H., Lachenbruch, A. H., and Munroe, R. J., 1971. Thermal conductivity of rocks from measurements on fragments and its application to heat-flow determinations: Journal of Geophysical Research, Vol. 76, pp. 3391-3401.

Sepaskhah, A.R., and L. Boersma. ,1979. Thermal conductivity of soils as a function of temperature and water content .Vol. 43, pp. 439-444.

Sepaskhah, A.R., and L. Boersma., 1979. Thermal conductivity of soils as a function of temperature and water content. Soil Sci. Soc. Am. J. ,Vol 43,pp. 439–444.

Sharqawy, M.H., Mokheimer, E.M., Badr, H.M., 2009. Effective pipe-to-borehole thermal resistance for vertical ground heat exchangers. Geothermics. Vol. 38,pp. 271– 277.

Shonder, J. A. and J. V. Beck.,1999. Determining Effective Soil Formation Thermal Properties From Field Data Using a Parameter Estimation Technique. ASHRAE Transactions, 105(1).

Steve Kavanaugh, 2010. Borehole ResistCalc xls: A program to Calculate Borehole Thermal Resistance from Formation Thermal Property Test Data.

Stuebi, R. T. ,2000. "Geothermal Heat Pumps: Green for Your Wallet, Green for Our Planet." Renewable Energies Conference. November 29,Denver.

Tarnawski Gori ,B. Wagner,G. D. Buchan,2000. Modelling approaches to predicting thermal conductivity of soils at high temperatures. Vol. 24**,** pp.403–423**.**

Tarnawski, V. R., W. H. Leong, F. Gori, G. D. Buchan, and J. Sundberg ,2002. Inter-particle contact heat transfer in soil systems at moderate temperatures. Vol. 26(15), pp. 1345 – 1358.

Thornton, J. W.; McDowell. T.P.; Hughes, P.J., 1997, Comparison of 5 Practical Vertical Ground Heat Exchanger Sizing Methods to a Fort Polk, LA Data/Model Benchmark, ASHRAE Transactions, 1997.

U.S. Department of Energy, 2008. American Reinvestment and Act.

Warren Adem Austin ,1995 . Development of an situ system for measuring ground thermal properties.

Walter J. Eugster, Ladislaus Rybach , 2000. Sustainable Production From Borehole Heat Exchanger Systems. Poly dynamics Engineering Zurich.

Yang, P. Cui, Z. Fang ,2010.Vertical-borehole ground-coupled heat pumps: A review of models and systems.

Yavuztruk, C., J.D. Spilter, S.J Rees. ,1999. A Transient Two-dimensional Finite Volume Model for Simulation of Vertical U-tube Ground Heat Exchangers.

Young, T. R. 2004. Development, Verification, and Design Analysis of the Borehole Fluid Thermal Mass Model for Approximating Short Term Borehole Thermal Response. Master of Science, Oklahoma State University.

Yutaka Genchi,, Yukihiro Kikegawa, Atsushi Inaba, 2002.CO_2 payback–time assessment of a regional-scale heating and cooling system using a ground source heat–pump in a high energy–consumption area in Tokyo.

Zeng, H., Diao, N., Fang, Z., 2003. Heat Transfer Analysis of Boreholes in Vertical Ground Heat Exchangers. International Journal of Heat and Mass Transfer Vol. 46, pp. 4467–4481.

Zheng, Q.-S.,Jiang, B., Liu, S.P.,2002. Self-retracting motion of graphite microflakes.

Zoi Sagia, Athina Stegou and Constantinos Rakopoulos, 2012. Borehole Resistance and Heat Conduction Around Vertical Ground Heat Exchangers